ISSN 1881-7831 Online ISSN 1881-784X

DD&T

Drug Discoveries & Therapeutics

Volume 10, Number 2
April, 2016

IRCA BSSA

IACMHR

www.ddtjournal.com

DD&T
Drug Discoveries & Therapeutics

ISSN: 1881-7831
Online ISSN: 1881-784X
CODEN: DDTRBX
Issues/Year: 6
Language: English
Publisher: IACMHR Co., Ltd.

Drug Discoveries & Therapeutics is one of a series of peer-reviewed journals of the International Research and Cooperation Association for Bio & Socio-Sciences Advancement (IRCA-BSSA) Group and is published bimonthly by the International Advancement Center for Medicine & Health Research Co., Ltd. (IACMHR Co., Ltd.) and supported by the IRCA-BSSA and Shandong University China-Japan Cooperation Center for Drug Discovery & Screening (SDU-DDSC).

Drug Discoveries & Therapeutics publishes contributions in all fields of pharmaceutical and therapeutic research such as medicinal chemistry, pharmacology, pharmaceutical analysis, pharmaceutics, pharmaceutical administration, and experimental and clinical studies of effects, mechanisms, or uses of various treatments. Studies in drug-related fields such as biology, biochemistry, physiology, microbiology, and immunology are also within the scope of this journal.

Drug Discoveries & Therapeutics publishes Original Articles, Brief Reports, Reviews, Policy Forum articles, Case Reports, News, and Letters on all aspects of the field of pharmaceutical research. All contributions should seek to promote international collaboration in pharmaceutical science.

Editorial Board

Editorial and Head Office:

Pearl City Koishikawa 603,
2-4-5 Kasuga, Bunkyo-ku,
Tokyo 112-0003, Japan
Tel.: +81-3-5840-9697
Fax: +81-3-5840-9698
E-mail: office@ddtjournal.com

Drug Discoveries & Therapeutics

Editorial and Head Office

Pearl City Koishikawa 603, 2-4-5 Kasuga, Bunkyo-ku,
Tokyo 112-0003, Japan

Tel: +81-3-5840-9697, Fax: +81-3-5840-9698
E-mail: office@ddtjournal.com
URL: www.ddtjournal.com

Editorial Board Members

Reviews

Original Articles

CONTENTS (*Continued*)

Brief Report

Case Reports

Guide for Authors

Copyright

Review

DOI: 10.5582/ddt.2016.01014

Regulation of food intake and the development of anti-obesity drugs

Yue Chen*

Pharmacy Department, PLA General Hospital, Beijing, China.

Summary **As the most significant cause of death worldwide, obesity has become one of the world's most important public health problems, but approved anti-obesity drugs are extremely limited. This article summarizes the feeding control circuits and regulators involved in obesity development, highlight the hypothalamus, melanocortin system and brain-gut peptide actions in this process, and the five US FDA approved anti-obesity medications in long term use, namely phentermine/topiramate, lorcaserin, naltrexone/bupropion, liraglutide and orlistat.**

Keywords: Anti-obesity drugs, feed control, brain gut peptide, hypothalamus

1. Introduction

In recent years, obesity has become the leading preventable cause of death worldwide, with increasing rates in adults and children. It was named as one of the greatest public health problem threats of this century (*1*). The American Medical Association named obesity as a disease in 2013 (*2*). Now it has been identified by World Health Organization as one of the five major health threats to human beings. In 2015, the world has more than 2.3 billion overweight adults, in which 700 million are obese (*3*). During the past 20 years, the population of overweight and obese individuals increased significantly in China, Japan and Southeast Asian countries. In addition, obese children and adolescents have increased markedly. It is now the world's largest chronic disease among adult patients and listed as one of the world's four major social medical problems (*4*).

Obesity may lead to several diseases particularly, heart disease, type 2 diabetes, certain types of cancer, osteoarthritis and obstructive sleep apnea. Moreover, obesity also makes people vulnerable to injury, and makes it easy to get joint disease, and vulnerable to post-operation infections (*5*). Because of the prevalence of obesity and high costs, obesity is also a public health and policy problem. It has a number of serious consequences for individuals and government health systems (*6*). In view of the health hazards and socioeconomic burden, anti-obesity has become a hot topic, but the misunderstanding of definition is prevalence, in which many people equate obesity and heaviness. In fact, patients should have excess body fat that may influence their health to be classified as obese. It is a medical condition that may have the potential to increase health problems and/or reduce life expectancy (*5*). The most common causes of obesity are excessive food energy intake and lack of physical activity. Some people may have genetic susceptibility. However, a few cases of obesity are caused primarily by genes and patients with medications, psychiatric illness or endocrine disorders. Normally, we refer to the most common cases.

In "2014 NICE Guidelines for the identification, assessment and management of overweight and obesity in children, young people and adults", obesity is defined by a measurement of Body Mass Index (BMI) (*7*). According to BMI, the degree of overweight or obesity in adults can be subdivided as healthy weight, overweight, obesity I, obesity II and obesity III. In addition to BMI, in people with a BMI less than 35 kg/m^2, the waist circumference is also considered as a factor and subdivided as low, high and very high. Assessment of the health risks associated with being overweight or obese in adults based on BMI and waist circumference can be seen in Table 1. The four levels of intervention are: 1. General advice for healthy weight and lifestyle; 2. Diet and physical activity; 3. Diet and

Released online in J-STAGE as advance publication April 11, 2016.

**Address correspondence to:*
Dr. Yue Chen, Pharmacy Department, PLA General Hospital, Beijing, 100853, China.
E-mail: metwen@163.com

Table 1. Identification, assessment and management of overweight and obesity

BMI (kg/m^2)		Intervention level			
		Waist circumference (cm)			Comorbidities present
		Low	High	Very high	
	Male	< 94	94-102	> 102	
	Female	< 80	80-88	> 88	
Over weight (25-29.9)		1	2	2	3
Obesity I (30-34.9)		2	2	2	3
Obesity II (35-39.9)		3	3	3	4
Obesity III (≥ 40)		4	4	4	4

physical activity; consider drugs; 4. Diet and physical activity; consider drugs; consider surgery.

In addition to these two indicators, the common factors assessing obesity may also include fat percentage and waist-hip ratio. Body fat percentage refers to the proportion of fatty tissue that reflects our body fat level (degree of obesity) (*8*). Waist-hip ratio (WHtR) is the ratio of waist to hip, which is an important indicator of central obesity. The WHtR measures the body fat distribution. A higher value means the individual may have higher risk of obesity-related cardiovascular diseases. When the male WHtR > 0.9 or female WHtR > 0.8, they can be diagnosed as central obesity (*9*).

Obesity intervention may be a long and arduous task that requires coordination of all aspects. There are three major methods: lifestyle interventions, including exercise, diet and cognitive - behavioral therapy, pharmacotherapy and surgery (*10*). Among them, lifestyle intervention is the foundation, namely of all treatments for obesity must consist of dieting and physical exercise. Using drugs or surgery both must meet some strict standards. In 2015, "Pharmacological Management of Obesity: An Endocrine Society Clinical Practice Guideline", was published by the American Endocrine Society (*11*). It recommended that all patients with a BMI ≥ 25 kg/m^2 should be given the treatment including diet, exercise, and behavioral modification. For those who cannot adhere to behavior change, drugs may be useful and may amplify the effects of behavioral regulation. Medications can be used in patients who have a history of failing in weight control or maintaining the lost weight. Moreover, only those who meet the deemed effective standard of medication treatment, namely weight loss ≥ 5% of body weight at 3 months, and have no side effects, can be continued. If the deemed effect is not obtained or has any safety or tolerability problem, the medication should be changed to other medications or alternative treatment approaches.

A long term imbalance of energy intake and energy consumption definitely leads to overweight and obesity. In modern society, eating style and sedentary lifestyles may be the major factors in the prevalence of obesity. Cheap, high fat and prepared food and modern transportation methods increase energy intake while reducing consumption (*12*). With the urgency of dealing with this arduous task, researchers try to explain the mechanisms involved in obesity and find proper treatments with sustained effects and less toxicity. This review sums up the latest understanding of feeding control in humans and FDA approved obesity drugs.

2. Feeding control circuits and regulators

To protect the human species from extinction through famine and war, the evolutionary protective mechanism resists fat loss and maintains weight. According to metabolic needs, several homeostatic brain circuits regulate feeding behavior by promoting food intake or suppressing appetite (*13*). The homeostatic control of food intake and the regulation of energy homeostasis takes place predominantly in the Central Nervous System (CNS), especially in the hypothalamus and brainstem, and responds to peripheral hormonal and neural signals. In the CNS, hypothalamus, the brain stem and reward systems combined regulate fluids and nerve messages. Specifically the hypothalamus plays a key role in monitoring, processing and responding to peripheral signals (*14*). Hunger hormones like Orexin and Ghrelin, or high-calorie food prompt people to eat. Satiety hormones such as leptin, insulin and other so called brain-gut peptides can inhibit feeding behavior (*15*). Long-term imbalance between hunger and satiety signals lead to weight increase and obesity. Besides, cognitive structures also involved in this process such as emotions can influence human eating behavior (*16*).

The main parts of the hypothalamus are the arcuate nucleus (ARC), the paraventricular nucleus (PVN), the ventromedial nucleus (VMN), the dorsomedial nucleus (DMN), and the lateral hypothalamic area (LHA), and all of them are involved in energy homeostasis-regulation (**17**). Peripheral signals contact the CNS to regulate energy homoeostasis. Gut hormones in the gastrointestinal tract communicate information and transfer it to regulatory appetite centers based in the CNS *via* the so-called 'Gut-Brain-Axis'. There are two ways of information communication, either *via* vagal non-vagal afferent nerve signaling, or *via* blood circulation directly. The ARC is adjacent to the third ventricle and the median eminence, where there is a thin blood-brain barrier. So hormones and nutrient signals can directly

diffuse into the extracellular fluid, which means both nerve regulation and humoral regulation affect the ARC, to give it a major role in feeding control circuits (*18*).

Several neuronal populations have been listed as key players in the hypothalamus, mainly the central melanocortin system (*19*). Three main components of the central melanocortin system are: the proopiomelanocortin (POMC) and cocaine-and-amphetamine-regulated transcript (CART)-coexpressing neurons (POMC/CART), the neuropeptide Y (NPY) and agouti-related peptide (AgRP)-coexpressing neurons located in the hypothalamic arcuate nucleus (NPY/AgRP), and the melanocortin receptors (MCRs) expressing neurons located in the hypothalamic paraventricular nucleus. The first one in the lateral ARC coexpress POMC and CART can depress appetite, leads to feeding decrease and weight loss. In contrast, the second one in the medial ARC coexpress NPY and AgRP, which increase appetite and stimulate eating, leads to weight gain.

Melanocortin receptors include five, class A, G protein-coupled receptors, namely MC1R-MC5R. All of them have diverse physiological roles, in which the melanocortin 4 receptors (MC4Rs) and melanocortin 3 receptors (MC3Rs) play critical roles in mediating energy homoeostasis (*20*). MC4R mainly binds to a-melanocyte stimulating hormone (aMSH) in the hypothalamus PVN to control food intake. MC4R inactivating mutations are the single most common cause of monogenic obesity in humans (*21*). The food intake reduction and energy expenditure increasing effects of anorexigenic POMC/CART neurons are through activating MC4Rs, while the orexigenic NPY/AgRP neurons increase food intake and decrease energy expenditure by antagonizing POMC action on MC4Rs, thus increasing body weight. Moreover, enteroendocrine L cells can express MC4Rs to regulate the release of certain types of brain-gut peptides, like peptide YY (PYY) and glucagon-like peptide 1 (GLP-1). MC3R is primarily expressed in the central nervous system in the ARC of the hypothalamus and limbic areas, where it affects food utilization/partitioning and food anticipatory behavior. In mice, MC3Rs plays an important role in the maintenance of a circadian rhythm of activity related to feeding behavior while obese humans show loss-of-function mutations in MC3Rs (*22*). However, the role of MC3R in energy homeostasis is unclear.

Several bioactive peptides, like adreno corticotrophin (ACTH), α-, β-, and γ-melanocyte stimulating hormone (α-MSH, β-MSH, and γ-MSH) and β-endorphin, are generated by the POMC protein precursor. Among them, α-MSH is the most well known anorexigenic peptide and MCR agonist. By binding and activating MCRs, α-MSH regulates food intake and energy consumption. POMC plays a critical role in the regulation of metabolism, in which its gene mutation will lead to early-onset obesity. AgRP neurons co-express the orexigenic NPY, and the neuro-transmitter gamma-aminobutyric acid (GABA), directly inhibit POMC neurons. AgRP is a high-affinity MCR antagonist. However, contrary to POMC mutations, NPY/ AgRP gene mutations do not have a significant effect on food intake and body weight, which means other compensatory mechanisms may be involved in the energy homeostasis-regulating process (*23*). Besides, peripheric hormones like leptin, glucocorticoids, insulin, estrogens, ghrelin, PYY, and GLP-1, and signals from nutrients can regulate POMC and AgRP neurons. Body energy status can also influence the melanocortin system.

Vagal afferent fibers can sense the signals of nutrients and transfer them to the CNS. Most of the vagal afferent fibers, that innervate the viscera and gastrointestinal tract, project to the nucleus of the solitary tract (NTS) rostral to obex (*24*). Within this region, several neurons project to the VTA and lateral hypothalamic areas, and may affect food intake through actions on dopamine signaling in motivation and reward-related areas. The pleasantness of food alongside the emotional and cognitive aspects of eating behavior is determined in the 'reward' system of the brain. This system is comprised of a number of limbic and cortical areas that communicate with each other and with the hypothalamus, predominantly through dopamine (DA), opioid and endocannabinoid neurotransmission (*25*). Moreover, metabolic pathways in the brainstem, like the orbitofrontal cortex (OFC), amygdala, insula, dorsal and ventral striatum, hippocampus, anterior cingulate cortex and dorsolateral prefrontal cortex, amongst others, also integrate and respond to short-term and long-term changes in energy homeostasis as part of a broader network.

3. Regulatory signals in the feeding control circuits

NPY, peptide YY (PYY) and pancreatic polypeptide (PP) are members of the neuropeptide Y (NPY) family. They are expressed by cell systems at different levels of the gut-brain axis (*26*). NPY is the most abundant neuropeptide in the brain. A lot of neuronal system regions, from the medullary brainstem to the cerebral cortex, can express NPY. It exerts a variety of physiological processes in humans *via* four different receptor subtypes Y1, Y2, Y4 and Y5. As one of the potent orexigenic peptides in the CNS, NPY/AgRP neurons have a critical role in feeding regulation. Y1 receptors play the main role in the orexigenic effect, although Y5 receptors also are involved in this process.

Through different neuronal circuits, neuropeptides like melanin-concentrating hormone (MCH) or orexins/hypocretins (OX) in LHA can regulate ingestion, arousal, and locomotor behavior as well as autonomic function (*27*). By activation of MCHR-1 in the nucleus accumbens (NA), MCH can coordinate energy need and feeding. This process possibly contributes to influence feeding in energy balance disorders. Central injection of the orexigenic neuropeptide MCH into the brain increases feeding in rodents and promotes obesity. Unlike strongly

orexigenic neuropeptide NPY, MCH only amplifies the size or amount of normally accepted food and water, and the forebrain can selectively control this effect.

The endocannabinoid system functions as a potent regulator of feeding behavior and energy balance through complex central and peripheral mechanisms (*28*). In general, increased endocannabinoid activity enhances food intake and favors fat storage. Endocannabinoids such as anandamide promote feeding mediated by the interaction of cannabinoid compounds with various types of receptors in the nervous system. The cannabinoid-type 1 (CB1) receptors are highly expressed in the brain, mainly in the ARC, the PVN, and the LHA. It colocalizes with opioid receptors and participates in the modulation of food palatability and ingestion. CB1 receptor inverse agonist/antagonist rimonabant was used as a weight loss drug but was withdrawn from the market for increasing the risk of psychiatric side-effects (*29*).

Highly flavored, energy-dense, "palliative foods" can override normal eating and weight-control mechanisms and generate paradoxically high but ineffective levels of appetite-suppressing hormones (*30*). There is evidence that these foods can affect the reward system through central monoamine neurotransmitters. In the reward system, neurotransmitter dopamine plays a key role in regulating feeding and emotion. However, the clear role of dopamine signaling in reward is controversial. There exists two hypotheses to explain the role of dopamine (*31*). The first one is the positive correlation between dopamine signaling and pleasure experience may overindulgence pleasurable stimuli. The second one is a compensatory response like overeating may result from decreased dopaminergic signaling.

4. Brain-gut peptides as feeding control regulators

The gastrointestinal tract is the largest endocrine organ in which many kinds of peptides are being produced and released and have several distinct effects (*32*). External cues contact the CNS to control feed and coordinate with the brain's internal signals, transferring messages about the presence and composition of foods in the gut. These gastrointestinal peptides are either orexigenic or anorexigenic related to food intake and named as brain-gut peptides. There are two types of brain-gut peptides (*33*): *i*) short-term signals, which are kept in step with each episode of eating, like, ghrelin, cholecystokinin (CCK), PP, PYY, GLP-1, nesfatin-1, oxyntomodulin (OXM), glucagon, gastric inhibitory polypeptide (GIP), amylin, and so forth.; *ii*) long-term signals, which reflect the metabolic state of adipose tissue, such as, insulin and leptin. Both of them interact with each other to determine eating behavior.

4.1. *Short-term signals*

As the first gut hormone known to affect feeding and appetite, CCK is secreted from enteroendocrine I-cells predominantly located in the proximal small intestine, mainly in response to fatty acids. After a meal, plasma CCK levels increase within 15 minutes and the life time of CCK is only a few minutes. The vagal nerve has CCK-1 receptors that can lead to early meal termination and reduce food intake once combining with CCK (*34*). The hypothalamus also has CCK-1 receptors, which means a direct communication without vagal regulation may exist. Besides, the synergistic interaction between CCK and several other anorexigenic peptides also have an important role in feeding regulation.

Ghrelin is a 28-amino-acid-long peptide that exerts its orexigenic effect *via* the growth hormone secretagogue receptor (GHS-R) to increase food intake in animals and humans (*35*). During fasting, the circulating levels of ghrelin increase and after eating, it falls to stimulate hunger. Until now, ghrelin is the only known orexigenic, peripherally active gut hormone. The plasma level of ghrelin is mainly regulated by nutrients but not water. Expressed within the ARC and PVN of the hypothalamus, ghrelin also plays a role as a neurotransmitter to adjust appetite. This effect is mediated through activation of NPY/AgRP co-expressing neurons. Both central and peripheral ghrelin administration have the same effect in reducing fat utilization and weight increase from overeating. Except for short term effects as a meal stimulator, ghrelin may also have long-term effects because its levels are inversely correlated to BMI. Further, ghrelin may influence the reward system through mesolimbic dopamine circuitry, in which the emotional wanting or reward value for highly desirable foods increased (*36*).

PP-fold peptide family includes NPY, PP and PYY. PP is a 36 amino-acid-long peptide released from the pancreas (*37*). The blood level of PP is proportional to the amount of ingested calories. It is believed that the anorectic effects of PP are transferred *via* the Y4-receptor in the brainstem and the hypothalamus. Compared to normal weight people, the circulating levels of PP in obese subjects and Pradere Willi syndrome patients are reduced and can't increase after feeding. Further, PP can reduce leptin in white adipose tissue and decrease the gene expression of ACTH-releasing factor. However, although intravenously administered PP can reduce food intake and increase energy expenditure, central administrated PP leads to increased food intake (*38*).

PYY also belongs to the PP-fold peptide family, secreted in proportion to nutrients ingested, but not affected by gastric distension. The secretion of PYY is mainly stimulated by fat. N-terminally truncated PYY3-36 is the major form of PYY that has high affinity for the Y2 receptor. Peripherally administrated PYY3-36 at physiological doses can decrease food intake in rodents, primates and humans. Circulating postprandial PYY levels are lower in obese individuals, suggesting

it may have a potential pathophysiological role in the development of obesity (*39*). However, different reports show large differences in fasting PYY levels between normal and obese patients.

Both L cells and neurons of the nucleus of the solitary tract in the hindbrain can produce GLP-1 (*40*). The release of GLP-1 is proportional to the amount of calories ingested, but normal and obese people have a different response to GLP-1 administration. Unlike PYY affected mainly by fat, the stimulators of GLP-1 are carbohydrate and fat. Protein has a relatively less effect on the release of GLP-1. By combining with GLP-1 receptor, a member of 'Family B' of the G-protein-coupled receptors widely distributed in the gastrointestinal tract, pancreas and brain, GLP-1 can activate neurons in the ARC, PVN, NTS and AP, lead to satiety and reduce hunger.

Nesfatin-1 is an 82 amino acid polypeptide. It is the cleavage product of NUCB2, mainly expressed in the CNS as part of the feeding regulatory system (*41*). As an anorexigenic modulator of feeding control, once injected into the brain, Nesfatin-1 can induce a prolonged decrease of dark phase food intake even at picomolar levels. Hypothalamic anorexigenic pathways such as corticotropin-releasing factor receptor 2 (CRF2), medullary pro-opiomelanocortin signaling, melanocortin and oxytocin can mediate the effect of Nesfatin-1.

4.2. *Long-term signals*

The long term signals of feeding regulators are leptin and insulin (*42*). The release of them are proportional to body fat content and the CNS level of them are determined by their plasma concentrations.

Insulin serves as an anorexigenic modulator of feeding control in the CNS by stimulating POMC/CART and inhibiting NPY/AgRP (*43*). It controls energy homeostasis by acting on the ARC, stimulating the synthesis of pro-opiomelanocortin that acts on melanocortin receptors MC3R and MC4R in hypothalamic nuclei. However, insulin is secreted into the blood in response to change in blood glucose concentrations, and lowered blood sugar level is a strong signal of hunger, which means it can't be used to control eating by peripheral administration. The release of insulin can also be influenced by incretin hormones such as GLP-1 (*44*). Thus, the relationship between insulin secretion and appetite regulation may be more complicated than current understanding.

Leptin acts directly on the feeding control neurons in CNS, suppressing NPY and increasing pro-opiomelanocortin, to stimulate the enzymes involved in lipid metabolism. It can reduce food intake and increase energy consumption. (*45*). It can prevent obesity by inhibiting appetite. Lacking leptin or leptin receptor dysfunction may lead to hyperphagia and obesity. Further, the expression and consolidation of learned appetitive behaviors can be depressed by leptin and dopamine signaling is influenced by leptin, as well, although the mechanism is not clear yet (*46*). It can also enhance the effect of CCK and heighten the sensitivity for sweetness.

5. Nutrients served as feeding control regulators

Nutrients can also transfer satiating signals to the hypothalamus. Specific receptors or transporters sense the signals from nutrients like carbohydrate, fat and protein. These receptors located in the entero-endocrine cells (EEC) in the intestinal epithelium can trigger the release of gastro-intestinal regulatory peptides such as CCK, ghrelin, PYY, serotonin, GLP-1 among others (*47*).

After absorption, glucose released in the portal vein bound to SGLT3, and served as a second message to the brain to reduce hunger (*48*). A broad range of G-protein-coupled receptors in the lumen sense the signal from non-esterified fatty acids (NEFA) in a length dependent manner. Among them, NEFA1 receptor and GPR120 respond to medium- and long-chain NEFA(C>12) and NEFA2 and NEFA3 receptors detect short-chain fatty acids (SCFA). After digestion, protein degrade to peptides in the portal vein, which antagonize MORs present in the peri-portal afferents to the brain. By vagal and spinal signals, these message are transferred to the brain by MOR-controlled ascending nerves.

6. Weight-loss products

Excessive body weight can lead to various diseases, such as diabetes mellitus type 2, cardiovascular diseases, certain types of cancer, obstructive sleep apnea, asthma and osteoarthritis. As a result, obesity may reduce life expectancy. With the dramatic increase in obesity in the population, a variety of weight-loss products have emerged, but effectiveness and safety are uncertain (*49*). To date, there are no regulations for the safety and effectiveness of weight-loss products and no strict criteria. The most common weight-loss products can be divided into four categories, which include: prevent the absorption of fat or carbohydrates to reduce the absorption of energy from food; promote metabolism, namely increasing energy expenditure; change the distribution of nutrients in body to reduce body fat while increasing lean tissue; reduce the body's energy intake by suppressing appetite and increasing satiety.

A-amylase inhibitor (*50*) and chitin (*51*) are two materials that can reduce energy intake by decreasing the absorption of carbohydrates and fat, respectively. These products have less toxicity but can cause stomach discomfort. Besides, there is no evidence or proof for the weight-loss effect of these products compared with placebo.

The body's metabolism determines the rate of energy consumption. Fast metabolism people can consume more energy compared with slower ones. Metabolism boosters reduce body weight by speeding up the body's calorie-burning furnace (*52*). Caffeine, ephedra (ephedrine), green tea, and cocoa are among this type of weight-loss products. However, the safety of metabolism boosters is uncertain and commodities on the market usually contain an excessive quantity of doping products, leading to serious side effects.

Calcium, conjugated linoleic acid, and chromium picolinate can change the ratio of fat tissue to muscle tissue in the body, and namely reduce fat and increase muscle (*53*). However, the weight loss effect of these products is insignificant with an uncertain mechanism. Moreover, relative high toxicity restrains their application.

As undigested carbohydrate, dietary fiber can be used as a physiological barrier to interfere with energy intake by replacing the available nutrients to promote weight reduction (*54*). Fiber reduces the absorption efficiency of the intestine. Dietary fiber can increase anaerobic microorganisms' reproduction, stimulate intestinal peristalsis, accelerate the discharge of food residues and reduce nutrient digestion and absorption. Further, fibers need more chewing action, which can limit food intake and promote gastric and saliva secretion, causing gastric distension and increasing satiety. Although inadequate dietary fiber intake can cause many diseases, excessive dietary fiber will affect the absorption of nutrients, resulting in malnutrition.

7. The history of anti-obesity drugs

Obesity is one of the world's most important public health problems, but the approved anti-obesity drugs are extremely limited. Currently, only two types of anti-obesity drugs for long term weight loss are on the market, pancreatic lipase inhibitors and central nervous system appetite suppressants. Those that can increase energy consumption and metabolism were withdrawn due to side effects. Until now, there are five drugs (orlistat, phentermine/topiramate, lorcaserin, naltrexone/bupropion and liraglutide) approved for long-term use and four sympathomimetic drugs approved for short-term treatment of obesity by the US FDA.

Medical treatment of obesity can be traced to the late 19th and early 20th century (*55*). Between 1887 and 1940 thyroid hormone, dinitrophenol and amphetamine were used to treat obesity. All of them were finally stopped due to side effects. Neuropathy and cataracts induced by dinitrophenol and trityl alcohol were named as one of the disasters caused by medicine in the 20th century (*56*). In the early 1950s, amphetamine and its congener methamphetamine, became widely abused street drugs. The side effects and addictive effect of them lead to the search for safer alternatives. Serotonergic agents like fenfluramine opened a new area of anti-obesity drugs, although the side effects like primary pulmonary hypertension lead to withdrawal later (*57*). Combination therapy for treatment of obesity was popular between 1973 and 1996, and one of the most popular combination drugs was d,l-fenfluramine and phentermine. However, they were removed from the market worldwide in 1997 because more than 30% of patients have the potential to develop valvular heart disease (*58*). A number of nervous system appetite suppressants were developed after 1996, but only a few approved by the FDA to treat obesity. The mechanism of these drugs were inhibiting monoamine action and modulating neuropeptides. However, nearly all of them were withdrawn from the market several years later. In 2001, the appetite suppressant phenylpropanolamine (PPA) was withdrawn from the market due to serious consequences like hemorrhagic stroke (*59*). In 2003, ephedrine was removed from the market because of heart disease and stroke (*60*). In 2009, rimonabant was withdrawn for enhancing suicidal tendency (*61*). Sibutramine is also a central appetite inhibitor, which inhibits norepinephrine and serotonin reuptake, leading to satiety and reducing appetite. After its approval by the US FDA, similar products swept the world, and became the gold standard for anti-obesity drugs. However, in 2010, it was withdrawn because of the risk of cardiovascular disease and stroke (*62*). Most recently, in early 2011, a pharmaceutical scandal in France shocked the world. The country's pharmaceutical giant Servier's anti-obesity drug Mediator lead to the death of hundreds of people because its main component benfluorex causes valvular side effects and death (*63*). Thus, since approved in 1999, lipases inhibitor orlistat (tetrahydrolipstatin) has long been the only drug available on the market (*64*).

The fact that obesity is increasingly more serious and treatment is extremely limited led to the development of new drugs and re-combination of old drugs (Table 2). To handle this global problem, FDA approved phentermine/topiramate (*65*) and lorcaserin (*66*) in 2012, then naltrexone/bupropion (*67*) and liraglutide (*68*) in 2014. However, to date, the anti-obesity drug market has one and only OTC drug, orlistat (*69*).

7.1. *Pancreatic lipase inhibitor approved by FDA for long-term use: Orlistat (marketed by prescription as Xenical and OTC as Alli)*

As the only long term used drug approved worldwide, orlistat was approved by FDA in 1999. It has long been the only long term used weight-loss medicine on the market until 2012. It is a potent long-acting gastrointestinal lipase inhibitor, directly blocking the absorption of fat (*70*). Serval long term clinical trials of orlistat have been published. Orlistat at a therapeutic

Table 2. Currently approved anti-obesity drugs

Name	Mechanism of Action	Average weight lost at 1 year (kg) *vs.* for placebo	Percentage of patients achieving > 5% loss of body weight at 1 year *vs.* for placebo	Safety warning	Contraindications
Orlistat	Pancreatic lipase inhibitor	10.3 kg	68.50%	Cyclosporine exposure, rare liver failure, concomitant	Chronic malabsorption, gall bladder disease
Lorcaserin	5-HT2C agonist	5.8 kg	47.50%	Serotonin syndrome, valvular heart disease, cognitive impairment, depression, hypoglycemia, priapism	MAOIs, use with extreme caution with serotonergic drugs (SSRIs, SNRIs), pregnancy
Phentermine/ topiramate	Sympathomimetic Anticonvulsant (GABA receptor modulation, carbonic anhydrase inhibition, glutamate antagonism)	8.1 kg (7.5/46 mg) 10.2 kg (15/92 mg)	62% (7.5/46 mg) 70% (7.5/46 mg)	Fetal toxicity; acute myopia, cognitive dysfunction, metabolic acidosis,	Glaucoma, hyperthyroidism, MAOIs, pregnancy
Naltrexone/ bupropion	Opioid receptor antagonist dopamine reuptake inhibitor	6.1 kg (360/32 mg)	39%	Boxed waning: suicidality; Warning: BP, HR, seizure risk, glaucoma, hepatotoxicity	Seizure disorder, uncontrolled HTN, chronic opioid use, MAOIs, pregnancy
Liraglutide 3.0 mg	GLP-1 receptor agonist	7.4% (*vs*. 3.0% for placebo)	62.3% (*vs*. 34.4% for placebo)	Boxed warning: thyroid c-cell tumorsin rodents. Warnings: acute pancreatitis, acute gallbladder disease, serious hypoglycemia if used with insulin secretagogue, heart rate increase,use caution in renal impairment; hypersensitivity reactions can occur, monitor for depression or suicidal	Patients with a personal or family history of medullary thyroid carcinoma or multiple endocrine neoplasia, pregnancy

dose (120mg, 3 times per day) will reduce fat absorption up to 30%. Patients in a one year treatment can lose 9% of their body weight by using orlistat, while the placebo group only lost 5.5%. It can also reduce waist, blood pressure, fasting glucose, BMI, glycated hemoglobin concentration in diabetic patients, as well as decrease low-density lipoprotein cholesterol (LDL-C), total cholesterol and increase high-density lipoprotein cholesterol (HDL-C) (*71*).

Orlistat can't be transfered into the bloodstream, so the side effects mainly involved triglyceride digestive dysfunction in the intestine, including fat diarrhea, abdominal distension, fecal urgency, fecal incontinence and oily stools (*72*). The incidence rate of these side effects can be 15% to 30%, and some patients considered this unacceptable. Certain researchers even consider the anti-obesity effect of orlistat mainly comes from the "punishment" of a high-fat diet that can lead to these embarrassments, so people will consciously decrease fat absorption to avoid them. Studies have shown that few people can stick to the treatment longer than 1 year (less than 10%), let alone 2 years (less than 2%). Further, absorption of fat soluble vitamins can be impaired by orlistat, so patients should take multivitamins with more than a 2 hour interval. Moreover, patients treated with orlistat may develop gall bladder disease (> 2%) and it can influence the absorption of cyclosporine. Very few cases of liver failure were reported recently.

Cetilistat is a novel, orally active, gastrointestinal and pancreatic lipase inhibitor developed by Takeda and approved by Japanese Ministry of Labor Health and Welfare (MHLW) as a drug for treatment of obese patients having both type 2 diabetes and dyslipidemia (*73*). Cetilistat acts similarly as orlistat with relatively mild side effects. Adverse events and discontinuation rates with cetilistat are less common than with orlistat.

7.2. *Serotinin-2C receptor agonist approved by FDA for long-term use: Lorcaserin (marketed as Belviq)*

In 2012, FDA approved a long-term medication for obesity, lorcaserin. It is a highly selective serotonin 2c receptors (5HT-2C) agonist that reduces appetite and increase satiety by binding to the 5HT-2C receptors on anorexigenic POMC neurons in the hypothalamus (*74*). Some removed anti-obesity drugs such as fenfluramine

and dexfenfluramine, also act on 5-HT receptors but increased the risk of serotonin-associated cardiac valvular disease by activating the 5HT-2B receptor (*75*). As a highly selective 5HT-2C agonist, the cardiac valvular effects of lorcaserin may not be serious (long-term data was asked for by FDA).

Three randomized, placebo-controlled trials of locraserin have been reported. Two of them were in nondiabetic patients (BLOOM29 (N=3182; 50% attrition) and BLOSSOM30 (N=4004; 45% attrition)) and one was in adults with type 2 diabetes (BLOOM-DM31 (N=603; 34% attrition)). It shows that compared with placebo, lorcaserin can cause decrease of more body weight, approximately 3.2 kg (≈3.2%of initial body weight) (*76*). Although the weight lost is modest, when it comes to the weight lost of at least 5% standard, patients treated with lorcaserin 10mg twice daily gave better data than with placebo (BLOOM (47% *vs.* 20%), BLOSSOM (47% *vs*. 25%), BLOOM-DM (37% *vs*. 16%)), and the weight lost of at least 10% standard shows the same results (BLOOM (23% *vs*. 8%), BLOSSOM(23% *vs*. 10%), BLOOM-DM(16% *vs*. 4%)). The only study involved where patients took lorcaserin for 2 years shows that an average weight loss of 5.6 kg, compared with 2.4 kg in the placebo group. Using locraserin can also decrease blood pressure, triglycerides, total cholesterol and low-density lipoprotein cholesterol. For diabetic patients, lorcaserin treatment can reduce body weight and improve glycated hemoglobin concentrations.

As one of the central appetite suppressants, lorcaserin is relatively well-tolerated. Common side effects of locraserin were headache, dizziness, nausea, dry mouth, constipation and fatigue (*77*). However, selective serotonin reuptake inhibitors (SSRIs) or monoamine oxidase inhibitors (MAOIs) should not be used with locraserin to avoid the risk of serotonin syndrome. Warnings of valvular heart disease and hypoglycemia are on the drug label. Last but not the least, like all the other weight loss medications, lorcaserin should be avoided in pregnancy.

7.3. *Combination of phentermine-topiramate approved by FDA for long-term use: Phentermine/Topiramate ER (marketed as Qsymia)*

The first FDA approved long-term anti-obesity combination drug was an extended release (ER) combination of phentermine and topiramate (marketed as Qsymia) in 2012 (*78*). Phentermine is an adrenergic agonist that reduces weight by activating the sympathetic nervous system and releasing endorphins to reduce energy intake and increase expenditure. Topiramate was approved by FDA to treat epilepsy and migraine prophylaxis. It has the effect of reducing weight through promoting taste aversion and reducing caloric intake. Combining these two with lower doses, at starting dose phentermine 3.75 mg and topiramate 23 mg, a recommended dose 7.5 mg and 46 mg respectively, and full dose 15 mg and 92 mg respectively, can reduce side effects and obtain weight loss results.

Three essential clinical trials were carried out (EQUIP, CONQUER and SEQUEL) (*79*). Treatment with Qsymia 56 weeks can obtain percent weight loss of approximately 10.6% (15/92 mg), 8.4% (7.5/46 mg,), and 5.1% (3.75/23 mg), respectively ($p < 0.0001$). 2 years study (SEQUEL) shows 9.3% (7.5/46mg) and 10.5% (15/92 mg) weight loss from baseline were sustained ($p < 0.0001$). Qsymia treatment can also reduce fasting triglycerides, fasting glucoses and waist circumference in obese patients.

Using a lower dose of these two drugs minimizes risks and adverse effects. The most common side effects of Qsymia were dizziness, paraesthesias, insomnia, dysgeusia, dry mouth and constipation. Like the other than-orexiants or nonselective monoamine oxidase inhibitors, Qsymia may induce the potential risk of cardiovascular and central nervous system effects (*80*). Besides, Qsymia may increase the risk of oral clefts and other craniofacial defects, and thus it should be avoided during pregnancy and lactation.

7.4. *Combination of Naltrexone and Bupropion approved by FDA for long-term use: Naltrexone SR/Bupropion SR (marketed as Contrave)*

Contrave is an extended-release tablet combining an opioid receptor inhibitor (naltrexone) and a dopamine and norepinephrine reuptake antagonist (bupropion) (*81*). It is the fourth long-term weight management medication approved by US FDA, in September 2014. Bupropion has been approved to treat depression and smoking cessation. Bupropion reduces weight by inhibiting reuptake of dopamine and norepinephrine to decrease the food activated reward system. Naltrexone has been approved to treat opioid and alcohol dependence and inhibiting opioid receptors may slow weight gain.

Four unique phase 3 studies of Contrave, all named as CONTRAVE Obesity Research (COR), involving approximately 4500 overweight and obese participants have proved efficacy and safety (*82*). COR-I trial shows that the mean change in body weight was 25.4% in 360/32 mg Contrave group, while 21.3% in the placebo group. As to clinically significance of at least 5% reduction in body weight, 42% patients in Contrave group and 17% in placebo group met this standard. In the COR-Diabetes trial, 44.5% in Contrave group and 18.9% in placebo group met the at least 5% reduction in body weight standard ($p < 0.001$). Contrave can also reduce HbA1c (0.6% *vs*. 0.1% in placebo group) and reduce waist circumference, visceral fat, triglycerides and increase HDL cholesterol.

For bupropion, the safety concerns are hypertension, depression and seizures, and for naltrexone, opioid

overuse and acute opioid withdrawal should be considered (*83*). On the label, Contrave warns the increased risk of depression and suicidal behavior, which is the side effect of bupropion alone, but not shown in the clinical trials of the combination. Contrave can't be used in patients with uncontrolled high blood pressure because of the potential of raising blood pressure and heart rate. Seizure patients and those already taking opioids should avoid using Contrave

7.5. *GLP-1 receptor agonist approved by FDA for long term use: Liraglutide 3.0 mg (marketed as Saxenda)*

It has long been considered that analogs of naturally occurring gut hormones (GLP-1, oxyntomodulin, PYY, ghrelin, *et al*.) engaged in energy balance regulation may represent a specific and low side-effect approach in the treatment of obesity. Liraglutide is a GLP-1 receptor agonist that has 97% homology to native GLP-1. After approval by US FDA to treat type 2 diabetes at a 1.5 mg dosage in 2010, the 3.0 mg dosage of liraglutide (marked name Saxenda) was approved to treat obesity in December 2014 (*84*).

Phase III studies have shown that compared with placebo and cognitive behavioral intervention, Saxenda treatment can achieve more weight loss, in the range of 26% to 28%. Data confirm that after using Saxenda, patients have shown improvements in systolic and diastolic blood pressure, LDL and triglycerides reduction, HDL cholesterol increasing and waist circumference reduction (*85*). Besides, Saxenda can improve glycemic control in a weight loss independent manor.

As to the side effects, some patients have shown transient nausea and vomiting. Of note is that Saxenda can increase heart rate slightly, which is opposed by its cardioprotective properties. A black box warning of Saxenda said it may increase the risk of thyroid C-cell tumors because Saxenda causes C-cell tumors in rodents but not in humans. Patients with a personal or family history of Multiple Endocrine Neoplasia or medullary thyroid carcinoma should avoid liraglutide for safety concerns. As with all the other weight loss drugs, Saxenda is contraindicated in pregnancy or hypersensitivity patients. Clinical trials have shown the potential risks of mild or moderate pancreatitis, thus the drug should be stopped if acute pancreatitis is suspected (*86*). Phase 3 studies also report cholecystitis and cholelithiasis, but whether it was caused by the drug or weight loss is uncertain.

7.6. *Noradrenergic drugs approved for short-term use*

Lots of sympathomimetic drugs, like diethylpropion, benzphetamine, phentermine and phendimetrazine, have a similar mechanism as norepinephrine and were tested to treat obesity before 1973 (Diethylpropion (1959), Phentermine (1959), Benzphetamine (1960), and Phendimetrazine (1959). These compounds work by stimulating adrenergic neurotransmitter pathways in the brain, however, they have varying degrees of amphetamine-like side effects, including insomnia, nervousness and irritability (*87*). They are approved only for use of less than 12 weeks (short-term use) and have the potential for abuse. There are no studies that support long-term use of these agents and the evidence that weight regain occurs when administration of these drugs is ceased limit the application of them.

8. Conclusion

Obesity has been recognized as a worldwide epidemic of the 21st century. In the past 30 years, obesity increased rapidly and obesity-related diseases surged. It is a complex medical problem with poor pharmacotherapy-based management. The major goal of obesity treatment is to reduce body weight, diminish the risk of weight associated disorders and to prevent regaining the lost weight. Despite the fact that obesity has become the most significant problem worldwide, efficient medication is limited and potential serious side effects associated with these drugs always outweigh the advantages. Bariatric surgery achieves greater and more sustained weight loss than non-surgical management in patients with severe obesity. However, not all patients can accept surgery.

Until now, studies show that the most effective way to prevent overweight and obesity during menopause is to follow a proper diet and do physical activity. That's why lifestyle interventions are required for all treatments. In the foreseeable future, lifestyle changes, like reducing fat intake and regular exercise, are still the most reliable way to lose weight. In order to achieve the desired outcomes, all patients (taking drugs or not) must combine treatment with lifestyle intervention to achieve sustained weight loss.

References

1. Dibaise JK, Foxx-Orenstein AE. Role of the gastroenterologist in managing obesity. Expert Rev Gastroenterol Hepatol. 2013; 7:439-451.
2. Xu W, Zhang H, Paillard-Borg S, Zhu H, Qi X, Rizzuto D. Prevalence of overweight and obesity among Chinese adults: Role of adiposity indicators and age. Obes Facts. 2016; 9:17-28.
3. Nguyen DM, El-Serag HB. The Epidemiology of obesity. Gastroenterol Clin North Am. 2010; 39:1-7.
4. Wilborn C, Beckham J, Campbell B, Harvey T, Galbreath M, La Bounty P, Nassar E, Wismann J, Kreider R. Obesity: Prevalence, theories, medical consequences, management, and research directions. J Int Soc Sports Nutr. 2005; 2:4-31.
5. Haslam DW, James WP. Obesity. Lancet. 2005; 366:1197-1209.
6. Yumuk V, Tsigos C, Fried M, Schindler K, Busetto L, Micic D, Toplak H; Obesity Management Task Force of the European Association for the Study of Obesity.

European guidelines for obesity management in adults. Obes Facts. 2015; 8:402-424.
7. Identification, assessment and management of overweight and obesity in children, young people and adults. NICE clinical guidelines, No. 189. National institute for health and clinical excellence. National Clinical Guideline Centre (UK); London, UK, 2014.
8. Oliveros E, Somers VK, Sochor O, Goel K, Lopez-Jimenez F. The concept of normal weight obesity. Prog Cardiovasc Dis. 2014; 56:426-433.
9. Kelishadi R, Mirmoghtadaee P, Najafi H, Keikha M. Systematic review on the association of abdominal obesity in children and adolescents with cardio-metabolic risk factors. J Res Med Sci. 2015; 20:294-307.
10. Swinburn B, Vandevijvere S, Kraak V, *et.al*. Monitoring and benchmarking government policies and actions to improve the healthiness of food environments: A proposed Government Healthy Food Environment Policy Index. Obes Rev. 2013; 14(Suppl 1):24-37.
11. Apovian CM, Aronne LJ, Bessesen DH, McDonnell ME, Murad MH, Pagotto U, Ryan DH, Still CD; Endocrine Society. Pharmacological management of obesity: An endocrine Society clinical practice guideline. J Clin Endocrinol Metab. 2015; 100:342-362.
12. Goodman C, Anise A. What is known about the effectiveness of economic instruments to reduce consumption of foods high in saturated fats and other energy-dense foods for preventing and treating obesity? Health Evidence Network, World Health Organisation. *http://www.euro.who.int/__data/assets/pdf_file/0010/74467/E88909.pdf* (accessed February 4, 2010).
13. Flier JS. Obesity wars: molecular progress confronts an expanding epidemic. Cell. 2004; 116:337-350.
14. Kim JD, Leyva S, Diano S. Hormonal regulation of the hypothalamic melanocortin system. Front Physiol. 2014; 5:480.
15. Burger KS, Berner LA. A functional neuroimaging review of obesity, appetitive hormones and ingestive behavior. Physiol Behav. 2014; 136:121-127.
16. Berridge KC. 'Liking' and 'wanting' food rewards: Brain substrates and roles in eating disorders. Physiol Behav. 2009; 97: 537-550.
17. Gao XB, Hermes G. Neural plasticity in hypocretin neurons: the basis of hypocretinergic regulation of physiological and behavioral functions in animals. Front Syst Neurosci. 2015; 9:142.
18. De Silva A, Salem V, Matthews PM, Dhillo WS. The use of functional MRI to study appetite control in the CNS. Exp Diabetes Res. 2012; 2012:764017.
19. Cone RD. Anatomy and regulation of the central melanocortin system. Nat Neurosci. 2005; 8:571-578.
20. Lantang AM, Innes BA, Gan EH, Pearce SH, Lash GE. Expression of melanocortin receptors in human endometrium. Hum Reprod. 2015; 30:2404-2410.
21. Jackson DS, Ramachandrappa S, Clark AJ, Chan LF. Melanocortin receptor accessory proteins in adrenal disease and obesity. Front Neurosci. 2015; 9:213.
22. Gregory M, Perez-Tilve D, Nogueiras R, Fang J, Kim JK, Cone RD, Gimble JM, Tschöp MH, Butler AA. The melanocortin-3 receptor is required for entrainment to meal intake. J Neurosci. 2008; 28:12946-12955.
23. Joly-Amado A, Cansell C, Denis RG, Delbes AS, Castel J, Martinez S, Luquet S. The hypothalamic arcuate nucleus and the control of peripheral substrates. Best Pract Res Clin Endocrinol Metab. 2014; 28:725-737.
24. Chambers AP, Sandoval DA, Seeley RJ. Integration of satiety signals by the central nervous system. Curr Biol. 2013; 23:R379-388.
25. Berthoud HR. Metabolic and hedonic drives in the neural control of appetite: Who's the boss? Curr Opin Neurobiol. 2011; 21:888-896.
26. Holzer P, Reichmann F, Farzi A. Neuropeptide Y, peptide YY and pancreatic polypeptide in the gut-brain axis. Neuropeptides. 2012; 46: 261-274. (check to ref No.38)
27. Brown JA, Woodworth HL, Leinninger GM. To ingest or rest? Specialized roles of lateral hypothalamic area neurons in coordinating energy balance. Front Syst Neurosci. 2015; 9:9.
28. Alén F, Ramírez-López MT, Gómez de Heras R, Rodríguez de Fonseca F, Orio L. Cannabinoid receptors and cholecystokinin in feeding inhibition. Vitam Horm. 2013; 92:165-196.
29. Salamone JD, McLaughlin PJ, Sink K, Makriyannis A, Parker LA. Cannabinoid CB1 receptor inverse agonists and neutral antagonists: effects on food intake, food-reinforced behavior and food aversions. Physiol Behav. 2007; 91:383-388.
30. deShazo RD, Hall JE, Skipworth LB. Obesity bias, medical technology, and the hormonal hypothesis: Should we stop demonizing fat people? Am J Med. 2015; 128:456-460.
31. Hong S. Dopamine system: manager of neural pathways. Front Hum Neurosci. 2013; 7:854.
32. Inui A, Asakawa A, Bowers CY, Mantovani G, Laviano A, Meguid MM, Fujimiya M. Ghrelin, appetite, and gastric motility: the emerging role of the stomach as an endocrine organ. FASEB J. 2004; 18:439-456.
33. Blundell JE. Perspective on the central control of appetite. Obesity (Silver Spring). 2006; 14(Suppl 4):160S-163S.
34. Sayegh AI. The role of cholecystokinin receptors in the short-term control of food intake. Prog Mol Biol Transl Sci. 2013; 114:277-316.
35. Camilleri M, Papathanasopoulos A, Odunsi ST. Actions and therapeutic pathways of ghrelin for gastrointestinal disorders. Nat Rev Gastroenterol Hepatol. 2009; 6:343-352.
36. Skibicka KP, Hansson C, Egecioglu E, Dickson SL. Role of ghrelin in food reward: impact of ghrelin on sucrose self-administration and mesolimbic dopamine and acetylcholine receptor gene expression. Addict Biol. 2012; 17:95-107.
37. Sobrino Crespo C, Perianes Cachero A, Puebla Jiménez L, Barrios V, Arilla Ferreiro E. Peptides and Food Intake. Front Endocrinol (Lausanne). 2014; 5:58.
38. Holzer P, Reichmann F, Farzi A. Neuropeptide Y, peptide YY and pancreatic polypeptide in the gut-brain axis. Neuropeptides. 2012; 46:261-274.
39. Merlino DJ, Blomain ES, Aing AS, Waldman SA. Gut-brain endocrine axes in weight regulation and obesity pharmacotherapy. J Clin Med. 2014; 3:763-794.
40. Barrera JG, Sandoval DA, D'Alessio DA, Seeley RJ. GLP-1 and energy balance: an integrated model of short-term and long-term control. Nat Rev Endocrinol. 2011; 7:507-516.
41. Stengel A, Goebel M, Taché Y. Nesfatin-1: A novel inhibitory regulator of food intake and body weight. Obes Rev. 2011; 12:261-271.
42. Woods SC, Lutz TA, Geary N, Langhans W. Pancreatic signals controlling food intake; insulin, glucagon and amylin. Philos Trans R Soc Lond B Biol Sci. 2006;

361:1219-1235.
43. Gerozissis K. Brain insulin and feeding: A bi-directional communication. Eur J Pharmacol. 2004; 490:59-70.
44. Barber TM, Begbie H, Levy J. The incretin pathway as a new therapeutic target for obesity. Maturitas. 2010; 67:197-202.
45. Morrison CD. Leptin signaling in brain: A link between nutrition and cognition? Biochim Biophys Acta. 2009; 1792:401-408.
46. Kanoski SE, Hayes MR, Greenwald HS, Fortin SM, Gianessi CA, Gilbert JR, Grill HJ. Hippocampal leptin signaling reduces food intake and modulates food-related memory processing. Neuropsychopharmacology. 2011; 36:1859-1870.
47. Rasoamanana R, Darcel N, Fromentin G, Tomé D. Nutrient sensing and signalling by the gut. Proc Nutr Soc. 2012; 71:446-455.
48. Mithieux G. Crosstalk between gastrointestinal neurons and the brain in the control of food intake. Best Pract Res Clin Endocrinol Metab. 2014; 28:739-744.
49. Vaughan RA, Conn CA, Mermier CM. Effects of commercially available dietary supplements on resting energy expenditure: A brief report. ISRN Nutr. 2014; 2014:650264.
50. Barrett ML, Udani JK. A proprietary alpha-amylase inhibitor from white bean (Phaseolus vulgaris): A review of clinical studies on weight loss and glycemic control. Nutr J. 2011; 10:24.
51. Jull AB, Ni Mhurchu C, Bennett DA, Dunshea-Mooij CA, Rodgers A. Chitosan for overweight or obesity. Cochrane Database Syst Rev. 2008; 3:CD003892.
52. Manore MM. Dietary supplements for improving body composition and reducing body weight: where is the evidence? Int J Sport Nutr Exerc Metab. 2012; 22:139-154.
53. van Meijl LE, Vrolix R, Mensink RP. Dairy product consumption and the metabolic syndrome. Nutr Res Rev. 2008; 21:148-157.
54. Schrenk D. Dietary fiber, low-molecular-weight food constituents and colo-rectal inflammation in animal models – A review. Mol Nutr Food Res. 2009; 53:1281-1288.
55. Bray GA. Medical treatment of obesity: The past, the present and the future. Best Pract Res Clin Gastroenterol. 2014; 28:665-84.
56. Grundlingh J, Dargan PI, El-Zanfaly M, Wood DM. 2,4-Dinitrophenol (DNP): A weight loss agent with significant acute toxicity and risk of death. J Med Toxicol. 2011; 7:205-212.
57. Surapaneni P, Vinales KL, Najib MQ, Chaliki HP. Valvular heart disease with the use of fenfluramine-phentermine. Tex Heart Inst J. 2011; 38:581-583.
58. Centers for Disease Control and Prevention (CDC). Cardiac valvulopathy associated with exposure to fenfluramine or dexfenfluramine: U.S. Department of Health and Human Services interim public health recommendations, November 1997. MMWR Morb Mortal Wkly Rep. 1997; 46:1061-1066.
59. Food And Drug Administration Public Health Service U S Department Of Health And Human Services. Food and Drug Administration recommends against the continued use of propoxyphene. J Pain Palliat Care Pharmacother. 2011; 25:80-82.
60. Food and Drug Administration, HHS. Final rule declaring dietary supplements containing ephedrine alkaloids adulterated because they present an unreasonable risk. Final rule. Fed Regist. 2004; 69:6787-6854.
61. Leite CE, Mocelin CA, Petersen GO, Leal MB, Thiesen FV. Rimonabant: an antagonist drug of the endocannabinoid system for the treatment of obesity. Pharmacol Rep. 2009; 61:217-224.
62. James WP, Caterson ID, Coutinho W, Finer N, Van Gaal LF, Maggioni AP, Torp-Pedersen C, Sharma AM, Shepherd GM, Rode RA, Renz CL; SCOUT Investigators. Effect of sibutramine on cardiovascular outcomes in overweight and obese subjects. N Engl J Med. 2010; 363:905-917.
63. European Medicines Agency. European Medicines Agency recommends withdrawal of benfluorex from the market in European Union. *http://www.ema.europa.eu/docs/en_GB/document_library/Press_release/2010/01/WC500059714.pdf* (accessed February 4, 2010).
64. Drew BS, Dixon AF, Dixon JB. Obesity management: update on orlistat. Vasc Health Risk Manag. 2007; 3:817-821.
65. "VIVUS, Inc. - Vivus Announces FDA Approval of Once Daily Qsymia™ (Phentermine and Topiramate Extended-release) Capsules CIV". Ir.vivus.com. (accessed June 19, 2014).
66. "DEPARTMENT OF JUSTICE Drug Enforcement Administration 21 CFR Part 1308, Placement of Lorcaserin into Schedule IV".
67. "FDA approves weight-management drug Contrave" (Press release). FDA. 10 September 2014.
68. FDA Approves Saxenda (liraglutide rDNA origin. injection) for Obesity. Dec 23, 2014.
69. FDA Approves Orlistat for Over-the-Counter Use. February 7, 2007.
70. Heck AM, Yanovski JA, Calis KA. Orlistat, a new lipase inhibitor for the management of obesity. Pharmacotherapy. 2000; 20:270-279.
71. O'Meara S, Riemsma R, Shirran L, Mather L, ter Riet G. A systematic review of the clinical effectiveness of orlistat used for the management of obesity. Obes Rev. 2004; 5:51-68.
72. Halpern B, Halpern A. Safety assessment of FDA-approved (orlistat and lorcaserin) anti-obesity medications. Expert Opin Drug Saf. 2015; 14:305-315.
73. Hainer V. Overview of new antiobesity drugs. Expert Opin Pharmacother. 2014; 15:1975-1978.
74. Meltzer HY, Roth BL. Lorcaserin and pimavanserin: emerging selectivity of serotonin receptor subtype-targeted drugs. J Clin Invest. 2013; 123:4986-4991.
75. Rothman RB, Baumann MH. Serotonergic drugs and valvular heart disease. Expert Opin Drug Saf. 2009; 8:317-329.
76. Yanovski SZ, Yanovski JA. Long-term drug treatment for obesity: A systematic and clinical review. JAMA. 2014; 311:74-86.
77. Hess R, Cross LB. The safety and efficacy of lorcaserin in the management of obesity. Postgrad Med. 2013; 125:62-72.
78. Alfaris N, Minnick AM, Hopkins CM, Berkowitz RI, Wadden TA. Combination phentermine and topiramate extended release in the management of obesity. Expert Opin Pharmacother. 2015; 16:1263-1274.
79. Smith SM, Meyer M, Trinkley KE. Phentermine/topiramate for the treatment of obesity. Ann Pharmacother. 2013; 47:340-349.
80. Sweeting AN, Tabet E, Caterson ID, Markovic TP.

Management of obesity and cardiometabolic risk – role of phentermine/extended release topiramate. Diabetes Metab Syndr Obes. 2014; 7:35-44.
81. Christou GA, Kiortsis DN. The efficacy and safety of the naltrexone/bupropion combination for the treatment of obesity: An update. Hormones (Athens). 2015; 14:370-375.
82. Fujioka K. Sustained-release Naltrexone/Bupropion – A Novel Pharmacologic Approach to Obesity and Food Craving. US Endocrinology, 2014; 10:53-58
83. Verpeut JL, Bello NT. Drug safety evaluation of naltrexone/bupropion for the treatment of obesity. Expert Opin Drug Saf. 2014; 13:831-841.
84. Nuffer WA, Trujillo JM. Liraglutide: A new option for the treatment of obesity. Pharmacotherapy. 2015; 35:926-934.
85. Lean ME, Carraro R, Finer N, Hartvig H, Lindegaard ML, Rössner S, Van Gaal L, Astrup A; NN8022-1807 Investigators. Tolerability of nausea and vomiting and associations with weight loss in a randomized trial of liraglutide in obese, non-diabetic adults. Int J Obes (Lond). 2014; 38:689-697.
86. Egan AG, Blind E, Dunder K, de Graeff PA, Hummer BT, Bourcier T, Rosebraugh C. Pancreatic safety of incretin-based drugs – FDA and EMA assessment. N Engl J Med. 2014; 370:794-797.
87. Bray GA. Use and abuse of appetite-suppressant drugs in the treatment of obesity. Ann Intern Med. 1993; 119(7 Pt 2):707-713.

(Received February 4, 2016; Revised March 25, 2016; Accepted April 2, 2016)

Mini-Review

DOI: 10.5582/ddt.2016.01003

Angiogenesis in refractory depression: A possible phenotypic target to avoid the blood brain barrier

Maki K. Yamada*

Isotope Science Center, The University of Tokyo, Tokyo, Japan.

Summary **Major depressive syndrome (so-called depression) is a common but serious mental disease that causes low mood. Most patients are treatable, mainly because of high response rates for medicines such as selective serotonin-reuptake inhibitors (SSRIs). However, there are still a considerable number of patients with refractory or drug-resistant depression. On the other hand, recent findings suggest that angiogenesis, *i.e.*, making new blood vessels, could have an important role in the recovery from depressive disorders, at least in part. It has been reported that the brain capillaries are physiologically capable of undergoing angiogenesis upon stimuli such as exercise and SSRIs seem to accelerate brain angiogenesis. Drugs targeting angiogenesis may possibly be another good concept. In addition, the blood brain barrier (BBB), which is a major obstacle for drug development for the central nervous system, would be circumvented. Here I summarize the reports that relate angiogenesis to a cure for major depression and discuss some of the potential molecular targets.**

Keywords: BBB, VEGF, pericyte, vasculogenesis, SERT

1. Introduction

The brain is filled with blood vessels. The mean distance from the center of the neuronal somata to the closest microvessel is reported to be 15 microns (*1*) and is of a certain variety (*2,3*). In the brain, angiogenesis, the process involving the budding and stretching of new brain capillaries from existing vasculatures, has been reported to be induced by physical exercise (*4-7*) in addition to normal growth in infancy (*8*).

Major depressive syndrome (so-called depression) is a common (~10%) and serious mental disease with long episodes of low mood, that can sometimes lead to suicide. The response rate for anti-depressants such as selective serotonin-reuptake inhibitors (SSRIs) is relatively high, and, together with good counseling therapy and changing the stressful environment, most patients recover well. However, there are a considerable number of drug-resistant patients. Most refractory patients stay socially inactive, and their life is heavily dependent on the support of families and social welfare systems. Thus, 'drug discoveries and therapies' are eagerly awaited.

Recent findings suggest that brain angiogenesis may be important in the recovery from depressive disorders, at least in some cases. Thus, here I will summarize these reports and focus on efficient cures.

1.1. *Mechanism of angiogenesis*

Angiogenesis is physiologically necessary for wound healing. It also has been highly studied in cancer development, and anti-angiogenic drugs have become good anti-cancer agents. Metabolically active cells such as growing tumor cells and working neurons should consume oxygen and enter an ischemic state. Ischemia is a trigger for cells to express then secrete an angiogenic factor, vascular endothelial growth factor (VEGF) (*6*), and this facilitates the growth and motility of endothelial cells for making new vessels. Since nutrients and oxygen supplied by vasculature are critical for neuronal function, angiogenesis is thought to work as the adaptive 'supply on demand system'.

Angiopoietin 2 (Ang-2) secreted by ischemic cells works as the first signal to make new vasculatures. Upon stimulation, the endothelial cells (or another

Released online in J-STAGE as advance publication February 19, 2016.

**Address correspondence to:*
Dr. Maki K. Yamada, Isotope Science Center, The University of Tokyo, 2-11-16, Yayoi, Bunkyo-ku, Tokyo, 113-0032, Japan.
E-mail: makiky-tky@umin.ac.jp

vessel cell, pericytes) secrete a protease and move inside, then, upon further stimulation by VEGF, grow then elongate as a tubule of the immature vessels. A brain capillary has a single endothelial layer folded by pericytes, then these pericytes follow to complete the structure, while pericytes may go faster (*9*).

The two secreted factors can dominate angiogenesis. Actually, mice treated with a VEGF protein infusion plus Ang-2 expression by a virus vector had significantly increased microvessels in their brains (*10*), while the mechanism to protect fragile newborns during angiogenesis from blood pressure is yet to be determined (Figure 1).

1.2. *SSRI*

SSRIs, the selective serotonin-reuptake inhibitors such as Fluoxetine and Paloxetine, are the major antidepressants currently used. Actually, whether patients show any signs of recovery by taking these drugs is the main branch point to 'drug-resistance'. The SSRIs inhibit the action of a molecule called serotonin transporter (SERT) and increase local concentrations of serotonin. Serotonin (Ser) is an amino acid that can be synthesized from tryptophan in serotonergic neurons in the brain, and works as a neurotransmitter/neuromodulator that regulates mood. SERT at the presynaptic terminal of neurons reuptake the released Ser, thus the SSRI enhances the action of Ser through inhibiting SERT and increasing Ser concentration in the synapses.

However, SSRIs are mysterious drugs. Their effects as antidepressants take a few to several weeks to become evident, even though the action on the SERT molecule is rapid. Furthermore, the mechanism of how SSRIs go through the blood brain barrier into the brain is not well known.

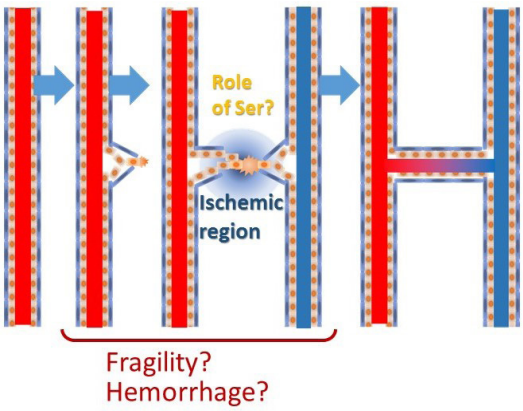

Figure 1. Diagram of the mechanism of angiogenesis in general. Blue arrow indicates progression of angiogenesis steps. Angiogenesis was induced by ischemia around the vessel. It evokes secretion of protease from the vessel cells, then the some of endothelial cells move into the tissue. They form tubules and grows till the tip cells from artery and vein meet. The detailed feature in the brain including the mechanism to protect fragile newborn vessels (brancket) from blood circulation is not well understood. Especially, in the brain, there should be multiple mechanisms for that, because the risk of hemorrhage (bleeding in the brain) should be avoided. SERT, the target of SSRI, might have some roles because it is expressed in the smallest of brain capillaries (*13*) and Ser can act as a vasoconstrictor (*12*).

Ser has many other functions in the body. It accelerates angiogenesis *in-vivo via* a receptor on endothelial cells (*11*). The intriguing thing is its role in hemostasis as a vasoconstrictor (*12*). Ser is released from activated platelets. Vasoconstriction activity stops or slows blood flow by this activity and generally protects injured vessel walls. SERT, the target of SSRIs has been found in the smallest of brain capillaries (*13*), while the role at the loci is not well understood. There is a possibility that Ser increased by SERT contracts the vessel to protect the site of angiogenesis in progress.

2. Angiogenesis might act as a cure for depression *via* neurogenesis

The hippocampal dentate gyrus is a particular place where many neuronal progenitors reside, and they keep on generating new neurons even in adults. This generation of neurons is called neurogenesis, and this has attracted attention as the target for SSRIs, because chronic administration of antidepressants up-regulates neurogenesis (*14*) and this cellular response is required for the effects of the drugs (*15*). I studied circuit generation by newly-born hippocampal granule cells (*16*) and considered that neurogenesis promotes the formation of novel neuronal circuits. The newly formed circuits would provide a curative effect for depression probably by supporting a different way of thinking.

On the other hand, there are some reports describing that angiogenesis acts on the SSRI-induced upregulation of neurogenesis (*17-19*). If this is true, angiogenesis may be a more promising phenotypic target for future drugs, because blood vessels are on the accessible side of the blood brain barrier (BBB). In addition, the action of angiogenesis will widely affect whole regions of the brain.

Another factor in the support for the role of neurogenesis in anti-depressive effects is in the treatment for drug-resistant depression, electric stimulation which stimulated neurogenesis. Also in this case, angiogenesis is accelerated (*20*).

Physical exercise has been known to have good effects on mental health (*22*), and it also has anti-depressant effects. At least in animals, angiogenesis seems to be indispensable, because an injection of an inhibitor for angiogenesis, not directly of neurogenesis, halted neurogenesis and deteriorated the action of exercise (*5*).

3. Relationship of angiogenesis-deficiency and refractive depression

The patients' status related to angiogenesis is summarized as follows.

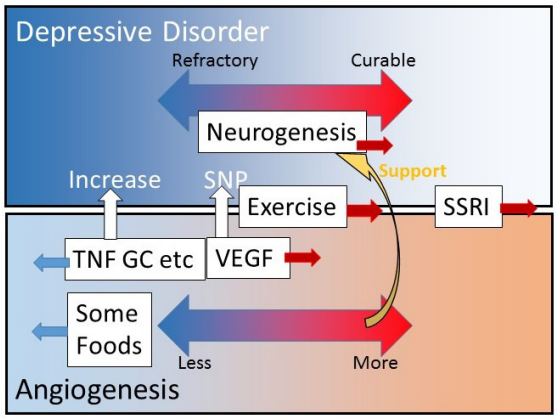

Figure 2. Accordance in action of factors on angiogenesis and on depressive disorder. There seems to be a good accordance in factors for angiogenesis and cure for depressive disorder, as if angiogenesis accompanies with the remedy of this disease. In this figure, red and blue arrows show the orientation of the effect of boxed factors for the included phenotypes.

3.1. *Angiogenesis deficiency in patients suffering from depression*

One of the signs of angiogenesis is said to be circulating endothelial progenitor cells (EPC). There is a report on decreased numbers of circulating EPCs in patients with a current episode of major depression with a significant inverse relationship between EPC levels and the severity of their depressive symptoms (*21*). A group of patients with major depressive disorders in general had a significantly higher VEGF level in serum concentration, while patients who had attempted suicide had a lower VEGF serum level compared to patients who had not attempted suicide (*22*). Further correlation analysis would be required for the patients. The accumulation of data on VEGF-related drugs may become clues in linking angiogenesis to the disease.

3.2. *Genetically different VEGF in a portion of the patients*

There are reports on genetics. One is VEGF polymorphism associated with treatment-resistant depression (*23,24*).

The other is on VEGF receptor gene polymorphism. It is in patients with a recurrent depressive disorder, not exactly matched for the refractory one, that distribution of the polymorphism differs significantly in patients compared to that of healthy subjects (*7*).

3.3. *Increased anti-angiogenic factors in refractory depression*

As above, genetically different patients would show insufficient angiogenesis that may lead to drug resistance. In addition, there may be a possible contribution of anti-angiogenic factors. Corticosterone or glucocorticoid (GC) is the so-called 'stress hormone', and is released from the adrenal gland upon mental and physical stress. It is reported to inhibit angiogenesis induced by electric shocks (*25*) and to damage pericytes forming brain capillaries (*26*).

Post stroke depression is a type of refractory depression seen in 20-60% of survivors of brain stroke. In these patients having depressive symptoms, serum interleukin (IL)-18 on day 7 was independently associated with incident post-stroke depression (*27*). IL-18 has been known to suppress angiogenesis (*28*), probably *via* interferon-γ (*29*). There is also a report on tumor necrosis factor (TNF)-alpha, showing a significant inverse correlation between TNF-alpha and EPC levels (*21*).

If there are obstacles for angiogenesis in the patients of refractory depression, removal of them might be a good concept for drug-development. Since anti TNF-alpha drugs are already on the market, research on the patients' mood may reveal a causal relationship.

4. Angiogenic regulators that might be future clues for remedy

As endogenous angiogenic regulators, the major ones are angiopoietin 2 and VEGF (*10*). Leptin, a satiety factor that supresses appetite, also works as an angiogenic factor (*30,31*), while serum levels of leptin were independently associated with post-stroke depression (*32*). Brain-specific angiogenesis inhibitor 2 (BAI2), that correlate with anti-angiogenesis in the brain, might be a candidate target protein, because BAI2 gene disruption in deficient mice showed significant antidepressant-like behavior (*33*).

In foods, there are reports of anti-angiogenic materials. For example, resveratrol in wine (*34,35*) curcumin in turmeric (*36,37*) and 6-gingerol in ginger (*38,39*) have all been reported to inhibit angiogenesis, even though they are seemingly good for the body. Ingesting too much of these foods would inhibit angiogenesis and might worsen depressive disorders.

More extensive research on these effectors would provide clues for the remedy of depressive symptoms.

5. Conclusion

There seems to be good reasons to think about angiogenesis as a therapeutic target for refractory depression, because there seems to be an accordance in roles of factors for angiogenesis and for depressive disorders (Figure 2). Extensive research on the above mentioned effectors should be further performed in light of angiogenesis and recovery from depression.

Acknowledgements

This work was supported by the Ministry of Education, Science, Sports and Culture, Grant-in Aid for Scientific

Research (A, 26250041) and JST Core Research for Evolutionary Science and Technology.

References

1. Tsai P S, Kaufhold J P, Blinder P, Friedman B, Drew P J, Karten H J, Lyden P D, Kleinfeld D. Correlations of neuronal and microvascular densities in murine cortex revealed by direct counting and colocalization of nuclei and vessels. J Neurosci. 2009; 29:14553-14570.
2. Wu J, Guo C, Chen S, Jiang T, He Y, Ding W, Yang Z, Luo Q, Gong H. Direct 3D Analyses Reveal Barrel-Specific Vascular Distribution and Cross-Barrel Branching in the Mouse Barrel Cortex. Cerebral cortex. 2016; 26:23-31.
3. Wu J, He Y, Yang Z, Guo C, Luo Q, Zhou W, Chen S, Li A, Xiong B, Jiang T, Gong H. 3D BrainCV: Simultaneous visualization and analysis of cells and capillaries in a whole mouse brain with one-micron voxel resolution. NeuroImage. 2014; 87:199-208.
4. Kerr A L, Steuer E L, Pochtarev V, Swain R A. Angiogenesis but not neurogenesis is critical for normal learning and memory acquisition. Neuroscience. 2010; 171:214-226.
5. Kiuchi T, Lee H, Mikami T. Regular exercise cures depression-like behavior *via* VEGF-Flk-1 signaling in chronically stressed mice. Neuroscience. 2012; 207:208-217.
6. Black J E, Isaacs K R, Anderson B J, Alcantara A A, Greenough W T. Learning causes synaptogenesis, whereas motor activity causes angiogenesis, in cerebellar cortex of adult rats. Proceedings of the National Academy of Sciences of the United States of America. 1990; 87:5568-5572.
7. Galecki P, Orzechowska A, Berent D, Talarowska M, Bobinska K, Galecka E, Lewinski A, Maes M, Szemraj J. Vascular endothelial growth factor receptor 2 gene (KDR) polymorphisms and expression levels in depressive disorder. J Affect Disord. 2013; 147:144-149.
8. Risser L, Plouraboue F, Cloetens P, Fonta C. A 3D-investigation shows that angiogenesis in primate cerebral cortex mainly occurs at capillary level. International journal of developmental neuroscience : The official journal of the International Society for Developmental Neuroscience. 2009; 27:185-196.
9. Gerhardt H, Betsholtz C. Endothelial-pericyte interactions in angiogenesis. Cell and tissue research. 2003; 314:15-23.
10. Zhu Y, Lee C, Shen F, Du R, Young W L, Yang G Y. Angiopoietin-2 facilitates vascular endothelial growth factor-induced angiogenesis in the mature mouse brain. Stroke; a journal of cerebral circulation. 2005; 36:1533-1537.
11. Profirovic J, Strekalova E, Urao N, Krbanjevic A, Andreeva A V, Varadarajan S, Fukai T, Hen R, Ushio-Fukai M, Voyno-Yasenetskaya T A. A novel regulator of angiogenesis in endothelial cells: 5-hydroxytriptamine 4 receptor. Angiogenesis. 2013; 16:15-28.
12. Machida T, Iizuka K, Hirafuji M. 5-hydroxytryptamine and its receptors in systemic vascular walls. Biol Pharm Bull. 2013; 36:1416-1419.
13. Young L W, Darios E S, Watts S W. An immunohistochemical analysis of SERT in the blood-brain barrier of the male rat brain. Histochem Cell Biol. 2015; 144:321-329.
14. Duman R S, Nakagawa S, Malberg J. Regulation of adult neurogenesis by antidepressant treatment. Neuropsychopharmacology : Official publication of the American College of Neuropsychopharmacology. 2001; 25:836-844.
15. Schmidt H D, Duman R S. The role of neurotrophic factors in adult hippocampal neurogenesis, antidepressant treatments and animal models of depressive-like behavior. Behav Pharmacol. 2007; 18:391-418.
16. Tamura M, Tamura N, Ikeda T, Koyama R, Ikegaya Y, Matsuki N, Yamada M K. Influence of brain-derived neurotrophic factor on pathfinding of dentate granule cell axons, the hippocampal mossy fibers. Molecular brain. 2009; 2:2.
17. Newton S S, Duman R S. Regulation of neurogenesis and angiogenesis in depression. Curr Neurovasc Res. 2004; 1:261-267.
18. Nakafuku M, Grande A. Neurogenesis in the Damaged Mammalian Brain. Comprehensive Developmental Neuroscience: Patterning and Cell Type Specification in the Developing CNS and PNS. Elsevier; 2013, pp. 552-608.
19. Boldrini M, Hen R, Underwood M D, Rosoklija G B, Dwork A J, Mann J J, Arango V. Hippocampal angiogenesis and progenitor cell proliferation are increased with antidepressant use in major depression. Biological psychiatry. 2012; 72:562-571.
20. Hellsten J, West M J, Arvidsson A, Ekstrand J, Jansson L, Wennstrom M, Tingstrom A. Electroconvulsive seizures induce angiogenesis in adult rat hippocampus. Biological psychiatry. 2005; 58:871-878.
21. Dome P, Teleki Z, Rihmer Z, Peter L, Dobos J, Kenessey I, Tovari J, Timar J, Paku S, Kovacs G, Dome B. Circulating endothelial progenitor cells and depression: A possible novel link between heart and soul. Mol Psychiatry. 2009; 14:523-531.
22. Berent D, Macander M, Szemraj J, Orzechowska A, Galecki P. Vascular endothelial growth factor A gene expression level is higher in patients with major depressive disorder and not affected by cigarette smoking, hyperlipidemia or treatment with statins. Acta Neurobiol Exp (Wars). 2014; 74:82-90.
23. Viikki M, Anttila S, Kampman O, Illi A, Huuhka M, Setala-Soikkeli E, Mononen N, Lehtimaki T, Leinonen E. Vascular endothelial growth factor (VEGF) polymorphism is associated with treatment resistant depression. Neurosci Lett. 2010; 477:105-108.
24. Galecki P, Galecka E, Maes M, Orzechowska A, Berent D, Talarowska M, Bobinska K, Lewinski A, Bienkiewicz M, Szemraj J. Vascular endothelial growth factor gene (VEGFA) polymorphisms may serve as prognostic factors for recurrent depressive disorder development. Progress in neuro-psychopharmacology & biological psychiatry. 2013; 45:117-124.
25. Ekstrand J, Hellsten J, Wennstrom M, Tingstrom A. Differential inhibition of neurogenesis and angiogenesis by corticosterone in rats stimulated with electroconvulsive seizures. Progress in neuro-psychopharmacology & biological psychiatry. 2008; 32:1466-1472.
26. Katychev A, Wang X, Duffy A, Dore-Duffy P. Glucocorticoid-induced apoptosis in CNS microvascular pericytes. Developmental neuroscience. 2003; 25:436-446.
27. Yang L, Zhang Z, Sun D, Xu Z, Zhang X, Li L. The serum interleukin-18 is a potential marker for development of post-stroke depression. Neurol Res. 2010; 32:340-346.

28. Cao R, Farnebo J, Kurimoto M, Cao Y. Interleukin-18 acts as an angiogenesis and tumor suppressor. FASEB J. 1999; 13:2195-2202.
29. Deng J, Liu X, Rong L, Ni C, Li X, Yang W, Lu Y, Yan X, Qin C, Zhang L, Qin Z. IFNgamma-responsiveness of endothelial cells leads to efficient angiostasis in tumours involving down-regulation of Dll4. J Pathol. 2014; 233:170-182.
30. Cao R, Brakenhielm E, Wahlestedt C, Thyberg J, Cao Y. Leptin induces vascular permeability and synergistically stimulates angiogenesis with FGF-2 and VEGF. Proceedings of the National Academy of Sciences of the United States of America. 2001; 98:6390-6395.
31. Bouloumie A, Drexler H C, Lafontan M, Busse R. Leptin, the product of Ob gene, promotes angiogenesis. Circulation research. 1998; 83:1059-1066.
32. Jimenez I, Sobrino T, Rodriguez-Yanez M, Pouso M, Cristobo I, Sabucedo M, Blanco M, Castellanos M, Leira R, Castillo J. High serum levels of leptin are associated with post-stroke depression. Psychological medicine. 2009; 39:1201-1209.
33. Okajima D, Kudo G, Yokota H. Antidepressant-like behavior in brain-specific angiogenesis inhibitor 2-deficient mice. J Physiol Sci. 2011; 61:47-54.
34. Chen P L, Easton A S. Anti-angiogenic effects of resveratrol on cerebral angiogenesis. Curr Neurovasc Res. 2011; 8:14-24.
35. Brakenhielm E, Cao R, Cao Y. Suppression of angiogenesis, tumor growth, and wound healing by resveratrol, a natural compound in red wine and grapes. FASEB J. 2001; 15:1798-1800.
36. Arbiser J L, Klauber N, Rohan R, Van Leeuwen R, Huang M T, Fisher C, Flynn E, Byers H R. Curcumin is an *in vivo* inhibitor of angiogenesis. Mol Med. 1998; 4:376-383.
37. Wang F, He Z, Dai W, Li Q, Liu X, Zhang Z, Zhai D, Chen J, Chen W. The role of the vascular endothelial growth factor/vascular endothelial growth factor receptors axis mediated angiogenesis in curcumin-loaded nanostructured lipid carriers induced human HepG2 cells apoptosis. J Cancer Res Ther. 2015; 11:597-605.
38. Kim E C, Min J K, Kim T Y, Lee S J, Yang H O, Han S, Kim Y M, Kwon Y G. [6]-Gingerol, a pungent ingredient of ginger, inhibits angiogenesis *in vitro* and *in vivo*. Biochemical and biophysical research communications. 2005; 335:300-308.
39. Brown A C, Shah C, Liu J, Pham J T, Zhang J G, Jadus M R. Ginger's (Zingiber officinale Roscoe) inhibition of rat colonic adenocarcinoma cells proliferation and angiogenesis *in vitro*. Phytother Res. 2009; 23:640-645.

(Received January 4, 2016; Revised February 9, 2016; Accepted February 10, 2016)

Mini-Review

DOI: 10.5582/ddt.2016.01004

A link between vascular damage and cognitive deficits after whole-brain radiation therapy for cancer: A clue to other types of dementia?

Maki K. Yamada*

Isotope Science Center, The University of Tokyo, Tokyo, Japan.

Summary **Whole brain radiation therapy for the treatment of tumors can sometimes cause cognitive impairment. Memory deficits were noted in up to 50% of treated patients over a short period of several months. In addition, an increased rate of dementia in young patients has been noted over the longer term, *i.e.* years. A deficit in neurogenesis after irradiation has been postulated to be the main cause of cognitive decline in patients, but recent data on irradiation therapy for limited parts of the brain appear to indicate other possibilities. Irradiation can directly damage various types of cells other than neuronal stem cells. However, this paper will focus on injury to brain vasculature leading to cognitive decline since vessels represent a better therapeutic target for drug development than other cells in the brain because of the blood-brain barrier.**

Keywords: Irradiation, angiogenesis, memory, learning, cognitive deficits, Alzheimer disease

1. Introduction

Whole brain radiation therapy (WBRT) is commonly used for the treatment of brain tumors and cancers with brain metastasis. Since growing cells such as tumor cells are more sensitive to irradiation than normal cells, irradiation can be used to kill the malignant cells and improve the survival rate in patients with tumors. However, cognitive impairment is a well-documented consequence of WBRT (*1-4*). In addition to acute encephalopathy (*5,6*), memory deficits have been noted in up to 50% of patients undergoing WBRT over a short period of several months. In addition, WBRT is reported to increase the rate of dementia three-fold in younger patients (< 65 years old, up to around 0.2% of irradiated persons) (*7*) and to lower the intelligence quotient (IQ) of children (*8*) over the longer term, *i.e*. years.

A deficit in neurogenesis has been postulated to be the main cause of cognitive decline (*9-11*), but recent data on irradiation therapy (RT) for various parts of the brain appear to indicate the complex causes of cognitive deficits. Analysis indicated that different regions are of varying importance when performing certain cognitive tasks, suggesting that hippocampal neurogenesis alone may be an oversimplification of the brain injury processes occurring after RT (*12*).

Irradiation can directly damage various types of cells other than neuronal stem cells for neurogenesis (*13*), but the current paper will focus on injury to the brain vasculature leading to cognitive decline. This is, at least partially, because vessels represent a better therapeutic target for drug development than other cells in the brain because of the blood-brain barrier.

2. Small blood vessels in the brain

The brain has an elaborate vascular system. Arteries and veins are joined by a fine network of capillaries that are intertwined with the surrounding neuronal architecture (*14,15*). A brain capillary has an endothelial cell layer tightly surrounded by thin pericytes and the diameter is often smaller than 10 micrometers (*16*). Since red blood cells are around 13 micrometers in diameter and monocytes are 22 (*17*), cells shinny through the dilated thin tubules in a physiological state. The mean distance

Released online in J-STAGE as advance publication April 18, 2016.

**Address correspondence to:*
Dr. Maki K. Yamada, Isotope Science Center, The University of Tokyo, 2-11-16, Yayoi, Bunkyo-ku, Tokyo, 113-0032, Japan. (*Present address*: Kagawa School of Pharmaceutical Sciences, Tokushima Bunri University, 1314-1 Shido, Sanuki city Kagawa 769-2193 Japan.)
E-mail: makiky-tky@umin.ac.jp

from the center of the neuronal somata to the closest microvessel is 15 microns (*14*). Neurons need a supply of nutrients and oxygen from vessels and would be affected by any defect in the immediate vasculature.

3. Radiation sensitivity of vascular cells

The endothelial cells of brain capillaries and their surrounding pericytes are known to display certain characteristics. Although these characteristics are not fully understood, studies have described their relationship to radiation.

3.1. *Cell viability*

AA study compared rat primary cerebromicrovascular endothelial cells in culture to neurons, microglia, and astrocytes in terms of their sensitivity to radiation. The endothelial cells had marked sensitivity to radiation (a ~2-fold larger number of dead cells) (*18*).

3.2. *Angiogenesis*

Angiogenesis, *i.e.*, the making of new blood vessels, could play an important role in natural cognition. Physical exercise is known to have beneficial effects on mental health (*19*) to have anti-depressant action (*20*), and on learning ability (*21*). In these instances, angiogenesis seems to be indispensable because injection of angiogenesis inhibitors canceled out the effects of exercise (*20*).

After irradiation, angiogenesis, *i.e*. CD31-positive capillary density, decreases substantially in laboratory mice (*22*) and is accompanied by learning deficits (*23*). Thus, a deficit in angiogenesis may cause cognitive decline. However, this decline might be inevitable for patients who have a tumor since the target for RT is not merely tumor cells but also angiogenesis inside the tumor. Limiting irradiation sites to areas around tumors seems to be the most ideal way to resolve this problem. Bevacizumab (Avastin) and other recent anti-cancer drugs inhibits angiogenesis, so this type of drugs should be used with caution in combination with RT (*6*).

3.3. *Transcriptome profiles*

A study reported on the transcriptome profiles of mouse brain tissue after whole-body irradiation. The study noted that the most altered genes involved ion channels, long-term potentiation, depression, and vascular damage (*22*).

4. Similarity and relationship to forms of senile dementia including Alzheimer's disease

Many possible remedies of irradiation-induced cognitive decline and precautions to limit that decline have been proposed and used (*24,25*) in patients and animals. Two effective remedies were memantine (*26,27*) and donepezil (*28,29*). Both are drugs to treat Alzheimer's disease and both have different targets of action (*30*).

Some recent studies of Alzheimer's disease have suggested that vascular defects in small capillaries may play a central role (*31-34*). In addition, cognitive decline as a result of radiation and cognitive decline as a result of senile dementia (*25,35*) seem to have common features. Animal models using radiation (*1,5,10*) would be of great benefit if they can serve as a general model of dementia because they can be produced in young animals in a short period of time.

5. Conclusion

Cognitive deficits after whole-brain radiation therapy for cancer should be studied in light of vascular damage along with forms of dementia, including Alzheimer's disease.

Acknowledgements

This work was supported by a Grant-in Aid for Scientific Research (A, 26250041) from the Ministry of Education, Science, Sports and Culture and a Core Research for Evolutionary Science and Technology grant from the Japan Science and Technology Agency.

References

1. Liu Y, Xiao S, Liu J, Zhou H, Liu Z, Xin Y, Suo WZ. An experimental study of acute radiation-induced cognitive dysfunction in a young rat model. AJNR Am J Neuroradiol. 2010; 31:383-387.
2. Meyers CA, Brown PD. Role and relevance of neurocognitive assessment in clinical trials of patients with CNS tumors. J Clin Oncol. 2006; 24:1305-1309.
3. Khasraw M, Posner JB. Neurological complications of systemic cancer. Lancet Neurol. 2010; 9:1214-1227.
4. Chang EL, Wefel JS, Hess KR, Allen PK, Lang FF, Kornguth DG, Arbuckle RB, Swint JM, Shiu AS, Maor MH, Meyers CA. Neurocognition in patients with brain metastases treated with radiosurgery or radiosurgery plus whole-brain irradiation: A randomised controlled trial. Lancet Oncol. 2009; 10:1037-1044.
5. Zhou H, Liu Z, Liu J, Wang J, Zhou D, Zhao Z, Xiao S, Tao E, Suo WZ. Fractionated radiation-induced acute encephalopathy in a young rat model: Cognitive dysfunction and histologic findings. AJNR Am J Neuroradiol. 2011; 32:1795-1800.
6. Jeyaretna DS, Curry WT, Jr., Batchelor TT, Stemmer-Rachamimov A, Plotkin SR. Exacerbation of cerebral radiation necrosis by bevacizumab. J Clin Oncol. 2011; 29:e159-162.
7. Chen JH, Yen YC, Liu SH, Lee FP, Lin KC, Lai MT, Wu CC, Chen TM, Yuan SP, Chang CL, Wu SY. Dementia risk in irradiated patients with head and neck cancer. Medicine (Baltimore). 2015; 94:e1983.
8. Schatz J, Kramer JH, Ablin A, Matthay KK. Processing

speed, working memory, and IQ: A developmental model of cognitive deficits following cranial radiation therapy. Neuropsychology. 2000; 14:189-200.
9. Snyder JS, Hong NS, Mcdonald RJ, Wojtowicz JM. A role for adult neurogenesis in spatial long-term memory. Neuroscience. 2005; 130:843-852.
10. Rola R, Raber J, Rizk A, Otsuka S, Vandenberg SR, Morhardt DR, Fike JR. Radiation-induced impairment of hippocampal neurogenesis is associated with cognitive deficits in young mice. Exp Neurol. 2004; 188:316-330.
11. Monje ML, Palmer T. Radiation injury and neurogenesis. Current opinion in neurology. 2003; 16:129-134.
12. Peiffer AM, Leyrer CM, Greene-Schloesser DM, Shing E, Kearns WT, Hinson WH, Tatter SB, Ip EH, Rapp SR, Robbins ME, Shaw EG, Chan MD. Neuroanatomical target theory as a predictive model for radiation-induced cognitive decline. Neurology. 2013; 80:747-753.
13. Otsuka S, Coderre JA, Micca PL, Morris GM, Hopewell JW, Rola R, Fike JR. Depletion of neural precursor cells after local brain irradiation is due to radiation dose to the parenchyma, not the vasculature. Radiat Res. 2006; 165:582-591.
14. Tsai PS, Kaufhold JP, Blinder P, Friedman B, Drew PJ, Karten HJ, Lyden PD, Kleinfeld D. Correlations of neuronal and microvascular densities in murine cortex revealed by direct counting and colocalization of nuclei and vessels. J Neurosci. 2009; 29:14553-14570.
15. Wu J, Guo C, Chen S, Jiang T, He Y, Ding W, Yang Z, Luo Q, Gong H. Direct 3D analyses reveal barrel-specific vascular distribution and cross-barrel branching in the mouse barrel cortex. Cerebral Cortex. 2016; 26:23-31.
16. Burke MJ, Nelson L, Slade JY, Oakley AE, Khundakar AA, Kalaria RN. Morphometry of the hippocampal microvasculature in post-stroke and age-related dementias. Neuropathol Appl Neurobiol. 2014; 40:284-295.
17. Mainland D, Coady BK. The investigation of cell size with special reference to the human lymphocyte. J Anat. 1938; 72:374-398.
18. Ungvari Z, Podlutsky A, Sosnowska D, Tucsek Z, Toth P, Deak F, Gautam T, Csiszar A, Sonntag WE. Ionizing radiation promotes the acquisition of a senescence-associated secretory phenotype and impairs angiogenic capacity in cerebromicrovascular endothelial cells: Role of increased DNA damage and decreased DNA repair capacity in microvascular radiosensitivity. J Gerontol A Biol Sci Med Sci. 2013; 68:1443-1457.
19. Matta Mello Portugal E, Cevada T, Sobral Monteiro-Junior R, Teixeira Guimaraes T, Da Cruz Rubini E, Lattari E, Blois C, Camaz Deslandes A. Neuroscience of exercise: From neurobiology mechanisms to mental health. Neuropsychobiology. 2013; 68:1-14.
20. Kiuchi T, Lee H, Mikami T. Regular exercise cures depression-like behavior *via* VEGF-Flk-1 signaling in chronically stressed mice. Neuroscience. 2012; 207:208-217.
21. Kerr AL, Steuer EL, Pochtarev V, Swain RA. Angiogenesis but not neurogenesis is critical for normal learning and memory acquisition. Neuroscience. 2010; 171:214-226.
22. Warrington JP, Csiszar A, Johnson DA, Herman TS, Ahmad S, Lee YW, Sonntag WE. Cerebral microvascular rarefaction induced by whole brain radiation is reversible by systemic hypoxia in mice. Am J Physiol Heart Circ Physiol. 2011; 300:H736-744.
23. Warrington JP, Csiszar A, Mitschelen M, Lee YW, Sonntag WE. Whole brain radiation-induced impairments in learning and memory are time-sensitive and reversible by systemic hypoxia. PloS one. 2012; 7:e30444.
24. Davis J, Ahlberg FM, Berk M, Ashley DM, Khasraw M. Emerging pharmacotherapy for cancer patients with cognitive dysfunction. BMC Neurol. 2013; 13:153.
25. Attia A, Page BR, Lesser GJ, Chan M. Treatment of radiation-induced cognitive decline. Curr Treat Options Oncol. 2014; 15:539-550.
26. Brown PD, Pugh S, Laack NN, Wefel JS, Khuntia D, Meyers C, Choucair A, Fox S, Suh JH, Roberge D, Kavadi V, Bentzen SM, Mehta MP, Watkins-Bruner D. Memantine for the prevention of cognitive dysfunction in patients receiving whole-brain radiotherapy: A randomized, double-blind, placebo-controlled trial. Neuro Oncol. 2013; 15:1429-1437.
27. Slade A, Stanic S. The impact of RTOG 0614 and RTOG 0933 trials in routine clinical practice: The US Survey of Utilization of Memantine and IMRT planning for hippocampus sparing in patients receiving whole brain radiotherapy for brain metastases. Contemp Clin Trials. 2015; 47:74-77.
28. Rapp SR, Case LD, Peiffer A, Naughton MM, Chan MD, Stieber VW, Moore DF, Jr., Falchuk SC, Piephoff JV, Edenfield WJ, Giguere JK, Loghin ME, Shaw EG. Donepezil for irradiated brain tumor survivors: A phase III randomized placebo-controlled clinical trial. J Clin Oncol. 2015; 33:1653-1659.
29. Shaw EG, Rosdhal R, D'agostino RB, Jr., Lovato J, Naughton MJ, Robbins ME, Rapp SR. Phase II study of donepezil in irradiated brain tumor patients: Effect on cognitive function, mood, and quality of life. J Clin Oncol. 2006; 24:1415-1420.
30. Mccaffrey P. Alzheimer's drug helps brain function after radiotherapy. Lancet Oncol. 2006; 7:371.
31. Drachman DA. The amyloid hypothesis, time to move on: Amyloid is the downstream result, not cause, of Alzheimer's disease. Alzheimers Dement. 2014; 10:372-380.
32. Giwa MO, Williams J, Elderfield K, Jiwa NS, Bridges LR, Kalaria RN, Markus HS, Esiri MM, Hainsworth AH. Neuropathologic evidence of endothelial changes in cerebral small vessel disease. Neurology. 2012; 78:167-174.
33. Okamoto Y, Yamamoto T, Kalaria RN, Senzaki H, Maki T, Hase Y, Kitamura A, Washida K, Yamada M, Ito H, Tomimoto H, Takahashi R, Ihara M. Cerebral hypoperfusion accelerates cerebral amyloid angiopathy and promotes cortical microinfarcts. Acta Neuropathol. 2012; 123:381-394.
34. Wang F, Guo X, Shen X, Kream RM, Mantione KJ, Stefano GB. Vascular dysfunction associated with type 2 diabetes and Alzheimer's disease: A potential etiological linkage. Med Sci Monit Basic Res. 2014; 20:118-129.
35. Cherry JD, Liu B, Frost JL, Lemere CA, Williams JP, Olschowka JA, O'banion MK. Galactic cosmic radiation leads to cognitive impairment and increased abeta plaque accumulation in a mouse model of Alzheimer's disease. PloS one. 2012; 7:e53275.

(Received January 4, 2016; Revised February 6, 2016; Accepted February 6, 2016)

Original Article

DOI: 10.5582/ddt.2016.01009

Tenascin C affects mineralization of SaOS2 osteoblast-like cells through matrix vesicles

Chengzhi Li[1,2], Yazhou Cui[1,2], Jing Luan[1,2], Xiaoyan Zhou[1,2], Haiying Li[1,2], Huaxin Wang[2,3], Liang Shi[1,2], Jinxiang Han[1,*]

[1] *School of Medicine and Life Sciences, University of Jinan-Shandong Academy of Medical Science, Ji'nan, Shandong, China;*
[2] *Key Laboratory for Rare Disease Research of Shandong Province, Key Laboratory for Biotech Drugs of the Ministry of Health, Shandong Medical Biotechnological Center, Shandong Academy of Medical Sciences, Ji'nan, Shandong, China;*
[3] *Shandong University of Traditional Chinese Medicine, Ji'nan, Shandong, China.*

Summary **Tenascin C (TNC) is an extracellular matrix glycoprotein involved in osteogenesis and bone mineralization. In a previous study, we identified TNC protein located in the matrix vesicles (MVs) of osteoblasts. MVs are determinant in the mineralization formation. Therefore, we hypothesize whether TNC can modulate osteoblast mineralization *via* MVs. In this study, we demonstrated that the expression level of TNC was increased with osteoblast differentiation of osteoblast-like SaOS2 cells, and down-regulation of TNC expression by siRNA could significantly inhibit SaOS2 differentiation toward osteoblasts and mineralization as evidenced by decreases in ALP activity, mineralized nodule formation, calcium deposition, and down-regulation of osteogenic marker genes *ALP*, and *COL1A1*. Furthermore, we validated that TNC located in the MVs of mineralized SaOS2 cells, and that down-regulation of TNC could decrease MVs mineralization ability *in vitro*, and the decrease of MVs mineralization ability was not associated with annexins. In conclusion, in this study, we extended the role of TNC during osteogenesis previous progresses, and that supported TNC as an important functional MVs component in modulating osteoblast mineralization.**

Keywords: Matrix vesicles, tenascin, mineralization

1. Introduction

Elucidation of novel cellular and molecular mechanisms in moderating osteoblast mineralization is of great significance in osteogenesis mechanism research and bone tissue engineering. During the process of osteoblast mineralization, matrix vesicles (MVs) function as an initial or primary nucleation site that may be the prerequisite to subsequent secondary mineralization (*1,2*). Aberrant function of MVs have been observed in multiple mineralization-defective diseases (*3*). MVs are highly enriched in proteins and lipids (*4*). Until now, about 2,000 proteins have been identified to be located in MVs. However, only a small set of MVs proteins such as annexins, had been demonstrated to be involved in osteoblast differentiation. The roles of most of the MVs proteins during mineralization remain unclear. Therefore, we hypothesized that these MVs-enriched proteins could be specific sources to identify novel regulators for the physiological and pathological mineralization process.

Tenascin C (TNC) is an extracellular matrix glycoprotein synthesized by osteoblasts during bone growth and morphogenesis (*5,6*). It has been established that TNC was implicated in osteoblastic differentiation and mineralization within bone. In the mechanism, TNC may act as a mediator of TGF-β-induced new bone formation (*7,8*). Additionally, bone morphogenetic protein (BMP) and Wnt growth factors, or mechanical loading and stress can also increase TNC expression in osteoblasts, but *via* distinct signaling pathways (*9,10*). However, little is known about the role of TNC in

Released online in J-STAGE as advance publication February 22, 2016.

*Address correspondence to:
Dr. Jinxiang Han, Key Laboratory for Rare Disease Research of Shandong Province, Key Laboratory for Biotech Drugs of the Ministry of Health, Shandong Medical Biotechnological Center, Shandong Academy of Medical Sciences, Ji'nan, Shandong 250062, China.
E-mail: jinxiang_han@163.com

the regulation of osteogenesis and mineralization. In a previous study, we identified TNC as a novel MVs protein, and raised our speculation that TNC might influence the mineralization process during osteoblast differentiation.

Therefore, in this study, we investigated the effect of TNC on mineralization formation and MVs activity in an osteosarcoma-derived osteoblast-like cell line SaOS2. Our findings suggest that endogenous TNC helps to maintain the mineralization activity and MVs function in SaOS2 cells as a novel MVs protein.

2. Materials and Methods

2.1. *Cell culture and osteoblast differentiation induction*

Human osteosarcoma-derived osteoblast-like cell line SaOS2 was acquired from the Cell Bank of Type Culture Collection of the Chinese Academy of Sciences (Shanghai, China), and was routinely maintained in McCoy's 5A medium (Gibco, Carlsbad, CA, USA), supplemented with 15% fetal bovine serum (Gibco, Carlsbad, CA, USA), 50 U/mL penicillin, and 50 μg/mL streptomycin (both from Invitrogen, Carlsbad, CA, USA) at 37°C under 5% CO_2 in a humidified atmosphere. To induce osteoblast differentiation, SaOS2 cells were treated with 10 mM β-glycerophosphate (β-GP) and 50 μg/mL L-ascorbic acid-2-phosphate as described previously (*9*).

2.2. *siRNA transfection*

TNC targeted siRNA and negative control siRNA were purchased from Guangzhou RiboBio Co., LTD (RiboBio Co., Ltd., Guangzhou, China). The target gene and siRNA sequences are shown in Table 1. Fifty nM of TNC siRNA or negative control siRNA were transfected using Ribo FECTTM CP Transfection Kit (RiboBio Co., Ltd., Guangzhou, China) according to the manufacturer's protocol. After 3 days of transfection, cells were collected and subjected to the subsequent analysis.

2.3. *Isolation of MVs*

MVs were harvested from SaOS2 cells with and without osteoblast induction, and also from cells with siRNA transfection and osteoblast induction. MVs were isolated using a strategy as described previously (*11,12*). Briefly, SaOS2 cells were digested with collagenase Type IA (1 mg/mL, Sigma, St. Louis, MO, USA) at 37°C for 3 h. Cells were then pelleted by centrifugation at 3,000 g for 30 min. The supernatant was concentrated by ultrafiltration using a 100 KD Amicon Ultra filter (Millipore Corporation, Billerica, MA, USA), and then mixed with ExoQuick precipitation reagent (System Biosciences, Mountain View, CA, USA). After incubation overnight, the mixture was centrifuged at 1,500 g for 30 min to collect the MVs precipitation.

2.4. *Alkaline phosphatase (ALP) activity, AlizarinRed staining, and measurement of matrix-deposited calcium*

After treatment with siRNA transfection and osteoblast induction, ALP expression was assayed by means of an ALP activity staining kit (GenMed Scientifics Inc., USA), and the activity was measured as described previously (*13*). Briefly, lysis buffer (25 mM Tris-HCL, 0.5% TritonX-100) was added to precipitated SaOS2 cells and MVs to release ALP at 4°C for 1 h respectively, and then after incubating with *p*-nitrophenyl phosphate (*p*-NPP) substrate at 37°C for 20 min, the absorbance of the mixture at 405 nm was measured using a micro plate reader.

After 6 days of osteoblast differentiation, cells were fixed with ice-cold 70% ethanol and stained with Alizarin Red to detect mineralization using a staining kit according to manufacturer's instruction (GenMed Scientifics Inc., USA) (*14*).

Matrix-deposited calcium was quantitatively measured as described previously (*15*). Briefly, SaOS2 cells were decalcified with 0.6 M HCl at 37°C for 12 h. The calcium content of supernatants was determined using a Calcium Colorimetric Assay Kit (Bioassay Systems, Carlsbad, CA, USA), and then the absorbance of the mixture was measured at 560 nm. After decalcification, cells were solubilized with 0.1 M NaOH/0.1% SDS at 4°C for 1 h. The protein content was measured with a BCA Protein Assay Kit (Thermo Scientific, Rockford, IL, USA), and the calcium content of the cell layer was normalized by protein content.

2.5. *Quantitative real-time polymerase chain reaction (RT-qPCR)*

Total RNA was extracted using Trizol reagent (Gibco, Carlsbad, CA, USA) and the purified total RNA was used for cDNA synthesis with a first-strand cDNA synthesis kit (Toyobo, Osaka, Japan). After the reverse transcription reaction, cDNA was used as the template for RT-qPCR of *ALP*, *COL1A1*, and *TNC*. RT-qPCR was

Table 1. The target sequences and the sequences of siRNA

Items	siRNA-1	siRNA-2
Target 5'→3'	CCTGGCCTATAAGCACTTT	CCAGTTTGCTGAGATGAAA
Forward 5'→3'	CCUGGCCUAUAAGCACUUUdTdT	CCAGUUUGCUGAGAUGAAAdTdT
Reverse 3'→5'	dTdTGGACCGGAUAUUCGUGAAA	dTdTGGUCAAACGACUCUACUUU

Table 2. Quantitative real-time PCR primer sequences

Gene	Sequences5'-3'
GAPDH	
forward	GCA CCG TCA AGG CTG AGA AC
reverse	ATG GTG GTG AAG ACG CCA GT
ALP	
forward	CCGTGGCAACTCTATCTTGG
reverse	GCC ATA CAG GAT GGC AGT GA
COL1A1	
forward	CCC TGG AAA GAA TGG AGA TGAT
reverse	ACT GAA ACC TCT GTG TCC CTT CA
TNC	
forward	GTG CAG AAC TCT CCT GTC CAA AT
reverse	ATC TTT GCT CCT TGC AGT CTT TG

carried out using a SYBR Green qPCR Kit (Toyobo, Osaka, Japan) by LightCycler 480 thermocycler (Roche Applied Science, Mannheim, Germany). The primer sequences of target genes that were used in this study are shown in Table 2.

2.6. *Western-Blot*

From each sample, 40 μg aliquots of total protein was subjected to 7.5% sodium dodecyl sulfate polyacrylamide gel electrophoresis (SDS-PAGE) gels and transferred to a polyvinylidene fluoride (PVDF) membrane. After 2 h of blocking with 5% low fat milk in TBST (10 mM Tris, 100 mM NaCl, and 0.05% Tween-20), the membrane was incubated overnight at 4°C with specific antibodies against TNC (1:500, Cell Signaling Technology, Danvers, MA, USA), annexin 2 (AnxA2, 1:500, Proteintech Group, Wuhan, China), annexin 5 (AnxA5, 1:500, Proteintech Group, Wuhan, China), annexin 6 (AnxA6, 1:500, Proteintech Group, Wuhan, China) and GAPDH (1:1,000, Santa Cruz Biotechnology, Carlsbad, CA, USA).

2.7. *MV-collagen calcification assay*

MVs-collagen calcification assay was used to evaluate the mineralization induction activity of MVs as described previously by Chen *et al*. with minor modifications *in vitro* (*16,17*). Briefly, isolated MVs were re-suspended in TBS (pH = 7.6) with 0.25 M sucrose and then added to type I collagen-coated glass cover slips, and incubated for 12 h. Then calcification media (DMEM medium with 15% FBS and 10 mM β-glycerophosphate) were added, and further incubated at 37°C for 72 h. To determine the magnitude of calcification, the MVs-collagen complex was incubated with 0.6 M HCl for 12 h, and the calcium content of HCL supernatants was determined as described above.

2.8. *Statistics*

Measurements in each experiment were run in triplicate. For quantitative data, results are reported as the mean ± S.D. To determine the differences between groups, one-way analysis of variance (ANOVA) was carried out using SPSS software (version 17.0), with significance accepted at $p < 0.05$.

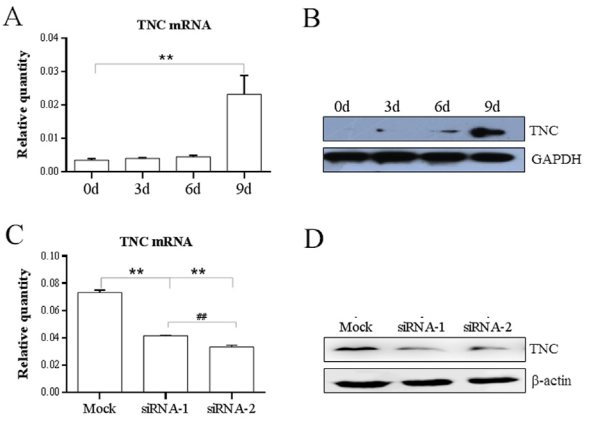

Figure 1. Expression of TNC during SaOS2 cells osteogenesis induction and expression after siRNA transfection. Quantitative real-time PCR analyses of TNC expression in mRNA level **(A)** and Western blotting analyses of TNC expression in protein level **(B)** during SaOS2 cells osteogenesis induction; expression of TNC in mRNA **(C)** and protein **(D)** level after siRNA transfection 3 days and 6 days respectively. Bars are shown as the mean ± S.D., $n = 3$. $^{**}p < 0.01$ *vs*. group 0 d and mock respectively.

3. Results

3.1. *Expression of TNC during SaOS2 cells osteogenesis induction*

First, we observed the expression pattern of TNC during osteogenesis at mRNA and protein levels. As seen in Figures 1A and 1B, TNC expression was elevated during SaOS2 osteoblast differentiation in a time-dependent manner and reached the highest level at 9 days after induction, suggesting that TNC may play an important role at the later mineralization stage.

3.2. *Effect of TNC siRNA on osteoblast differentiation of SaOS2 cells*

After siRNA transfection, the expression of TNC was significantly decreased (60%-70%) at both mRNA and protein levels as measured by RT-qPCR and Western-blot analyses (Figures 1C and 1D). We further observed that down-regulation of TNC by siRNA had a significant inhibitory effect on SaOS2 cell osteogenic differentiation, as manifested by down-regulated expression of osteogenic marker genes *COL1A1*, and *ALP*, and decreased ALP activity and matrix mineralization (Figure 2).

3.3. *Effect of TNC siRNA on the function of MVs*

We confirmed that TNC protein located in the

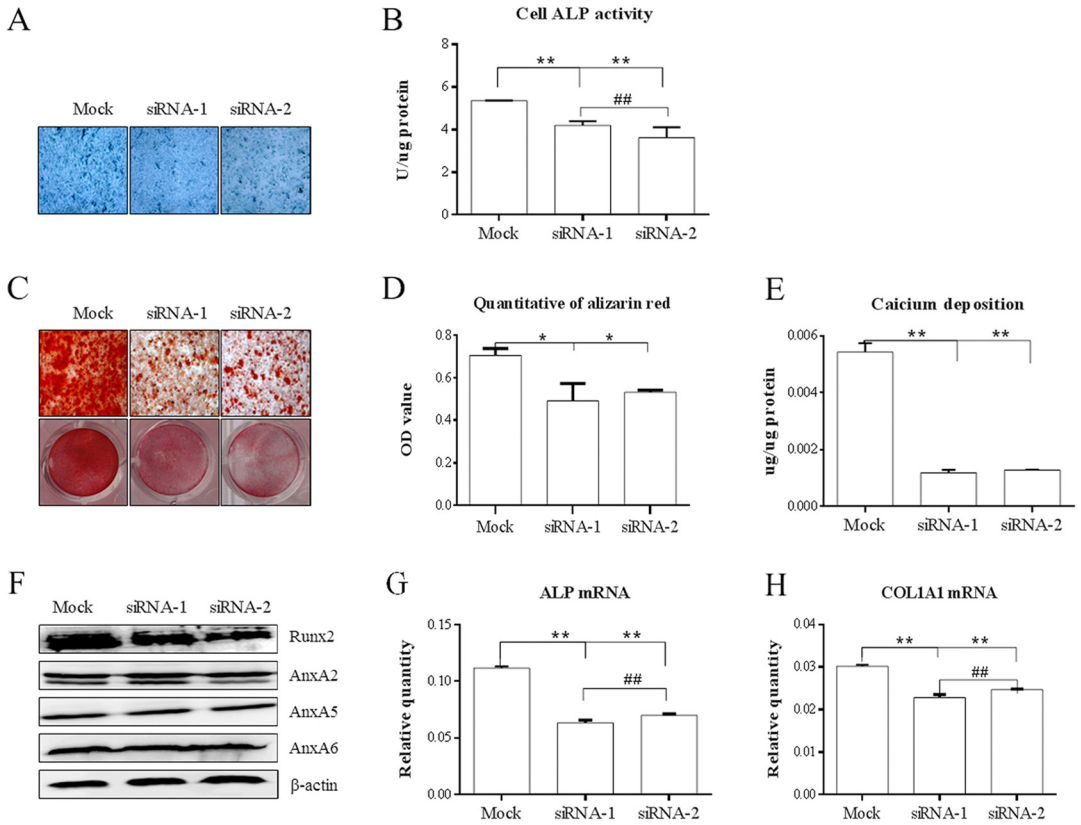

Figure 2. Effect of TNC siRNA on osteoblast differentiation of SaOS2 cells. ALP activity was assayed by means of an ALP expression staining kit **(A)** and the activity was measured by *p*-NPP **(B)**; the calcium deposits in the mineralized matrix were analyzed by Alizarin Red staining **(C)** which was quantified at 562 nm **(D)** and Calcium Assay Kit **(E)**; Western blot analyses of expression of Runx2, AnxA2, AnxA5, and AnxA6 in siRNA transfected and osteoplastic inducted SaOS2 cells **(F)**; quantitative real-time PCR analyses of expression of osteoplastic marker genes: *ALP* **(G)**, *COL1A1* **(H)**. Bars are shown as the mean ± S.D., $n = 3$. $^{*}p < 0.05$ *vs*. mock, $^{**}p < 0.01$ *vs*. mock, $^{\#\#}p < 0.01$, siRNA-1 *vs*. siRNA-2.

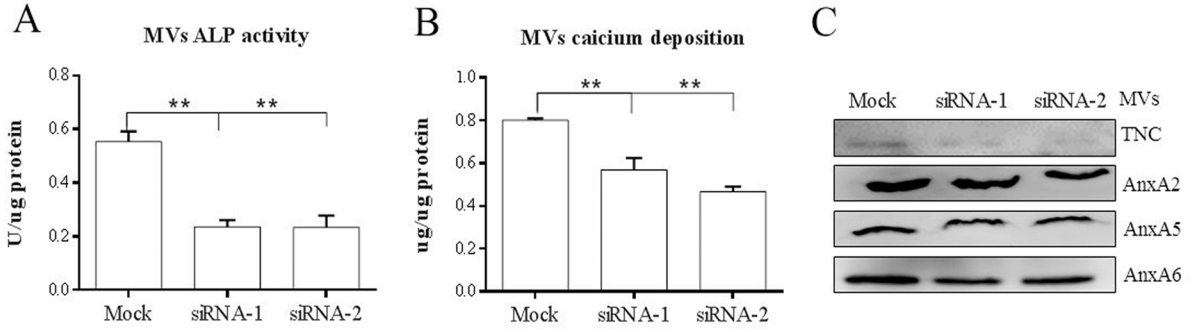

Figure 3. Effect of TNC siRNA on the function of MVs. The activity of MVs was measured by *p*-NPP **(A)**, and the calcium deposits caused by MVs in vitro were analyzed by Calcium Assay Kit **(B)**; Western blot analyses of expression of TNC, AnxA2, AnxA5, and AnxA6 in MVs after siRNA transfection **(C)**. Bars are shown as the mean ± S.D., $n = 3$. $^{**}p < 0.01$ *vs*. mock.

mineralized SaOS2 cell derived MVs, which was consistent with our previous finding (Figure 3C). Furthermore, accompanying the decrease of TNC expression in SaOS2 cells, siRNA also significantly inhibited TNC expression in MVs derived from mineralized SaOS2 cells (Figure 3C). Moreover, we also observed that ALP activity of MVs was markedly inhibited after TNC siRNA transfection (Figure 3A). Meanwhile, MVs induced calcium deposition was significantly decreased by TNC down-regulation (Figure 3B). Therefore, our above findings suggest that TNC expression is necessary for MVs in directly inducing mineralization *in vitro*.

3.4. *Effects of TNC siRNA on annexins expression in SaOS2 cells and MVs*

Annexin proteins are confirmed to be functional MVs components participating in mineralization. Therefore, we next explored whether there was some association

between TNC and annexins. We observed the expression of three annexin members, AnxA2, AnxA5, and AnxA6 in SaOS2 cells and their released MVs after TNC siRNA transfection, and found that TNC siRNA exerted no effect on the expression of three annexins on both cell and MVs levels (Figure 2F, Figure 3C), indicating that the influence of TNC on MVs function seems not to be associated with annexins.

4. Discussion

TNC is an osteoblast-secreted extracellular matrix protein which is able to stimulate osteoblastic differentiation and help to maintain the functional state of cultured osteoblast-like cells including SaOS2 cells (*18,19*). Meaningfully, TNC has been indicated to be associated with chronic kidney disease mineral and bone disorder, suggesting TNC may act as a key mediator and target for osteogenesis, especially for mineralization formation (*20*).

Most of the previous studies focused on the role of TNC on the early events of osteogenesis (*21*). In this present study, we identified that TNC expression level reached a peak at the late mineralization stage. Inhibiting TNC expression can decrease the early marker genes for osteoblast differentiation such as *COL1A1* and *ALP*, which was consistent with previous studies. Moreover, we also observed that TNC down-regulation could significantly inhibit late mineralization as manifested by decreased matrix calcium deposition and lower *COL1A1* gene expression. These findings are helpful to explain the close association between TNC and pathologic ossification, and suggest TNC may play an important role in mediating mineralization.

It has been believed that tenascin is absent from mineralized bone matrix (*22*). Different from the previous study, in this study, we confirmed that TNC was located in the MVs released from the mineralized matrix. Matrix vesicles (MVs) are specific membranous nanovesicles released by cells capable of mineralization such as chondrocytes, osteoblasts or odontoblasts (*23*). It has been shown that MVs play a critical role in modulating mineralization through modulating the local Pi/PPi ratio in the mineralizing matrix or providing initial mineral nucleation sites (*24*). In this study, for the first time, we found that the presence of TNC in MVs is necessary for the normal mineralization function of MVs.

Currently, over 2,000 proteins have been identified in MVs. Among them, annexin family transport proteins, especially, annexin 1, annexin 5, and annexin 6, are key components which have been shown to be linked to the two key functions of MVs in modulating mineralization (*16,25*). However, our results indicate that TNC cannot affect the expression of annexins in both cell and MVs levels. This finding suggests that the role of TNC involving MVs function seems not to be associated with annexins. TNC may participate in the mineralization process directly. Considering a calcium-binding domain existing at the C-terminal end of TNC, we speculate that TNC may regulate the MVs activity to initiate mineralization by combining Ca^{2+} and influx into MVs, but the exact mechanism needs further investigation.

In conclusion, our results indicate that TNC plays an important role during early and late osteoblast differentiation. For the first time we linked the effect of TNC on osteoblast mineralization with its regulatory function on MVs activity. We conclude that TNC is an important and functional component of MVs that might participate in physiological and pathological mineralization.

Acknowledgements

This study was supported by National Natural Science Foundation of China (81371909) and Key Projects in the National Science & Technology Pillar Program during the Twelfth Five-year Plan Period (2013BAI07B01).

References

1. Genge BR, Wu LNY, Wuthier RE. Mineralization of annexin-5-containing lipid-calcium-phosphate complexes: Modulation by varying composition and incubation with cartilage collagens. J Biol Chem. 2008; 283:9737-9748.
2. Wu LNY, Genge BR, Wuthier RE. Analysis and molecular modeling of the formation, structure, and activity of the phosphatidylserine-calcium-phosphate complex associated with biomineralization. J Biol Chem. 2008; 283:3827-3838.
3. Golub EE. Biomineralization and matrix vesicles in biology and pathology. Semin Immunopathol. 2011; 33:409-417.
4. Zhou X, Cui Y, Zhou X, Han J. Phosphate/pyrophosphate and MV-related proteins in mineralisation: Discoveries from mouse models. Int J Biol Sci. 2012; 8:778-790.
5. Ruth CE, Matthias C. Tenascins: Regulation and putative functions during pathological stress. J Pathol. 2003; 200:488-499.
6. Sato R, Fukuoka H, Yokohama-Tamaki T, Kaku M, Shibata S. Immunohistochemical localization of tenascin-C in rat periodontal ligament with reference to alveolar bone remodeling. Anat Sci Int. 2016; 91:196-206.
7. Li C, Li G, Liu M, Zhou T, Zhou H. Paracrine effect of inflammatory cytokine-activated bone marrow mesenchymal stem cells and its role in osteoblast function. J Biosci Bioeng. 2016; 121:213-219.
8. Laura DL, Rice JJ, Federico T, Hubbell JA. Tenascin C promiscuously binds growth factors *via* its fifth fibronectin type III-like domain. PLoS One. 2013; 8:376-380.
9. Anxun W, Xueqiang D, Shihu S, Zhaoyou Y. Bone morphogenetic protein receptor in the osteogenic differentiation of rat bone marrow stromal cells. Yonsei

Med J. 2010; 51:740-745.
10. Shinohara Y, Okamoto K, Goh Y, Kiga N, Tojyo I, Fujita S. Inhibition of fibrous adhesion formation in the temporomandibular joint of tenascin-C knockout mice. Eur J Histochem. 2014; 58:2337.
11. Zhou X, Cui Y, Luan J, Zhou X, Zhang G, Zhang X, Han J. Label-free quantification proteomics reveals novel calcium binding proteins in matrix vesicles isolated from mineralizing Saos-2 cells. Biosci Trends. 2013; 7:144-151.
12. Jiang L, Cui Y, Luan J, Zhou X, Zhou X, Han J. A comparative proteomics study on matrix vesicles of osteoblastlike Saos-2 and U2-OS cells. Intractable Rare Dis Res. 2013; 2:59-62.
13. Ge P, Cui Y, Liu F, Luan J, Zhou X, Han J. L-carnitine affects osteoblast differentiation in NIH3T3 fibroblasts by the IGF-1/PI3K/Akt signalling pathway. Biosci Trends. 2015; 9:42-48.
14. Luan J, Cui Y, Zhang Y, Zhou X, Zhang G, Han J. Effect of CXCR4 inhibitor AMD3100 on alkaline phosphatase activity and mineralization in osteoblastic MC3T3-E1 cells. Biosci Trends. 2012; 6:610-618.
15. Hernandez L, Park KH, Cai SQ, Ling Q, Partridge N, Sesti F. The antiproliferative role of ERG K+ channels in rat osteoblastic cells. Cell Biochem Biophys. 2007; 47:199-208.
16. Chen NX, O'Neill KD, Chen X, Moe SM. Annexin-mediated matrix vesicle calcification in vascular smooth muscle cells. J Bone Miner Res. 2008; 23:1798-1805.
17. Chen NX, Fatih K, O'Neill KD, Xianming C, Moe SM. Verapamil inhibits calcification and matrix vesicle activity of bovine vascular smooth muscle cells. Kidney Int. 2010; 77:436-442.
18. Pillarisetti S, Jones P, Xiao H. Involvement of matrix metalloproteinases and tenascin-C in elastin calcification. Cardiovasc Pathol. 2004; 13:146-155.
19. Ikemura S, Hasegawa M, Iino T, Miyamoto K, Imanaka-Yoshida K, Yoshida T, Sudo A. Effect of tenascin-C on the repair of full-thickness osteochondral defects of articular cartilage in rabbits. J Orthop Res. 2015; 33:563-571.
20. Ozkan G, Ulusoy S, Guvercin B, Mentese A, Karahan SC, Yavuz A. A new player in chronic kidney disease mineral and bone disorder: Tenascin-C. Int J Artif Organs. 2015; 38:481-487.
21. Morgan JM, Wong A, Yellowley CE, Genetos DC. Regulation of tenascin expression in bone. J Cell Biochem. 2011; 112:3354-3363.
22. Mackie EJ, Abraham LA, Taylor SL, Tucker RP, Murphy LI. Regulation of tenascin-C expression in bone cells by transforming growth factor-beta. Bone. 1998; 22:301-307.
23. Thouverey C, Malinowska A, Balcerzak M, Strzelecka-Kiliszek A, Buchet R, Dadlez M, Pikula S. Proteomic characterization of biogenesis and functions of matrix vesicles released from mineralizing human osteoblast-like cells. J Proteomics. 2011; 74:1123-1134.
24. Harmey D, Hessle L, Narisawa S, Johnson KA, Terkeltaub R, Millán JL. Concerted regulation of inorganic pyrophosphate and osteopontin by akp2, enpp1, and ank: An integrated model of the pathogenesis of mineralization disorders. Am J Pathol. 2004; 164:1199-1209.
25. Wei W, Jinping X, Thorsten K. Annexin-mediated Ca^{2+} influx regulates growth plate chondrocyte maturation and apoptosis. J Biol Chem. 2003; 278:3762-3769.

(Received January 8, 2016; Revised February 2, 2016; Accepted February 3, 2016)

Original Article

DOI: 10.5582/ddt.2016.01019

Generic selection criteria for safety and patient benefit [V]: Comparing the pharmaceutical properties and patient usability of original and generic nasal spray containing ketotifen fumarate

Yuko Wada[1], Shyoko Ami[1], Mitsuru Nozawa[2], Miho Goto[2], Ken-ichi Shimokawa[1], Fumiyoshi Ishii[1,*]

[1] *Department of Pharmaceutical Sciences, Meiji Pharmaceutical University, Tokyo, Japan;*
[2] *Triad Japan Co. Ltd., Kanagawa, Japan.*

Summary **The pH, osmotic pressure (cryoscopy), viscosity, squeeze force, spray angle, and spraying frequency of nasal spray containing ketotifen fumarate (1 brand-name product and 8 generic products) were measured. Based on the results of pH measurement, all products were weakly acidic (4.0 to 5.1). For all products, the osmotic pressure ratio to physiological saline was approximately 1. The viscosity of various products ranged from approximately 1.0 to 1.5 mPa·s. The spray angle of drug solution differed among the products: minimum, 46 degrees (Sawai and Fusachol); and maximum, 68.7 degrees (Sekiton). In particular, TOA, Sawai, Fusachol, and TYK showed significantly smaller angles compared to Zaditen (brand-name product). Container properties varied among the products: minimum squeeze force, 19.0 N (Sekiton); and maximum squeeze force, 43.1 N (Sawai). Based on these results, although all the above products are identical in dosage form and active ingredient, the differences in pharmaceutical properties, such as container operations and drug-solution spraying/attachment, may markedly influence patients' subjective opinions.**

Keywords: Brand-name product, generic products, pharmaceutical properties, ketotifen fumarate, nasal spray

1. Introduction

In Japan, health expenditures have rapidly increased with the aging of society. Since the establishment of the Medical System for the Elderly in 2006, the budget deficits of health insurance societies have exceeded 300 billion yen (6 consecutive years) (*1*). As a strategy to efficiently improve the public finance of pharmaceutical insurance, the widespread use of generic products has been emphasized, and official name-based prescriptions have been promoted under the government's policy so that pharmacists may recommend and deliver generic products (*2*). In this prescription system, the selection of generic products depends on pharmacists' evaluation. Therefore, pharmacists must select safe, equivalent generic products from a pharmaceutical point of view, and explain them to patients.

In March 2015, the National Federation of Health Insurance Societies published the results of a survey regarding health insurance societies' health expenditure in 2013, in which the contents of the total health expenditure of 609 societies (1,456.4 billion yen) were investigated (*3*). According to this report, health expenditure for respiratory diseases accounted for 15.43%, and was the highest percentage among 19 disease categories. In particular, health expenditure for allergic rhinitis accounted for 2.93%, the second highest percentage, following that for asthma (3.07%). Furthermore, the number of patients with a type of seasonal allergic rhinitis, hay fever, is still increasing.

In the "Practical Guideline for the Management of Allergic Rhinitis in Japan" (*4*), a second-generation antihistaminic drug, ketotifen fumarate, is recommended as a first-choice drug for mild, rhinorrhea-type moderate, or severe allergic rhinitis. It exhibits antihistaminic actions (*5*) by suppressing

**Address correspondence to:*
Dr. Fumiyoshi Ishii, Department of Pharmaceutical Sciences, Meiji Pharmaceutical University, 2-522-1, Noshio, Kiyose, Tokyo 204-8588, Japan.
E-mail: fishii@my-pharm.ac.jp

Table 1. Various products used in this experiment

Product name	Abbreviated name	Class	Company	Price (¥)/bottle	Serial number
Zaditen® nasal solution 0.05%	Zaditen	brand-name	Novartis Pharma K. K.	781.1	375
Electer® nasal solution 0.05%	Electer	generic	Mylan Seiyaku Ltd.	442.6	M001AU3
Ketotifen nasal solution 0.05% "TOA"	TOA	generic	Toa Pharmaceutical Co., LTD.	442.6	S01SF
Sekiton® nasal solution 0.05%	Sekiton	generic	Kyorin Rimedio Co., Ltd.	341.1	18KA
Ketotifen nasal solution 0.05% “CH”	CH	generic	Choseido Pharmaceutical Co., Ltd.	341.1	WK031
Supdel® nasal solution 0.05%	Supdel	generic	Towa Pharmaceutical Co., Ltd.	341.1	A015
Ketotifen nasal solution 0.05% "Sawai"	Sawai	generic	Sawai Pharmaceutical Co., Ltd.	341.1	12108
Fusachol® nasal solution 0.05%	Fusachol	generic	Nitto Medic Co., Ltd.	341.1	11601
Ketotifen nasal solution 0.05% "TYK"	TYK	generic	Taisho Pharm. Ind., Ltd	341.1	WJ01

the release of chemical mediators (*6*), reducing the hypersensitivity of the nasal mucosa (antiallergic actions) (*7*).

In Japan, capsules, syrup, nasal drops, and eye drops have been approved as the dosage forms of ketotifen fumarate. In the package inserts of a brand-name product, Zaditen, it is described that patients with allergic rhinitis who responded to capsules and nasal drops accounted for 59.0% (138/234) and 60.1% (184/306), respectively; the percentages were similar. However, the incidences of an adverse reaction of the central nervous system, sleepiness, were 4.4 and 1.0%, respectively. Nasal drops have the merit of reducing adverse reactions. On the other hand, such drops are characterized by differences in availability, such as the availability of spraying containers or intranasal sensation on drug-solution attachment, among products from different manufacturers, differing from oral formulations, such as capsules. This leads to switching of a generic product to the brand-name product in some cases. In others, switching of the brand-name product to a generic product improves availability, increasing the degree of satisfaction (*8*). The patient-based selection of formulations may facilitate the use/promotion of generic products, improving the comfortableness, degree of satisfaction, and adherence, and leading to favorable treatment responses.

We previously reported the physical properties of various formulations with respect to brand-name and generic products (*9-12*). However, few studies have compared the pharmaceutical properties of various formulations, including brand-name and generic products. In this study, the pharmaceutical properties of brand-name and generic products of nasal sprays containing ketotifen fumarate were investigated to provide information to patients and health-care professionals.

2. Materials and Methods

2.1. *Materials*

Ethical pharmaceuticals of nasal sprays containing ketotifen fumarate (1 brand-name and 8 generic products) were used in this study. The names, manufacturers, sales agencies, prices, and lot numbers of these products are presented in Table 1.

2.2. *Measurement of pH*

The fluid content pH of each nasal-spray preparation was measured using a Benchtop pH meter F-74 (HORIBA, Ltd., Kyoto, Japan). Measurement was performed 3 times at 25 ± 5°C, and the mean ± standard deviation (S.D.) was calculated.

2.3. *Measurement of osmotic pressure*

The fluid content osmotic pressure of each nasal-spray preparation was measured using cryoscopy with an OSMOMAT device (030-D, Gonotec GmbH, Berlin, Germany). The osmotic pressure ratio to physiological saline was calculated. Measurement was performed 3 times, and the mean ± S.D. was calculated.

2.4. *Measurement of viscosity*

The viscosity of the fluid content of each nasal-spray preparation was measured using a cone-plate-type rotary viscometer (TPE-100, Toki Sangyo Co., Ltd., Tokyo, Japan) at 100 rpm at 3 different temperatures (20, 25, and 35°C). Measurement was performed 3 times, and the mean ± S.D. was calculated.

2.5. *Measurement of power on the finger required for a mist*

Using a ZTS-50N digital force gauge (Imada Co., Ltd., Aichi, Japan), each nasal-spray preparation was covered with a test tube, set in a stand, and pressed from the upper side for measurement. Measurement was performed 10 times, and the mean ± S.D. was calculated.

2.6. *Measurement of the mist angle*

Video filming of the mist angle of each nasal-spray preparation was performed from the side, and the angle was measured using a protractor. Measurement was performed 3 times, and the mean ± S.D. was calculated.

2.7. *Measurement of the number of mists*

The number of mists from each preparation was measured at room temperature. The values (%) represent the number of effective mists as a percentage of the total number of mists. The total number of mists was defined as that until the residual drug solution volume became zero. Based on the results of measurement, the number of effective mists was defined as the number of mists until the slope of a graph for the standard deviation increased. Measurement was performed 3 times, and the results are expressed as the mean ± S.D.

2.8. *Investigation of ingredient composition*

We investigated the composition of ingredients using the package inserts and interview form for each sample.

3. Results and Discussion

3.1. *Measurement of pH*

The nasal mucosal pH is reportedly approximately 5.5 to 6.5 in healthy adults and approximately 7.2 to 8.3 in those with rhinitis (*13*). On the other hand, a study reported that when buffer solution was sprayed into the nasal cavity, the nasal mucosal pH changed through the effects of the buffer solution (*14*). We measured the pH of each preparation. The results are shown in Figure 1.

As shown in Figure 1, all preparations were weakly acidic: pH range, 4.0 (TYK) to 5.1 (Electer). This was possibly because the pH was established, considering the stability of each preparation, based on the finding that the water solubility of ketotifen fumarate is higher at a lower pH (*15*). According to a study, pollen rupture, which is the process of allergen release from pollen, may occur in an alkaline state (*16*). Low-pH preparations may adjust the nasal cavity, which tends to become weakly alkaline, to a weakly acid state.

In the package inserts, it is described that the standard pH values of preparations other than Electer range from 3.8 to 4.6, whereas that of Electer ranges from 4.9 to 5.5. It was reported that the partition coefficient of ketotifen was greater at a higher solution pH (*17*). The absorption of high-pH preparations through the nasal mucosa may be promoted with a higher molecule-type percentage of ketotifen in comparison with low-pH preparations.

3.2. *Measurement of osmotic pressure*

With respect to the osmotic pressure of nasal spray, a study using rabbits indicated that the hypotonic adjustment of preparations improved drug permeability (*18*). On the other hand, according to a survey using guinea pigs, the infusion of low-osmotic-pressure liquid, such as tap water, led to marked enlargement of the intercellular space of the nasal mucosa (*19*).

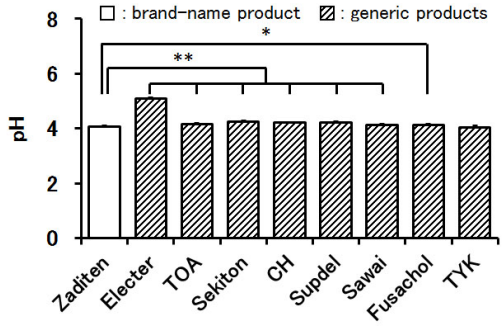

Figure 1. pH comparison of various products (*n* = 3). $^{*}p <$ 0.05, $^{**}p < 0.01$ (brand-name *vs*. generics, *Dunnett's* test).

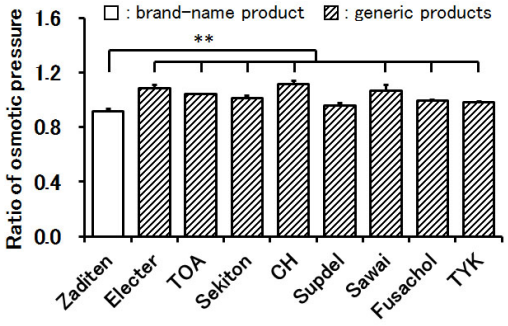

Figure 2. Osmolarity comparison of the various products (*n* = 3). The ratio of osmotic pressure to isotonic saline containing 0.9% NaCl. $^{**}p < 0.01$ (brand-name *vs*. generics, *Dunnett's* test).

Furthermore, a study regarding the influence of the osmotic pressure of nebulizer solution on the human nasal mucosa reported that the administration of hypertonic salt solution significantly increased the volume of nasal discharge (*20*).

To examine the influence of the osmotic pressure of preparations on the nasal mucosa, nasal discharge, and drug permeability, the osmotic pressure was measured. The osmotic pressure ratio of each sample is shown in Figure 2.

As presented in Figure 2, all preparations showed an osmotic pressure ratio of approximately 1. It was possibly established to reduce the influence of stimuli on the mucosa. Furthermore, these preparations may have been designed to avoid hypertonic solution-related nasal discharge.

3.3. *Measurement of viscosity*

The viscosity of drug solution may influence its retention at the affected site or dripping. We measured the viscosity of each preparation. The results are shown in Figure 3. Concerning temperatures of measurement, 20 and 25°C were established as room temperature, and 35°C as intranasal temperature.

As presented in Figure 3, the viscosity of each preparation ranged from approximately 1.0 to 1.5 mPa·s. After spraying, more viscous preparations may

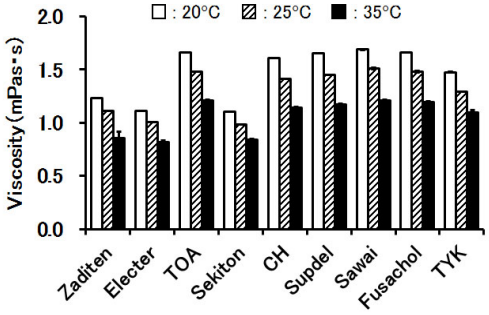

Figure 3. Viscosity comparison of the various products (*n* = 3).

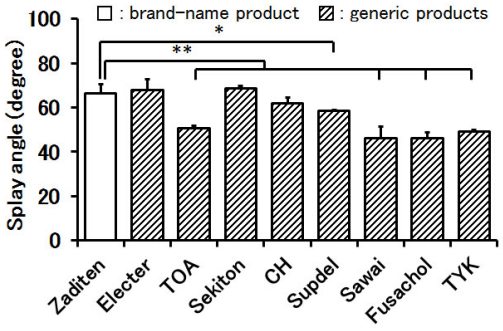

Figure 4. Comparison of spray angle of the various products (*n* = 3). $^{*}p < 0.05$, $^{**}p < 0.01$ (brand-name *vs*. generics, *Dunnett's* test).

be retained at the affected site without dripping in comparison with less viscous preparations.

3.4. *Measurement of the spray angle of drug solution*

The spray angle of drug solution may contribute to the retention of drug solution at the affected site and dripping. We measured the spray angle of drug solution for each preparation. The results are shown in Figure 4.

The spray angle of drug solution differed among the preparations: 46 (Sawai and Fusachol) to 68.7 degrees (Sekiton). In particular, the spray angles of TOA, Sawai, Fusachol, and TYK were significantly smaller than that of the brand-name product (Zaditen), suggesting that sprayed drug solution reaches the deep area of the nasal cavity, reducing the volume of drug solution directly attached to the lateral side of the nasal cavity. This also reflects that there is no dripping after spraying, whereas the effects on symptoms of the lateral side, onto which drug solution is not readily attached, are reduced.

3.5. *Measurement of the force required for spraying*

Container-operating properties on spraying contribute to availability for patients. They may influence adherence. We measured the finger force required for spraying, that is, the squeeze force for each sample container. The results are shown in Figure 5.

The container properties varied among the preparations: 19.0 (Sekiton) to 43.1 N (Sawai). Preparations that can be sprayed using a relatively light force may be appropriate for children, females, elderly persons, and hand-disabled persons, whose finger forces are weak. When switching from the brand-name product to a generic product, patients may feel difficulty in spraying, if the force required for spraying is greater than that for the brand-name product; caution is needed.

These results showed that there were differences in the pharmaceutical properties among the products. Although the efficacy of each product may be similar, the differences in pharmaceutical properties, such as container-operating properties and drug-solution spraying/attachment, may markedly influence

Figure 5. Comparison of squeeze force requirement of the various products (*n* = 3). $^{**}p < 0.01$ (brand-name *vs*. generics, *Dunnett's* test).

availability for patients. As TYK contains peppermint oil, its scent-related freshness may be obtained on spraying, but some persons may dislike it. Pharmacists may play an important role in the selection of nasal spray, as an external preparation, for which usability may contribute to adherence, in accordance with individual patients' needs.

Acknowledgements

We thank Chuo Kagaku Sangyou Co., Ltd., (Tokyo, Japan) for providing compounds of various reagents.

References

1. 2014 Coercive union budget early aggregate result summary, National Federation of Health Insurance Societies, April 18, 2014. *http://nakyblog.cocolog-nifty.com/blog/2014/04/26-514e.html* (accessed April 9, 2016). (in Japanese)
2. 2012 Ministry of health, labour and welfare notification No. 76. Partial revision of the calculation method of medical treatment fees (Notification). http://www.mhlw.go.jp/stf/seisakunitsuite/bunya/kenkou_iryou/iryouhoken/iryouhoken15/index.html (accessed April 9, 2016). (in Japanese)
3. National Federation of Health Insurance Societies IT Promotion Department data analysis Promotion Group, Research and analysis report on trends in the 2013 fiscal health insurance medical expenses, p23 (2015) *http://www.kenporen.com/study/toukei_data/pdf/chosa_h27_3.*

pdf (accessed April 9, 2016). (in Japanese)
4. Okubo K. Practical guideline for the management of allergic rhinitis in Japan. Jpn Soc Allergol. 2013; 62:1458-1463. (in Japanese)
5. Ney UM, Bretz U, Martin U, Mazzoni L. Pharmacology of ketotifen. Res Clin Forums. 1982; 4:9-16.
6. Martin U, Römer D. The pharmacological properties of a new, orally active anti-anaphylactic compound: Ketotifen, a benzocyloheptathiophene. Arzneim Forsch. 1978; 28:770-782.
7. Usui N, Iwata A, Uchiyama M, Tsukasa M. Study of inhibitory effect of Ketotifen (HC 20-511) for the nasal provocation test by house dust antigen. JIBI INKOKA TEMBO. 1984; 27(Suppl 1):107-114. (in Japanese)
8. Kakuyama A, Tamaki T, Iizuka T, Ariumi H, Miyazaki T, Kido M, Kumai M, Noda T, Ohodo S, Yoshiyama Y. Database of value added generic drugs. JIBI INKOKA TEMBO. 2010; 53(Suppl 2):85-89. (in Japanese)
9. Wada Y, Nozawa M, Goto M, Shimokawa K, Ishii F. Generic selection criteria for safety and patient benefit [I] Comparing the original drugs and generic ones in pharmaceutical properties. J Community Pharm Pharm Sci. 2014; 6:97-105. (in Japanese)
10. Nozawa M, Wada Y, Yamazaki N, Shimokawa K, Ishii F. Generic selection criteria for safety and patient benefit [II] Physicochemical characteristics of original versus generic drugs for different difluprednate-containing products (ointment, cream, and lotion). Jpn Soc Community Pharm Pharm. 2014; 2:37-48. (in Japanese)
11. Wada Y, Nozawa M, Goto M, Shimokawa K, Ishii F. Generic selection criteria for safety and patient benefit [III] Comparing the pharmaceutical properties and patient usability of original and generic ophthalmic solutions containing Timolol maleate. Jpn Soc Pharm Health Care Sci. 2015; 41:394-403. (in Japanese)
12. Wada Y, Kihara M, Nozawa M, Shimokawa K, Ishii F. Generic selection criteria for safety and patient benefit [IV] Physicochemical and pharmaceutical properties of brand-name and generic ketoprofen types. Drug Discov Ther. 2015; 9:229-233.
13. England RJ, Homer JJ, Knight LC, Ell SR. Nasal pH measurement: A reliable and repeatable parameter. Clin Otolaryngol Allied Sci. 1999; 24:67-68.
14. Washington N, Steele RJC, Jackson SJ, Bush D, Mason J, Gill DA, Pitt K, Rawlins DA. Determination of baseline human nasal pH and the effect of intranasally administered buffers. Int J Pharm. 2000; 198:139-146.
15. Abd El-Bary AA, Salem HF, Kharshoum RM. 2-Hydroxypropyl-ß-cyclodextrin complex with ketotifen fumerate for eye drops preparations. Int J Drug Delivery. 2011; 3:228-240.
16. Nohara O. The effect of nasal fluid on the release of major allergens from Japanese cedar (Cryptomeria japonica) pollens. JIBI INKOKA TEMBO. 1996; 39:483-495. (in Japanese)
17. Kimura C, Tojo K. Development of a stick-type transdermal eyelid delivery system of ketotifen fumarate for ophthalmic diseases. Chem Pharm Bull. 2007; 55:1002-1005.
18. Nishibe Y, Nagano A, Uejima Y. Nasal suspensions with low osmolality and drug permeability. JIBI INKOKA TEMBO. 2002; 45(Supplement 1):46-49. (in Japanese)
19. Odaira H, Koike S, Takasaka T, Sawai T. Influence of various solutions injected into the nasal cavity on nasal epithelium. Nippon Jibiinkoka Gakkai Kaiho 1987; 90:1951-1962. (in Japanese)
20. Komori M, Miwa M, Mamiya T, Kondo Y, Miyagishima T, Takasu A, Iwata S. Effects of osmolality changes in nebulizar solutions on nasal mucosa. JIBI INKOKA TEMBO. 1999; 42(Supplement 2):181-185. (in Japanese)

(Received February 18, 2016; Revised April 4, 2016; Re-revised April 9, 2016; Accepted April 9, 2016)

Original Article

DOI: 10.5582/ddt.2016.01028

1,4-Naphthoquinone, a pro-oxidant, ameliorated radiation induced gastro-intestinal injury through perturbation of cellular redox and activation of Nrf2 pathway

Lokesh Gambhir*

Department of Life Sciences, Shri Guru Ram Rai Institute of Technology & Sciences, Dehradun, Uttarakhand, India.

Summary **Detrimental effects of ionizing radiation (IR) are observed at the doses above 1 Gy. Treatment modalities are available up to doses of 6 Gy including bonemarrow transplantation and administration of antibiotics. However, exposure to IR doses above 8 Gy results in gastro-intestinal (GI) syndrome characterised by denudated villi, apoptosis of crypt cells and elevated inflammatory responses. Multiple strategies have been employed to investigate novel agents to protect against IR induced injury. Since cellular redox homeostasis plays a pivotal role in deciding the cell fate, present study was undertaken to explore the potential of 1,4-naphthoquinone (NQ), a pro-oxidant, to ameliorate IR induced GI syndrome. NQ protected INT 407 cells against IR induced cell death of intestinal epithelial cells *in vitro*. NQ induced perturbation in cellular redox status and induced the activation of nuclear factor-erythroid 2-related factor 2 (Nrf2) pathway. Thiol antioxidant and inhibitors of Nrf2 pathway abrogated the radioprotection offered by NQ. Further, knocking down Nrf2 rescind the NQ mediated protection against IR induced cell death. In conclusion, NQ protects against IR radiation induced GI syndrome *in vitro* by perturbing cellular redox and activating Nrf2 pathway. This is the first report highlighting the potential of a pro-oxidant to ameliorate IR induced GI injury.**

Keywords: Radioprotection, cellular redox status, ERK/Nrf2 pathway, Nrf2 knockdown

1. Introduction

Increased use of ionising radiation (IR) as treatment modality in multiple carcinomas and augmented risk of unplanned exposure due to nuclear proliferation and radioactive waste disposal have potentiated the need of a potent radioprotective agent which would be useful in multiple operational scenarios. Acute illness caused due to high doses of IR is termed as acute radiation syndrome (ARS). ARS is a dose dependent damage affecting the hematopoietic, gastro-intestinal (GI), cerebrovascular and cutaneous systems in the body (*1,2*). Rapidly proliferating cells and their respective organs are more sensitive towards IR induced cell death. Epithelial cells located in the small intestinal crypts divide rapidly and are among the most susceptible cells in the body to IR induced death. Higher susceptibility of GI tract to IR is the major limiting factor in radiation therapy of abdominal and pelvic malignancies (*3-5*).

Acute effects after doses above 8 Gy are known as gastrointestinal syndrome which causes mortality in 8 to 12 days. GI syndrome is characterized by loss in the absorptive surface of small intestine called as jejunum due to denudation of villi and apoptosis in submucosal invaginations called crypts of Lieberkuhn resulting in vomiting, diarrhoea, anorexia, dehydration, systemic infection and septic shock induced death in severe cases (*6*). Each crypt in jejunum contains intestinal stem cells (ISC) at the base which are responsible to supply the differentiated enterocytes to maintain homeostasis (*7,8*). Lineage-tracing experiments illustrated that a $Lgr5^+$ cell produced terminally differentiated epithelial lineages of mouse intestine (*9*). Further, a single $Lgr5^+$ stem cell is capable of generating crypt/villus organoids i*n vitro*

Released online in J-STAGE as advance publication April 13, 2016.

**Address correspondence to:*
Dr. Lokesh Gambhir, Department of Life Sciences, Shri Guru Ram Rai Institute of Technology and Sciences, Dehradun, Uttarakhand, India.
E-mail: gambhir.lokesh@gmail.com

containing differentiated intestinal mucosa cell lineages (*10*). However, exposure to radiation induces apoptosis in ISC, thus delimiting their potential to repopulate the denudated absorptive surface (*4,8,11*).

Since large part of IR induced damages are mediated due to generation of reactive oxygen species (ROS), much of the efforts in past were targeted to explore the potential of antioxidants to ameliorate IR induced toxicities. However recent advances have highlighted that activation of pro-survival pathways could serve as a novel target in developing a potent radioprotector. CBLB502 protected against IR induced mortality due to GI syndrome by activating NF-κB pathway (*12*). An anti-ceramide monoclonal antibody protected against apoptosis in the small intestine and whole body irradiation (WBI) induced mortility in mice (*13*). Lactobacillus probiotic was shown to protect against WBI induced apoptosis in intestinal epithelial cells in TLR-2 and cyclo-oxygenase-2 dependent manner (*14*). Sphingosine-1-phosphate, a ceramide antagonist, protected against WBI induced endothelial apoptosis in intestine by activating Akt pathway (*15*). R-spondin 1 improved survival percentage in mice exposed to WBI doses inducing GI syndrome by activating Wnt/β-catenin pathway (*16*). Despite of the potent efficacy of investigated agents, associated toxicity delimits their use in operational scenarios creating the dearth of agents with prolonged efficacy, broad specificity, and minimal toxicity to increase the benefit of radiation therapy in cancer treatment *(2*).

Recently, activation of redox sensitive pro-survival transcription factor nuclear factor-erythroid 2-related factor 2 (Nrf2) was shown to protect colonic epithelial cells from IR induced loss in cell viability (*17*). Activation of Nrf2 was shown to protect against oxidative stress induced cell death implicated in pathogenesis of ischemia, inflammation and cancer. Nrf2 has been shown to control the expression of intestinal detoxification and intestinal stem cell proliferation in drosophila. Previously, 1,4-naphthoquinone (NQ), a pro-oxidant, was shown to ameliorate radiation induced hematopoietic syndrome and exhibit anti-inflammatory effects by activation of Nrf2 pathway (*18,19*). Based on the embroiled role of Nrf2 in maintaining intestinal homeostasis, we hypothesised that modulation of cellular redox mediated activation of Nrf2 by a pro-oxidant might provide an adaptive response to confer protection against radiation induced GI syndrome. In the present study we highlight the potential of NQ, a pro-oxidant, to ameliorate radiation induced GI syndrome by activating Nrf2 pathway.

2. Materials and Methods

2.1. *Chemicals*

NQ, HEPES, ethylenediaminetetracetate (EDTA), ethylene glycol tetraacetic acid (EGTA), phenylmethylsulfonyl fluoride (PMSF), dimethyl sulfoxide (DMSO), leupeptin, aprotinin, benzamidine, dithiothreitol (DTT), dichlorofluorescein diacetate (H2DCF-DA), penicillin, streptomycin, crystal violet, N-acetyl cysteine (NAC) and Nonidet P-40 were purchased from Sigma Chemical Co. (St. Louis, MO, USA). cDNA synthesis kit, chemiluminiscence kit and SYBR green PCR mix were procured from Roche Chemical Co. (San Francisco, CA, USA). Roswell Park Memorial Institute (RPMI-1640) medium and fetal bovine serum (FBS) was obtained from HiMedia (Kennett Square, PA, USA). All-trans-retinoic acid (ATRA), PD98059 (ERKi) and JC-1 fluorescent dye were purchased from Calbiochem (Billerica, Massachusetts, USA). Hoechst 33342 was procured from Invitrogen (Carlsbad, CA, USA). Antibodies against pERK, ERK, pMEK, MEK and β-actin were procured from Cell Signalling Technologies (Danver, MA, USA). Anti-Nrf2 antibody and oligonucleotide probe for Nrf2 was procured from Santacruz Biotechnology (Santa Cruz, CA, USA). All other chemicals were purchased from reputed local manufacturers.

2.2. *Cell culture*

INT 407 (human intestinal epithelial cell line) cells were obtained from Health Protection Agency Culture Collections (HPACC, Salisbury, Wiltshire, UK) were cultured in Roswell Park Memorial Institute (RPMI-1640) medium containing 10% fetal bovine serum and antibiotics (100 U/mL penicillin and 100 µg/mL streptomycin) at 37°C in an atmosphere of 5% CO_2.

2.3. *Treatment with NQ*

Stock solution of NQ was prepared in DMSO, stored as small aliquots at -20ºC. In all *in vitro* experiments, cells were treated with different doses of NQ for 2 h or NQ 1 µM for indicated time interval before the initiation of culture. DMSO was used as vehicle control.

2.4. *Irradiation schedule*

INT 407 cells in medium were irradiated at a dose rate of 1.2 Gy/min in a blood irradiator (BRIT, Mumbai, India).

2.5. *Measurement of change in mitochondrial membrane potential (MMP)*

INT 407 Cells were treated with NQ 1 µM for 2 h followed by radiation dose of 15 Gy and were cultured for 24 h at 37°C. MMP was assessed using the mitochondrial-specific cationic fluorescent probe JC-1 (10 µM) by spectroflourimetric method as described previously (*20*).

2.6. *Caspase 3 assay*

INT 407 Cells were treated with NQ 1 μM for 2 h followed by radiation dose of 15 Gy and were cultured for 24 h at 37°C. Caspase 3 activity was measured following manufacturer`s protocol (Caspase 3 Assay Kit, Colorimetric, Sigma Aldrich, St. Louis, MO, USA).

2.7. *Clonogenic cell survival assay*

One thousand INT 407 cells were cultured in 100-mm culture dishes and treated with ATRA (Nrf2 inhibitor) or PD98059 (ERK inhibitor) or NAC for 2 h followed by treatment with NQ 1 μM for 2 h and then irradiated with dose of 6 Gy or 7 Gy or 8 Gy. Cells were allowed to grow for 14 days to form colonies, which were then stained with crystal violet (0.4 g/L), and colonies were counted using colony counter (*20*).

2.8. *Intracellular ROS measurements*

INT 407 cells were incubated with 20 μM oxidation-sensitive dichlorofluorescein diacetate (H_2DCF-DA) for 25 min at 37°C and then treated with NQ 1 μM for indicated time points. After incubation, the increase in fluorescence resulting from oxidation of H2DCF to DCF was measured using a spectrofluorimeter (*21*).

2.9. *Determination of intracellular glutathione (GSH) and glutathione disulfide (GSSG) levels*

INT 407 cells were pre-treated with NQ 1 μM for indicated points. Intracellular GSH/GSSG ratio was measured spectrophotometrically by conventional enzyme cycling method (*22*).

2.10. *Quantitative Real Time PCR*

INT 407 cells were pre-treated with NQ 1 μM for indicated points. RNA isolation, cDNA synthesis and RT-PCR were performed as described previously (*21*). Briefly, total RNA was isolated from the samples using Trizol reagent. One μg of total RNA was used for preparation of cDNA by reverse transcription (cDNA synthesis kit, Roche Chemical Co, San Francisco, CA, USA) following the manufacturer's instructions. Quantitative PCR was carried out using a Rotor Gene 3000 (Corbett Research, Mortlake, NSW, Australia) machine. The threshold cycle values were used for calculating the expression levels of genes by REST-384 version-2 software (*23*). PCR efficiency was calculated for individual primer pairs. Specific primer sequences were obtained from primer bank (Table 1). Expression of the genes was normalized against a house keeping gene, β-actin and plotted as relative change in expression with respect to control.

Table 1. List of specific primers for RT-PCR

Gene	Sequence
HO-1	Forward: AGGTACACATCCAAGCCGAGA
	Reverse: CCATCACCAGCTTAAAGCCTT
GCLC	Forward: CTACCACGCAGTCAAGGACC
	Reverse: CCTCCATTCAGTAACAACTGGAC
Nrf2	Forward: CTTTAGTCAGCGACAGAAGGAC
	Reverse: AGGCATCTTGTTTGGGAATGTG
MnSOD	Forward: CAGACCTGCCTTACGACTATGG
	Reverse: CTCGGTGGCGTTGAGATTGTT
Catalase	Forward: AGCGACCAGATGAAGCAGTG
	Reverse: AGGACATCAGGTCTCTGCGA
β-actin	Forward: GCGGGAAATCGTGCGTGACATT
	Reverse: GATGGAGTTGAAGGTAGTTTCGTG

2.11. *Western blot analysis*

INT 407 cells were pre-treated with different concentrations of NQ for 12 h or NQ (1 μM) for indicated time points. Cytosolic extracts were prepared as described earlier (*20*). Vehicle treated cells served as a control. Equal amount of protein was resolved by SDS-PAGE (10%), transferred to nitrocellulose membrane, blocked and incubated overnight with the primary antibody specific to pERK, ERK, pMEK, MEK and β-actin. After subsequent washing, membrane was further incubated with horseradish peroxidase-labeled secondary antibody for 2 h and specific bands were visualized on X-ray films using Enhanced Chemiluminiscence Kit. β-actin was used as loading control.

2.12. *Determination of nuclear levels of Nrf2 using confocal microscopy*

INT 407 cells were treated with NQ (1 μM) at indicated time intervals. The cells were labelled with anti-Nrf2 antibody as described previously (*24*). Further, these cells were stained with FITC-labelled secondary antibody followed by PI staining. Slides were examined using an LSM510 confocal microscope (Carl Zeiss, Jena, Germany) with a krypton-argon laser coupled to an Orthoplan Zeiss photomicroscope.

2.13. *Electrophoretic mobility shift assay*

INT 407 cells were pre-treated with NQ 1 μM for indicated time points and different concentrations of NQ for 12 h at 37°C. Nuclear extracts were prepared as described earlier (*19*). EMSA was performed by incubating 8μg of nuclear proteins with 16 fmol of ^{32}P-end-labeled, 45-mer double stranded NF-κB oligonucleotides from the human immunodeficiency virus long terminal repeat (5′-TTGTTACAA**GGGA CTTTCCGCTGGGGACTTTCC**AGGGAGGCG TGG-3′; boldface indicates NF-κB binding sites) in the presence of 0.5 μg of poly (2′-deoxyinosinic-2′-deoxycytidylic acid) in binding buffer for 30 min

at 37°C. The DNA-protein complex formed was separated from free oligonucleotide on 7.6% native polyacrylamide gels. The dried gel was exposed to phosphorimage plate and the radioactive bands were visualized using a PhosphorImage plate scanner (Amersham Biosciences, Piscataway, NJ, USA).

2.14. *shRNA knockdown studies*

Nrf2 shRNA plasmid (cat no. TF515053, Origene, Rockville, MD, USA) was used for knocking down Nrf2 in INT 407 cells. Transfection was performed using Neon® Transfection System (Invitrogen, Carlsbad, CA, USA) following manufacturer`s protocol. Briefly, 5 million cells were electroporated (pulse voltage 1005 and pulse width 35 ms) using 1 µg of nrf2 shRNA in antibiotic free medium. Cells were further cultured for 48 h for transgene expression. Knockdown INT 407 cells were treated with NQ 1 µM for 2 h followed by radiation dose of 6 Gy. Cells were further subjected to clonogenic assay as discussed earlier (*20*).

2.15. *Statistical analysis*

The statistical analysis was done using analysis of variance with Microcal OriginPro 8.0 software followed by post hoc analysis using Schiffe's test. * refers to $p < 0.01$, as compared to control, # refers to $p < 0.01$ as compared to irradiated group and $ refers to $p < 0.01$ as compared to NQ + IR group. Data points represent mean ± SEM from three replicates, and two independent experiments were performed.

3. Results

3.1. *NQ significantly protected against radiation induced cell death of INT 407 cells*

INT 407, a human intestinal epithelial cell line, was used as an *in vitro* model system to decipher the potential of NQ to protect against radiation induced GI syndrome. Cells were pre-treated with NQ 1 µM for 2 h followed by exposure to radiation 6 Gy or 7 Gy or 8 Gy. Vehicle treated cells served as control. Effect of radiation on viability of INT 407 cells was assessed by monitoring changes in proliferating potential which is defined by the ability of a single cell to grow as a colony. Clonogenic assay is the method of choice to determine cell reproductive death after treatment with radiation. Exposure to radiation induced significant reduction in the percent surviving fraction. Interestingly, treatment with NQ significantly (55% at 6 Gy, 38% at 7 Gy and 28% at 8 Gy) protected against radiation induced loss of clonogenicity (Figure 1A). Further, modulation in mitochondrial membrane potential and caspase 3 activity was also monitored to decipher the effect of NQ on radiation induced apoptosis. Vehicle treated cells served as control. Exposure to radiation induced a significant reduction in MMP (64%) and increase in caspase 3 activity indicating the induction of

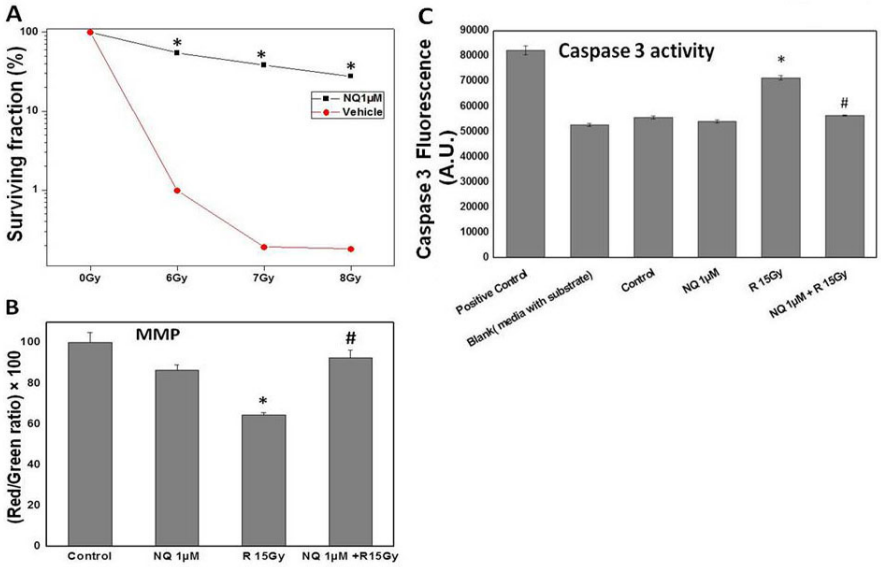

Figure 1. NQ offered radioprotection in INT 407 cells. (A) INT 407 cells were treated with NQ 1 µM for 2 h followed by radiation exposure of 6 Gy or 7 Gy or 8 Gy. Vehicle treated cells served as control. Cells were incubated for 14 days to monitor the clonogenic potential. Line graphed is the percent surviving fraction at the indicated doses of IR. **(B)** Cells were treated with NQ 1 µM or vehicle for 2 h followed by exposure to radiation dose of 15 Gy and were incubated for 24 h. Cells were harvested and stained with JC-1 dye to monitor IR induced loss in mitochondrial membrane potential in respective groups. Graphed is the percentage loss of mean (red/green) fluorescence of JC-1. **(C)** NQ inhibited IR induced increase in Caspase 3 activity. Cells were treated with NQ 1 µM or vehicle for 2 h followed by exposure to radiation dose of 15 Gy and were incubated for 24 h. Graphed is the arbitrary fluorescence unit representing the caspase 3 activity. Each bar represents mean ± S.E.M. from three replicates and two such independent experiments were carried out. The statistical analysis was done using analysis of variance followed by post hoc analysis using Schiffe's test. *$p < 0.01$, as compared to control, # refers to $p < 0.01$ as compared to irradiated group.

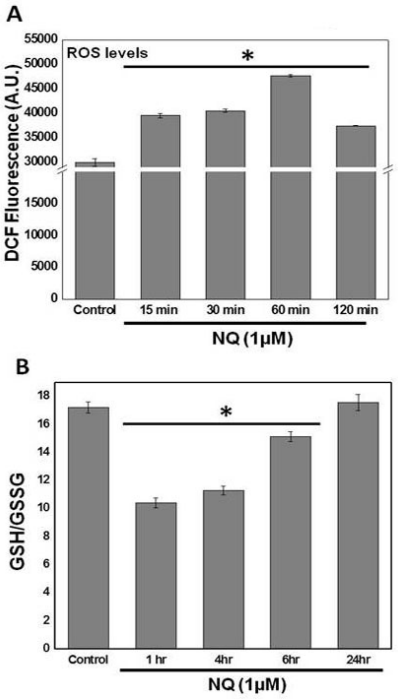

Figure 2. NQ induced perturbation of cellular redox status. (A) NQ induced a transient increase in the basal ROS levels. DCFH2-DA-stained INT 407 were treated with NQ 1 μM for indicating time intervals at 37°C and fluorescence emission was measured at 535 nm. **(B)** NQ induced a transient decrease in the levels of redox couple GSH/GSSG. INT 407 cells were treated with NQ 1 μM for indicated time intervals. GSH/GSSG ratio was estimated using enzyme cycling method. Each bar represents mean ± S.E.M. from three replicates and two such independent experiments were carried out. The statistical analysis was done using analysis of variance followed by post hoc analysis using Schiffe's test. *$p < 0.01$, as compared to control.

apoptosis. Interestingly, treatment with NQ significantly ameliorated radiation induced apoptosis by protecting against loss of mitochondrial membrane potential (92%) and abrogated the increase in caspase 3 activity (Figures 1B and 1C).

3.2. *NQ modulated cellular redox status in INT 407 cells*

Cellular redox status is impervious for normal functioning of cell. Pro-oxidants being a strong electrophile are known to modulate the cellular redox status which serves as the prime mediator of its effect. Effect of NQ to modulate cellular redox status was evaluated by monitoring changes in ROS and GSH/GSSG levels. DCFDA stained INT 407 cells were treated with NQ 1 μM at indicated time points to monitor the changes in levels of ROS. NQ treatment induced a transient increase in basal ROS levels (Figure 2A) indicating its pro-oxidant effect. GSH/GSSG, endogenous antioxidant, is a major redox couple involved in maintaining the cellular redox homeostasis. Being a strong electrophile, NQ exhibits a strong attraction towards cellular nucleophiles like GSH and may modulate their levels. Thus, effect of NQ was observed on the levels of GSH/GSSG. NQ induced a fleeting depletion in GSH/GSSG ratio which with long time exposure came back to control levels (Figure 2B). These results further highlight the non toxic effect of NQ as incessant depletion in the levels of GSH may be associated to cell death.

3.3. *NQ induced activation of Nrf2, a pro-survival transcription factor, pathway in INT 407 cells*

NQ previously has been shown to activate mitogen activated protein kinases (MAPK) in lymphocytes (*18*). Also, perturbation in cellular redox status is known to activate key redox sensitive regulatory transcription factor Nrf2. Therefore, potential of NQ to activate MAPK upstream of Nrf2 was explored. MEK-1 is a dual threonine and tyrosine recognition kinase that phosphorylates and activates extracellular-signal-regulated kinases (ERK). NQ induced activation of MEK and ERK, upstream kinases in Nrf2 pathway, in concentration and time dependent manner (Figure 3A). Since NQ modulated cellular redox status and activated upstream ERK, the effect of NQ on redox sensitive cytoprotective transcription factor Nrf2 was monitored. NQ increased the mRNA levels of Nrf2 and its dependent cytoprotective/antioxidant genes (MnSOD, HO-1, GCLC and Catalase) in a time dependent manner (Figure 3B). INT 407 cells were treated with NQ 1 μM for different time points to monitor the nuclear translocation of Nrf2. NQ induced Nrf2 nuclear translocation at 12 h and 24 h (Figure 3C). Further, INT 407 cells were treated with different concentrations of NQ for 12 h to monitor the binding of Nrf2 to its consensus sequence (Antioxidant Response Element). It was observed that NQ markedly increase the activation of Nrf2 as evident by enhanced DNA binding in EMSA (Figure 3D).

3.4. *Thiol antioxidants and Nrf2 inhibitor abrogated NQ mediated protection against radiation induced cell death*

Contribution of NQ induced perturbation of cellular redox status and activation of ERK/Nrf2 pathway in its radioprotective effect was monitored by employing pharmacological inhibitors ERKi (PD98059, ERK inhibitor) and ATRA (Nrf2 inhibitor) and NAC (thiol antioxidant). Clonogenic method was employed to monitor the effect of inhibitors on radioprotective potential of NQ. Employing these inhibitors alone does not offer any protection against radiation induced loss of proliferating potential in clonogenic assay. NQ treatment significantly (41% surviving fraction) protected against radiation induced loss (5% surviving fraction) of clonogenicity. Intriguingly, employment of NAC and ERKi along with NQ showed 11% and 15% surviving fraction indicating a significant abrogation of the NQ mediated radioprotection. Employing

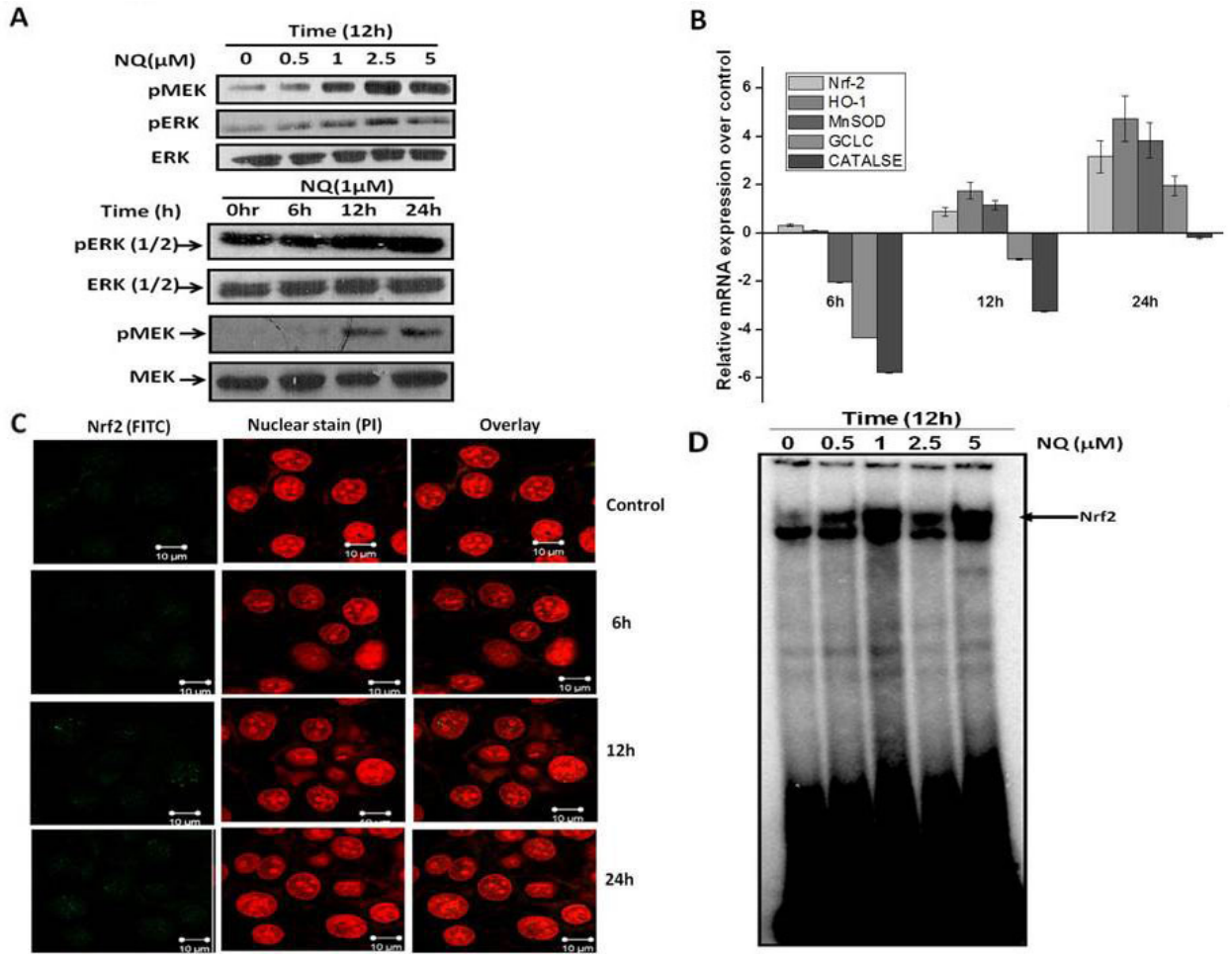

Figure 3. NQ induced activation of ERK/Nrf2 pathway. (A) INT 407 cells were treated with different concentrations of NQ for 12 h or with NQ 1 μM for indicated time intervals. Cytoplasmic extracts were fractionated on 10% non-reducing SDS-PAGE, and electrotransferred to nitrocellulose membrane. Western blot analysis was performed using antibodies specific for pMEK, MEK, pERK, ERK and β-actin. **(B)** INT 407 cells were treated with NQ 1 μM for 6 h, 12 h and 24 h, mRNA was isolated and used for real time RT-PCR. Bar diagram shows relative mRNA copy number of Nrf2, HO-1, MnSOD, GCLC and Catalase over control. Each bar represents mean ± S.E.M. from three replicates and two such independent experiments were carried out. **(C)** INT 407 cells were treated with NQ 1 μM for 6 h, 12 h and 24 h, stained with FITC labelled anti-Nrf2 antibody and PI. FITC (left)/PI(mid)/ overlay(right) is shown. **(D)** INT 407 cells were treated with NQ 1 μM for 6 h, 12 h and 24 h, EMSA was performed using nuclear extracts.

ATRA showed complete abrogation (4% surviving fraction equivalent to radiation treatment) of NQ induced protection against radiation induced loss of clonogenicity in INT 407 cells (Figures 4A and 4B). These results indicated that the modulation in cellular redox and activation of Nrf2 might be the underlying mechanism of NQ mediated protection against radiation induced GI syndrome.

3.5. *Knocking down Nrf2 significantly abrogated the NQ mediated radioprotection*

Knock down studies were adopted to contemplate the central role of Nrf2 pathway in NQ mediated protection against radiation induced cell death. INT 407 cells were transfected with Nrf2 shRNA or scrambled shRNA to create a transient knock down. After 24 h, transfected cells with ablated Nrf2 were washed and treated with NQ 1 μM for 2 h prior to radiation exposure of 6 Gy and were further monitored for loss in clonogenicity. NQ treatment offered significant (57% survival fraction) protection against radiation induced cell death in mock control and scrambled shRNA transfected cells. Interestingly, knocking down Nrf2 pathway completely abrogated (8% survival fraction in cells with ablated Nrf2) the NQ mediated protection against radiation induced clonogenic death (Figures 5A and 5B). Further, ablation in ERK and Nrf2 dependent cytoprotective gene, HO-1, also showed the significant abrogation of NQ mediated radioprotection (data not shown). These results contemplated our hypothesis that activation of Nrf2 is a central regulator and pivotal for NQ induced protection against radiation induce GI syndrome.

4. Discussion

Maintenance of cellular redox homeostasis is impervious to maintain cell viability and normal physiological

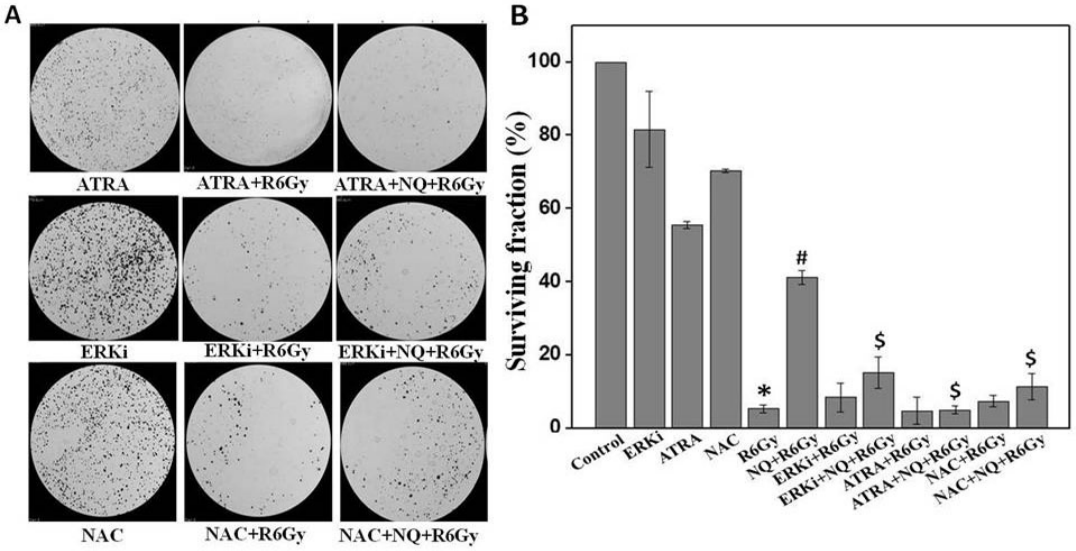

Figure 4. Thiol antioxidant and ERK/Nrf2 pathway inhibitors abrogated the NQ mediated radioprotection. INT 407 cells were pretreated with NQ or NAC (1 mM) or ERKi (PD98059, 5 μM) or ATRA (Nrf2i, 1 μM) for 2 h before being exposed to IR dose of 6 Gy and cultured for 14 days to monitor the clonogenic potential. Vehicle treated cells served as control. Visible colonies were enumerated after staining with crystal violet. **(A)** Pictures shown represent the observed stained colonies from the respective groups. **(B)** Graphed is the percent surviving fraction obtained after enumerating the visible colonies. Each bar represents mean ± S.E.M. from three replicates and two such independent experiments were carried out. The statistical analysis was done using analysis of variance followed by post hoc analysis using Schiffe's test. *$p < 0.01$, as compared to control, # refers to $p < 0.01$ as compared to irradiated group and $ refers to $p < 0.01$ as compared to NQ + IR group.

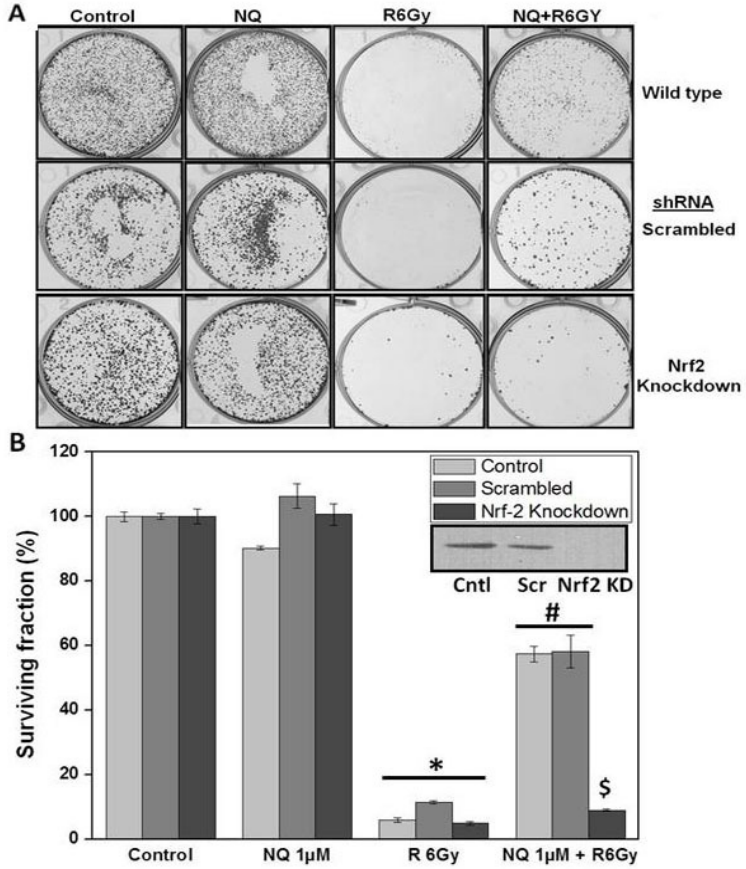

Figure 5. Knocking down Nrf2 reversed the radioprotection offered by NQ in INT 407 cells. INT 407 cells were transfected with scrambled shRNA or Nrf2 shRNA plasmid and were incubated for 24 h. Transfected cells were treated with vehicle or NQ 1 μM for 2 h followed by exposure to IR dose of 6 Gy. Cells were further cultured for 14 days to monitor the clonogenic potential. Visible colonies were enumerated after staining with crystal violet. **(A)** Pictures shown represent the observed stained colonies from the respective groups. **(B)** Graphed is the percent surviving fraction obtained after enumerating the visible colonies. Each bar represents mean ± S.E.M. from three replicates and two such independent experiments were carried out. The statistical analysis was done using analysis of variance followed by post hoc analysis using Schiffe's test. *$p < 0.01$, as compared to control, # refers to $p < 0.01$ as compared to irradiated group and $ refers to $p < 0.01$ as compared to NQ + IR group.

responses. Under normal physiological conditions, cells are exposed to multiple exogenous and endogenous oxidative stresses (*25*). Cells are equipped with network of antioxidant enzymes that plays a pivotal role in detoxification of ROS. The equilibrium between generation and elimination of ROS maintains the cellular redox homeostasis which acts to resist against various stress conditions. ROS are known to play dual role depending upon the magnitude of generation (*26*). High levels of ROS induce activation of apoptotic pathway whereas low levels of ROS initiate the induction of cytoprotective responses. The functional status of cellular antioxidant systems and the redox-sensitive survival signaling pathways can significantly influence the cell-fate against deleterious stimuli (*27*). Therefore, perturbation of cellular redox status by inducing mild oxidative stress may lead to activation of redox sensitive pro-survival pathways. Mild oxidative stress may thus serve as an amenable strategy to develop novel redox based therapeutics/preventive agents.

As radiation induced toxicity is mediated by generation of ROS, employing a potent antioxidant as agents to act as radioprotector seem to be the promising strategy. Though most of the agents investigated have been associated with off target effects and none have been approved by FDA to be used as radioprotector except amifostine (*28-30*). Amifostine has been approved to be used along with cisplatin in radiotherapy however it's not been approved for use outside clinic as it is also associated with the induction of multiple side effects, including nausea, vomiting, sneezing and hypertension (*31-34*). Thus multiple efforts have been undertaken to identify novel targets that could be exploited to develop novel radioprotective agents. Although plethora of agents has been shown to protect against IR induced hematopoietic syndrome, few have been documented to protect against IR induced GI syndrome (*2,35*). Radiation induced GI syndrome is one of the major cause of health impairments or in extreme cases death characterised by denudated villi and apoptosis in crypts. Humans are at higher risk of developing acute and chronic symptoms known as intestine mucositis including pain, ulceration, vomiting and diarrhoea at doses above 2 Gy (*36,37*). ISC present at the base of the crypts called as columnar base cells are responsible for maintaining the homeostasis in intestine. Exposure to ionising radiation induces apoptosis in the ISC which abolishes the regeneration of the denudated villi and marks the rapid onset of GI syndrome (*8,38-40*). Multiple strategies have been employed to investigate the novel targets as well as agents with potential to ameliorate or mitigate the radiation induced damages with lesser side effects.

NQ, a pro-oxidant, has been shown to protect against radiation induced hematopoietic syndrome and its potential to act as anti-inflammatory agent by activating Nrf2 pathway in lymphocytes. Present study was undertaken to investigate the potential of NQ to protect at high doses of IR using *in vitro* model, human intestinal epithelial cell, INT 407. Interestingly, NQ protected against radiation induced cell death in INT 407 cells (Figure 1). Since NQ is a known pro-oxidant, it perturbs the cellular redox status of the INT 407 cells by increasing the basal level of ROS and depleting GSH/GSSG (Figure 2). Higher redox potential and electrophilic nature of quinones imparts high affinity for cellular nucleophiles like thiols of cysteine group present in proteins and glutathione contributing to its biological activity (*41*). Perturbation in cellular redox status is known to activate redox sensitive pro-survival transcription factor Nrf2 and its dependent cytoprotective genes (*42-45*). Activation of Nrf2 has been shown to maintain intestine homeostasis, protect against radiation induced DNA strand breaks in intestine and to regulate the intestinal stem cell proliferation. Activation of Nrf2 results in elevated levels of cytoprotective genes which provide an adaptive response to protect against radiation induced damage (*17,46,47*). NQ induced the activation of ERK/Nrf2 axis in time and concentration dependent manner in INT 407 cells (Figure 3). Captivatingly, thiol antioxidant and inhibitors of ERK/Nrf2 pathway abrogated NQ mediated radioprotection contemplating the imperative role of Nrf2 (Figure 4). Further, knock down studies using shRNA of Nrf2 corroborated the significance of activation of Nrf2 pathway as underlying mechanism of NQ induced protection against IR induced GI syndrome (Figure 5). Further investigations in *in vivo* model system are required to corroborate the present findings.

To best of our knowledge, this is the first report illustrating the salutary effect of a pro-oxidant in the perspective of radiation induced GI syndrome where it played a protective role by inhibiting radiation induced cell death. Since, NQ has a profound anti-cancer activity; it may find application in increasing the therapeutic ratio of abdominal irradiation in GI malignancies. These findings further provide evidence for the putative role of Nrf2 as a key player in developing novel radioprotective agents.

Acknowledgements

The author is grateful for the guidance and support provided by Dr. S. Santosh kumar and Dr. Deepak Sharma (Bhabha Atomic Research Centre). The financial support from Homi Bhabha National Institute is kindly acknowledged.

References

1. Lopez M, Martin M. Medical management of the acute radiation syndrome. Rep Pract Oncol Radiother. 2011; 16:138-146.

2. Singh VK, Romaine PL, Seed TM. Medical countermeasures for radiation exposure and related injuries: Characterization of medicines, FDA-approval status and inclusion into the strategic national stockpile. Health Phys. 2015; 108:607-630.
3. Potten CS. A comprehensive study of the radiobiological response of the murine (BDF1) small intestine. Int J Radiat Biol. 1990; 58:925-973.
4. Potten CS, Booth C, Tudor GL, Booth D, Brady G, Hurley P, Ashton G, Clarke R, Sakakibara S, Okano H. Identification of a putative intestinal stem cell and early lineage marker; musashi-1. Differentiation. 2003; 71:28-41.
5. Williams JP, Brown SL, Georges GE, Hauer-Jensen M, Hill RP, Huser AK, Kirsch DG, Macvittie TJ, Mason KA, Medhora MM. Animal models for medical countermeasures to radiation exposure. Radiat Res. 2010; 173:557-578.
6. Zimmerer T, Bocker U, Wenz F, Singer MV. Medical prevention and treatment of acute and chronic radiation induced enteritis--is there any proven therapy? a short review. Z Gastroenterol. 2008; 46:441-448.
7. Cheng H, Leblond CP. Origin, differentiation and renewal of the four main epithelial cell types in the mouse small intestine. V. Unitarian Theory of the origin of the four epithelial cell types. Am J Anat. 1974; 141:537-561.
8. Potten CS, Owen G, Booth D. Intestinal stem cells protect their genome by selective segregation of template DNA strands. J Cell Sci. 2002; 115:2381-2388.
9. Barker N, van Es JH, Kuipers J, Kujala P, van den Born M, Cozijnsen M, Haegebarth A, Korving J, Begthel H, Peters PJ. Identification of stem cells in small intestine and colon by marker gene Lgr5. Nature. 2007; 449:1003-1007.
10. Sato T, Vries RG, Snippert HJ, van de Wetering M, Barker N, Stange DE, van Es JH, Abo A, Kujala P, Peters PJ. Single Lgr5 stem cells build crypt-villus structures *in vitro* without a mesenchymal niche. Nature. 2009; 459:262-265.
11. Qiu W, Leibowitz B, Zhang L, Yu J. Growth factors protect intestinal stem cells from radiation-induced apoptosis by suppressing PUMA through the PI3K/AKT/p53 axis. Oncogene. 2010; 29:1622-1632.
12. Burdelya LG, Krivokrysenko VI, Tallant TC, Strom E, Gleiberman AS, Gupta D, Kurnasov OV, Fort FL, Osterman AL, Didonato JA. An agonist of toll-like receptor 5 has radioprotective activity in mouse and primate models. Science. 2008; 320:226-230.
13. Rotolo J, Stancevic B, Zhang J, Hua G, Fuller J, Yin X, Haimovitz-Friedman A, Kim K, Qian M, Cardo-Vila M. Anti-ceramide antibody prevents the radiation gastrointestinal syndrome in mice. J Clin Invest. 2012; 122:1786-1790.
14. Ciorba MA, Riehl TE, Rao MS, Moon C, Ee X, Nava GM, Walker MR, Marinshaw JM, Stappenbeck TS, Stenson WF. Lactobacillus probiotic protects intestinal epithelium from radiation injury in a TLR-2/cyclo-oxygenase-2-dependent manner. Gut. 2012; 61:829-838.
15. Bonnaud S, Niaudet C, Legoux F, Corre I, Delpon G, Saulquin X, Fuks Z, Gaugler MH, Kolesnick R, Paris F. Sphingosine-1-phosphate activates the AKT pathway to protect small intestines from radiation-induced endothelial apoptosis. Cancer Res. 2010; 70:9905-9915.
16. Bhanja P, Saha S, Kabarriti R, Liu L, Roy-Chowdhury N, Roy-Chowdhury J, Sellers RS, Alfieri AA, Guha C. Protective role of R-spondin1, an intestinal stem cell growth factor, against radiation-induced gastrointestinal syndrome in mice. PLoS One. 2009; 4:e8014.
17. Kim SB, Pandita RK, Eskiocak U, Ly P, Kaisani A, Kumar R, Cornelius C, Wright WE, Pandita TK, Shay JW. Targeting of Nrf2 induces DNA damage signaling and protects colonic epithelial cells from ionizing radiation. Proc Natl Acad Sci U S A. 2012; 109:E2949-2955.
18. Khan NM, Sandur SK, Checker R, Sharma D, Poduval TB, Sainis KB. Pro-oxidants ameliorate radiation-induced apoptosis through activation of the calcium-ERK1/2-Nrf2 pathway. Free Radic Biol Med. 2011; 51:115-128.
19. Gambhir L, Checker R, Thoh M, Patwardhan RS, Sharma D, Kumar M, Sandur SK. 1,4-Naphthoquinone, a pro-oxidant, suppresses immune responses *via* KEAP-1 glutathionylation. Biochem Pharmacol. 2014; 88:95-105.
20. Wilankar C, Sharma D, Checker R, Khan NM, Patwardhan RS, Patil A, Sandur SK, Devasagayam TP. Role of immunoregulatory transcription factors in differential immunomodulatory effects of tocotrienols. Free Radic Biol Med. 2011; 51:129-143.
21. Patwardhan RS, Checker R, Sharma D, Kohli V, Priyadarsini KI, Sandur SK. Dimethoxycurcumin, a metabolically stable analogue of curcumin, exhibits anti-inflammatory activities in murine and human lymphocytes. Biochem Pharmacol. 2011; 82:642-657.
22. Rahman I, Kode A, Biswas SK. Assay for quantitative determination of glutathione and glutathione disulfide levels using enzymatic recycling method. Nat Protoc. 2006; 1:3159-3165.
23. Pfaffl MW, Horgan GW, Dempfle L.Relative expression software tool (REST) for group-wise comparison and statistical analysis of relative expression results in real-time PCR. Nucleic Acids Res. 2002; 30:e36.
24. Checker R, Sharma D, Sandur SK, Subrahmanyam G, Krishnan S, Poduval TB, Sainis KB. Plumbagin inhibits proliferative and inflammatory responses of T cells independent of ROS generation but by modulating intracellular thiols. J Cell Biochem. 2010; 110:1082-1093.
25. Adler V, Yin Z, Tew KD, Ronai Z. Role of redox potential and reactive oxygen species in stress signaling. Oncogene. 1999; 18:6104-6111.
26. Trachootham D, Lu W, Ogasawara MA, Nilsa RD, Huang P. Redox regulation of cell survival. Antioxid Redox Signal. 2008; 10:1343-1374.
27. Thannickal VJ, Fanburg BL. Reactive oxygen species in cell signaling. Am J Physiol Lung Cell Mol Physiol. 2000; 279:L1005-1028.
28. Andreassen CN, Grau C, Lindegaard JC. Chemical radioprotection: A critical review of amifostine as a cytoprotector in radiotherapy. Semin Radiat Oncol. 2003; 13:62-72.
29. Hensley ML, Schuchter LM, Lindley C, Meropol NJ, Cohen GI, Broder G, Gradishar WJ, Green DM, Langdon RJ, Mitchell RB. American Society of Clinical Oncology clinical practice guidelines for the use of chemotherapy and radiotherapy protectants. J Clin Oncol. 1999; 17:3333-3355.
30. Yuhas JM. Radiotherapy of experimental lung tumors in the presence and absence of a radioprotective drug, S-2-

(3-aminopropylamino)ethylphosphorothioic acid (WR-2721). J Natl Cancer Inst. 1973; 50:69-78.
31. Citrin D, Cotrim AP, Hyodo F, Baum BJ, Krishna MC, Mitchell JB. Radioprotectors and mitigators of radiation-induced normal tissue injury. Oncologist. 2010; 15:360-371.
32. Eisbruch A. Amifostine in the treatment of head and neck cancer: Intravenous administration, subcutaneous administration, or none of the above. J Clin Oncol. 2011; 29:119-121.
33. Hosseinimehr SJ. Trends in the development of radioprotective agents. Drug Discov Today. 2007; 12:794-805.
34. Landauer MR, Davis HD, Kumar KS, Weiss JF. Behavioral toxicity of selected radioprotectors. Adv Space Res. 1992; 12:273-283.
35. Singh S, Khar A. Biological effects of curcumin and its role in cancer chemoprevention and therapy. Anticancer Agents Med Chem. 2006; 6:259-270.
36. Inoue T, Hirabayashi Y, Mitsui H, Sasaki H, Cronkite EP, Bullis JE, Bond VP, Yoshida K. Survival of spleen colony-forming units (CFU-S) of irradiated bone marrow cells in mice: Evidence for the existence of a radioresistant subfraction. Exp Hematol. 1995; 23:1296-1300.
37. van Bekkum DW. Radiation sensitivity of the hemopoietic stem cell. Radiat Res. 1991; 128:S4-8.
38. Booth C, Potten CS. Gut instincts: Thoughts on intestinal epithelial stem cells. J Clin Invest. 2000; 105:1493-1499.
39. Schepers AG, Vries R, van den Born M, van de Wetering M, Clevers H. Lgr5 intestinal stem cells have high telomerase activity and randomly segregate their chromosomes. EMBO J. 2011; 30:1104-1109.
40. Umar S. Intestinal stem cells. Curr Gastroenterol Rep. 2010; 12:340-348.
41. Hoarau E, Chandra V, Rustin P, Scharfmann R, Duvillie B. Pro-oxidant/antioxidant balance controls pancreatic beta-cell differentiation through the ERK1/2 pathway. Cell Death Dis. 2014; 5:e1487.
42. Chen XL, Dodd G, Thomas S, Zhang X, Wasserman MA, Rovin BH, Kunsch C. Activation of Nrf2/ARE pathway protects endothelial cells from oxidant injury and inhibits inflammatory gene expression. Am J Physiol Heart Circ Physiol. 2006; 290:H1862-1870.
43. Chen ZJ. Ubiquitin signalling in the NF-kappaB pathway. Nat Cell Biol. 2005; 7:758-765.
44. Cullinan SB, Gordan JD, Jin J, Harper JW, Diehl JA. The Keap1-BTB protein is an adaptor that bridges Nrf2 to a Cul3-based E3 ligase: Oxidative stress sensing by a Cul3-Keap1 ligase. Mol Cell Biol. 2004; 24:8477-8486.
45. Cullinan SB, Zhang D, Hannink M, Arvisais E, Kaufman RJ, Diehl JA. Nrf2 is a direct PERK substrate and effector of PERK-dependent cell survival. Mol Cell Biol. 2003; 23:7198-7209.
46. Hochmuth CE, Biteau B, Bohmann D, Jasper H. Redox regulation by Keap1 and Nrf2 controls intestinal stem cell proliferation in Drosophila. Cell Stem Cell. 2011; 8:188-199.
47. McMahon M, Itoh K, Yamamoto M, Chanas SA, Henderson CJ, McLellan LI, Wolf CR, Cavin C, Hayes JD. The Cap'n'Collar basic leucine zipper transcription factor Nrf2 (NF-E2 p45-related factor 2) controls both constitutive and inducible expression of intestinal detoxification and glutathione biosynthetic enzymes. Cancer Res. 2001; 61:3299-3307.

(Received March 18, 2016; Revised April 1, 2016; Accepted April 8, 2016)

Original Article

DOI: 10.5582/ddt.2016.01029

Generation and purification of monoclonal antibodies against Der f 2, a major allergen from *Dermatophagoides farinae*

Huifang Chen, Kejun Zhang, Shan Wang, Chenxia Xu, Zehong Zou, Ailin Tao*

The Second Affiliated Hospital of Guangzhou Medical University, The State Key Laboratory of Respiratory Disease, Guangdong Provincial Key Laboratory of Allergy & Clinical Immunology, Guangzhou, China.

Summary **Monoclonal antibodies (mAbs) are needed for the quantitation of environmental allergens for precise diagnosis and immunotherapy. In this study, we produced and purified monoclonal antibodies against Der f 2, one of the major allergens of the house dust mite *Dermatophagoides farina*, in order to develop an assay for the detection of this allergen. BALB/c mice were immunized four times with the protein Der f 2 together with an adjuvant after which splenocytes were collected and fused with SP2/0 (myeloma cells) in the presence of polyethylene glycol (PEG). The fused cells were selected in the presence of Hypoxanthine-Aminopterin-Thymidine (HAT) and then Hypoxanthine-Thymidine (HT) medium. Positive cells were screened with ELISA and subcloned by limited dilution at least three times to achieve stable mAb-producing clones. Four stable mAb-producing clones were obtained. One clone with IgG1 isotype and another with IgG2b isotype were chosen to produce large amounts of mAb by inoculation of the cells into the abdominal cavity of mice. Ascites were collected and the mAbs were purified using protein A affinity chromatography. Testing of the ascites by ELISA showed the titration of IgG1 and IgG2b to be higher than $1/10^6$ dilution. The specificity of both antibodies was confirmed by immunoblotting. Thus, we produced two mAb clones against Der f 2 that can be used to create a precise quantitative method to identify allergen components in dust samples and facilitate further study in Der f 2 component-resolved diagnosis (CRD).**

Keywords: *Dermatophagoides farina*, environmental allergen, house dust mite monoclonal antibody

1. Introduction

House dust mite (HDM) is one of the most common causes of respiratory allergic diseases such as allergic asthma and allergic rhinitis (*1*). HDM allergens can be found in dust samples from the bedding of 95% of Chinese households (2). The higher average relative humidity in the south of China, especially in the coastal cities, may be a factor in promoting exposure to mites and, thus, result in an increasing prevalence of asthma (*3*). Because of the warm climate (average temperature: 22°C) and humidity (average relative humidity: 76%), more than 90% of children with asthma have positive skin test responses to HDM in Taipei, China (*4*). *Dermatophagoides pteronyssinus* (D. *pteronyssinus*) (65.3%) and *Dermatophagoides farina* (D. farina) (20.6%) are two of the most common groups of dust in the household environment (*5,6*). Currently, there are nearly 30 kinds of allergenic components in HDM that have been cloned and identified (*7*). Approximately 80% to 100% of HDM allergic patients respond to group 1 and group 2 allergens (*8*).

Allergen avoidance is widely recommended to reduce the symptom severity of allergic diseases in sensitized individuals (*9-11*). Therefore, it is important to monitor the amount of allergens in dust samples to evaluate the correlation between the environmental allergens and the occurrence and severity of allergic diseases (*12*).

Allergen immunotherapy (AIT) is the only

**Address correspondence to:*
Dr. Ailin Tao, The Second Affiliated Hospital of Guangzhou Medical University, The State Key Laboratory of Respiratory Disease, Guangdong Provincial Key Laboratory of Allergy & Clinical Immunology, 250# East Changgang Road, Guangzhou 510260, Guangdong, China.
E-mail: taoailin@gzhmu.edu.cn

treatment approach that can improve the immune response of patients to allergens (*13*). AIT with HDM extract is one of the most common treatments for mite allergy. Furthermore, several new strategies such as the administration of recombinant and genetically modified allergens are being explored for their use in new types of AIT (*14*). However, the amount of each allergen component in both the crude extract and other new types of AIT is not exactly known, which could lead to serious side-effects in the course of treatment (*15*), especially in patients who have experienced anaphylactic reactions. It is important to detect the concentration of each allergen component exactly in the HDM extract. However, efficient tools for quantification of allergen components are still limited.

MAbs against specific allergen components could be used in their quantification as well as for the further improvement of HDM allergy immunotherapy. In 2013, a mAb against Der p 2 was generated for the development of a Der p 2 ELISA (*16*) that was used to monitor environmental mite infestation and estimate the number of mites in house dust samples. However, currently, there is no commercial antibody kit against the allergen Der f 2. In this study, we produced and purified mAbs against Der f 2, which might be used in the quantification of this allergen component.

2. Materials and Methods

2.1. *Materials*

Recombinant Der f 2 protein was generated and purified in a routine process similar to a method described elsewhere (*17*). BALB/c mice were obtained from the Medical Laboratory Animal Center (Guangdong, China. License No.: SCXK 2013-002). Complete Freund's Adjuvant (CFA) and Incomplete Freund's Adjuvant (IFA) were purchased from Sigma-Aldrich Co (St. Louis, America). The Sp 2/0 myeloma cell line was obtained from CAS Shanghai Life Science Cell Resource Center (Shanghai, China). HAT medium, HT medium, penicillin, streptomycin, fetal bovine serum (FBS), RPMI-1640 medium plus L-glutamine were purchased from Life Technologies Inc (New York, USA). Horse anti-mouse IgG-HRP conjugate was purchased from Cell Signaling Technology (Shanghai, China). Polyethylene glycol (PEG 4000) was bought from Sigma-Aldrich Co. HiTrap Protein A (5 × 1 mL Lot: 17-0402-01) was bought from GE Healthcare (Freiburg, Germany).

2.2. *Immunization of mice*

All procedures performed in this study involving animals were in accordance with the ethical standards of the institution and have been approved by a research ethics committee of The Second Affiliated Hospital of Guangzhou Medical University. Five mice were subcutaneously (*s.c.*) immunized with purified Der f 2 protein emulsified with CFA at the first injection. The total amount of protein was 36 μg/mouse. After two weeks, the mice were given a second subcutaneous injection of 36 μg/mouse in IFA followed by a third injection in IFA two weeks later in the same manner. After another two weeks, serum was obtained from the tail and the titer of Der f 2 specific IgG antibodies was investigated. The mice with highest titers of positive antibodies were then selected for administration of the final intraperitoneally (*i.p.*) injected protein without adjuvant and were sacrificed three days later.

2.3. *Fusion*

Peritoneal cells were obtained from a healthy non-immunized mouse and cultured in 96-well plates as primary feeder cells. Spleen cells from the immunized mice were fused with SP2/0 cells in the presence of PEG 4000. The fused cells were suspended in HAT medium containing 10% FBS and 1% penicillin-streptomycin and distributed into prepared 96-well plates. Culture supernatant was semi-replaced with fresh HAT medium on the 4th, 7th, and 10th day after fusion. After ten days of culture in HAT medium, the hybridoma cells were transferred to HT medium.

2.4. *Screening of antibody-producing cells*

Wells of a 96-well plate were coated with 2 ng of purified Der f 2 protein and then incubated at 4°C overnight. After washing four times with PBS containing 0.05% tween 20, the plates were blocked with 2% BSA solution. 100 μL of hybridoma supernatant was added to each well and incubated for 1 h at 37°C. After plate washing, secondary antibody was added (horse anti-mouse IgG at 1/4,000 dilution) to each well and incubated for another hour at 37°C. After washing, the plate was developed with TMB and the absorbance was checked using an ELISA Reader (Thermo Scientific, Varioskan Flash) at 450 nm.

2.5. *Subcloning and immunoglobulin isotyping of mAb-producing hybridomas*

The hybridomas that generated the highest antibody titers were selected for subcloning by limited dilution. Briefly, cell suspension was distributed at concentrations of 10, 5, or 2 cells/well in 100 μL medium and cultured in 96-well plates containing feeder cells. The clone supernatants were tested using ELISA after ten days in culture. In order to obtain stable antibody-secreting clones, the positive clones were subcloned at least three times using the limited dilution method (*18*). The isotype of the mAb was qualitatively analyzed using a commercial ELISA kit (Sino Biological.inc, SEK003),

following the manufacturer's guidelines.

2.6. *Mass production and verification of mAbs*

Six-eight weeks old female mice were *i.p.* with 0.5 mL of priming reagent per mouse. Ten days later, 1 × 10^6 stable mAb-producing cells suspended in 0.5 mL RPMI-1640 medium were injected into the abdominal cavity of each mouse. Production of ascites as noted by abdominal distension was observed a few days after inoculation and was collected after seven to ten days.

Der f 2 protein was resolved through SDS-PAGE and then transferred onto a PVDF membrane. The membrane was then blocked with 2% BSA and incubated for 2 h at room temperature. Either cell supernatants or ascites were diluted and added as primary antibody. After the incubation and washing steps, goat anti-mouse IgG antibody (1/4,000) was added as the secondary antibody. The membrane was developed in ECL reagent and images were acquired using ImageQuant LAS 4000 mini.

2.7. *Purification of Der f 2 monoclonal antibody*

The ascites was diluted with normal saline and precipitated by 50% ammonium sulfate. The precipitate was dissolved and dialyzed into 20 mM phosphate-buffered saline (PBS) followed by antibody purification using protein A chromatography according to the manufacturer's recommendation. In brief, the resin was equilibrated with PBS pH 7.4. After protein loading, the resin was washed with at least a 20-fold column volume of PBS pH 7.4. The target protein was eluted using 100 mM citric acid buffer (pH 4.0) and the mAb concentration was monitored by UV absorption at 280 nm.

3. Results

3.1. *Serum titration of the immunized mice*

Serum from three of the immunized mice was diluted 1:5,000, 1:10,000, 1:20,000 and 1:40,000 and tested for titers of Der f 2 specific IgG antibody. Control serum of non-immunized mice was tested at a 1:10,000 dilution. All the serum from the immunized mice had antibody titers that could be detected at a dilution of 1:40,000 (Table 1) and the mouse with the highest titer was selected for fusion.

Table 1. OD 450 nm of serum titers in immunized mice

Immunized Mice	1:5,000	1:10,000	1:20,000	1:40,000	Ctrl
1*	1.858	1.561	1.174	0.679	0.079
2	1.508	1.075	0.717	0.341	/
3	1.019	0.900	0.643	0.421	/

Ctrl: negative control using the serum from non-immunized mouse with the a dilution of 1:10,000. *Immunized mouse 1 was selected for fusion.

3.2. *Isotype of the mAb and ascites titration*

After fusion, 130 clones were found to have antibody titers that were significantly higher than the negative control and eight of them were selected for limited dilution (Table 2). After the first subcloning, four stable clones were retained for further limited dilution. Two of the four stable clones, which were classified as either IgG1 or IgG2b isotype (Table 3), were selected for ascites induction for mass production of mAb. ELISA results showed that the antibody titer in the ascites was higher than $1:10^6$, indicating a mAb with high potency (Table 4).

3.3. *Characterization and purification of the mAbs*

The high specificity of the mAbs against Der f 2 was confirmed by immunoblotting assay in both the supernatant of the mAb-producing clones and the ascites before purification (Figure 1A). The ascites was first precipitated by 50% ammonium sulfate and then purified by protein A chromatography. The highest

Table 2. Absorbance of the selected clones after fusion and after the first subcloning detected by ELISA

Clones selection after fusion		Clones selection after the first subcloning	
Clones	OD at 450 nm	Clones	OD at 450 nm
neg.ctrl	0.059	neg.ctrl	0.090
pos. ctrl	3.496	pos. ctrl	4.147
1B12	4.921	1-1B12[a]	5.519
1G4	1.081	1-1G4[b]	0.114
3A12	2.257	3-1A12[a]	4.163
3E1	3.108	3-1E1	4.406
3G5	2.406	3-1G5[b]	0.927
3A7	1.325	3-1A[7]	1.570
3F9	1.381	3-1F9[b]	0.180
4B10	1.092	4-1B10[b]	0.081

neg.ctrl: negative control, serum from non-immunized mouse. pos.ctrl: positive control, serum from immunized mouse. [a]: The individual clones selected for mAb mass production are labeled as 1-1 and 3-1. [b]: The four clones that showed decreasing antibody production.

Table 3. Isotype identification as determined by absorbance at 450 nm

Clones	IgG1	IgG2a	IgG2b	IgG3	IgM	Control
1-1	2.089	0.071	0.169	0.086	0.043	0.043
3-1	0.293	0.165	1.251	0.398	0.220	0.155

Table 4. Titration of Der f 2 mAbs in ascites as shown by absorbance at 450 nm

Clones	$1:10^2$	$1:10^3$	$1:10^4$	$1:10^5$	$1:10^6$	$1:10^7$	blank
1-1	/	4.865	4.513	2.450	0.573	0.112	0.045
3-1	5.645	3.467	1.957	0.943	0.216	/	0.044

/: means not done because of too high in $1:10^2$ and too low in $1:10^7$.

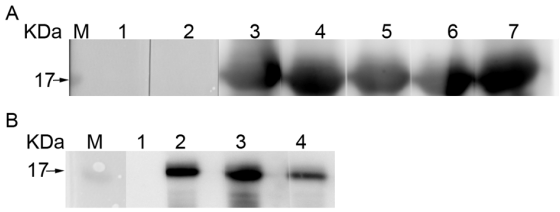

Figure 1. Characterization of Der f 2 mAbs by immunoblotting. A: Characterization of Der f 2 mAbs before purification. M: Marker. Lane 1: SP2/0 culture medium. Lane 2: Serum of non-immunized mouse. Lane 3: Serum of Der f 2 immunized mouse. Lane 4: Supernatant of Der f 2 mAb clone 3-1. Lane 5: Ascites of Der f 2 mAb clone 3-1. Lane 6: Supernatant of Der f 2 mAb clone 1-1. Lane 7: Ascites of Der f 2 mAb clone 1-1. **B:** Characterization of Der f 2 mAbs after purification. M: Marker. Lane 1: Serum of non-immunized mouse. Lane 2: Serum of Der f 2 immunized mouse. Lane 3: Purified Der f 2 mAb clone 1-1. Lane 4: Purified Der f 2 mAb clone 3-1.

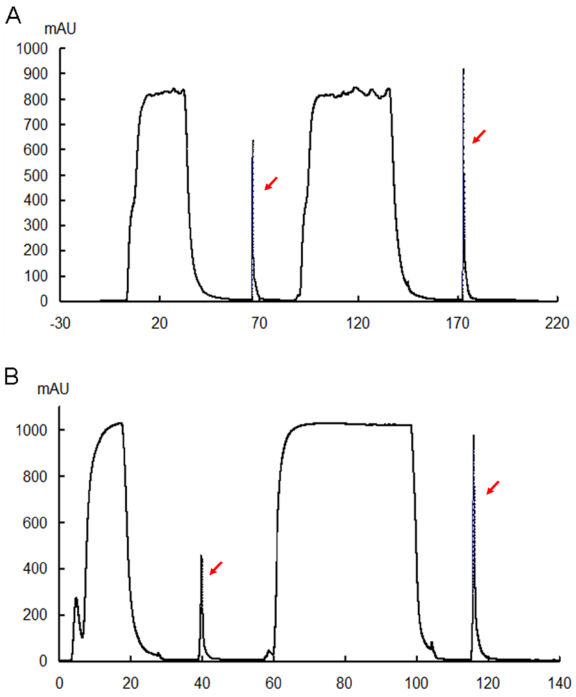

Figure 2. Purification of Der f 2 mAbs. A: Purification of Der f 2 mAb clone 1-1. **B:** Purification of Der f 2 mAb clone 3-1. The arrows indicate the elution peak of the target protein.

elution peaks were collected as purified antibodies (Figure 2), which were then verified by SDS-PAGE electrophoresis (Figure 3) and immunoblotting assay (Figure 1 B).

4. Discussion

In this study, we produced and purified two different isotypes of specific monoclonal antibodies against Der f 2 mite allergen. These antibodies could be used to develop an assay for the quantification of Der f 2 in environmental allergens.

In our study, the fusion rate between the splenocytes and SP2/0 cells was approximately 79% as screened

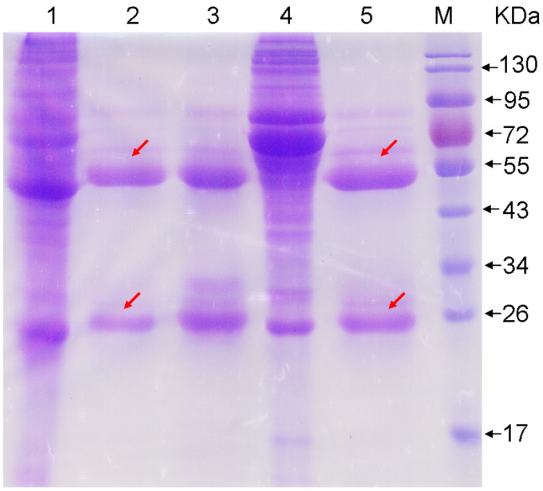

Figure 3. The mAbs after purification. Lane 1: Der f 2 mAb clone 1-1 before purification. **Lane 2:** Purified Der f 2 mAb clone 1-1 collected from the first part of elution peak. **Lane 3:** Purified Der f 2 mAb clone 1-1 collected from the second part of elution peak. **Lane 4:** Der f 2 mAb clone 3-1 before purification. **Lane 5:** Purified Der f 2 mAb clone 3-1. **M:** Markers. The arrows indicate the heavy chain and light chain of the purified antibodies, individually.

by ELISA, which demonstrated the efficiency of PEG 4000 in the production of monoclonal antibodies. Eight clones with the highest ODs were selected for limited dilution. However, after the first subcloning, four of the clones showed a gradual decrease in antibody production, while the other four clones grew well. This situation has been described during other mAb production procedures and could be due to chromosomal instability (*19*).

BALB/c mice are most commonly used for ascites production because this strain of animals is syngeneic with the myeloma cells that are most frequently used for fusion (*20*). Mice were first given a priming agent by *i.p.* injection. After seven days, the hybridoma cells were inoculated by *i.p.* injection. Ascites induction is a life-threatening procedure due to tumor growth, metastatic spreading and infiltrative growth. Mineral oil was first tried as the priming agent but failed to prevent negative side effects related to the growth of the hybridoma cells and resulted in too much bleeding in the abdominal cavity. Thus, we used IFA for priming agent (*21*), which significantly alleviated the negative side effects of tumor growth and increased the amount of ascites production. We also analyzed the differences in ascites induction in different ages and genders of mice and we found that the yield of ascites was greater in 10-12 week-old mice than 6-8 week-old ones, while the gender had no significant influence on ascites production.

During the last several decades, the prevalence of allergic disease has steadily increased in developed countries. Among atopic patients in China, approximately 87% are sensitive to one or more species of HDM (*22*) indicating that it is the main allergen for these patients.

Another study from Taiwan showed that more than 90% of children with asthma had positive skin test responses to HDM (*23*). The high humidity and high ambient temperature in the southern coastal regions of China is suitable for the growth of dust mites. HDM is abundant in the dust samples collected from carpets, mattresses and air-conditioners. There is convincing evidence that avoidance of mite allergen can effectively reduce allergic symptoms (*24*). Thus, it is very important to develop an effective tool to monitor the concentration of allergen components in the indoor environment. The high titer, highly specific antibodies that have been produced in this work could be used to develop assays that can help the physician educate patients in creating an environment with lower concentrations of mite allergen, which would therefore reduce patient exposure to HDM in their residences.

Although HDM allergen is a major cause of respiratory allergic disease, there are still unresolved challenges in both the specific diagnosis and effective treatment (*17*). Purified allergens are helpful for CRD and immunotherapy of HDM allergy (*25*). Treatments for HDM allergy include HDM avoidance and AIT, which is a widely recommended strategy and well documented (*26*). AIT is effective when appropriate doses of allergens are administrated (*27*). Several studies showed that an optimal maintenance dose needed for AIT through the subcutaneous route is in the range of 5-20 μg of the major allergen found in aeroallergens (*28-31*). Therefore, it is quite important to develop a tool for the precise quantitation of allergen components in the allergen extract or the recombinant protein to ensure that it contains an effective therapeutic dose of each of its individual allergen components.

In summary, to better evaluate the correlation between symptom relief and HDM avoidance, we produced and purified two different isotypes of monoclonal antibodies against Der f 2 that might facilitate CRD as well as identify the effective doses of this HDM major allergen component when used in component-resolved immunotherapy.

Acknowledgements

This work was supported by the National Science and Technology Major Project of China (2014ZX08011-005B) and the National Science and Technology Major Project of China (2014ZX08011-005). We thank Dr. Zhou Yanchun for providing us with technical support.

References

1. Custovic A, Simpson A, Woodcock A. Importance of indoor allergens in the induction of allergy and elicitation of allergic disease. Allergy. 1998; 53:115-120.
2. Zheng YW, Lai XX, Zhao Y, Zhang CQ, Chen JJ, Zhang L, Wei QY, Chen S, Liu EM, Norback D, Gjesing B, Zhong NS, Spangfort DM. Indoor Allergen Levels and Household Distributions in Nine Cities Across China. Biomed Environ Sci. 2015; 28:709-717.
3. Vesper S, Choi H, Perzanowski MS, Acosta LM, Divjan A, Bolanos-Rosero B, Rivera-Mariani F, Chew GL. Mold populations and dust mite allergen concentrations in house dust samples from across Puerto Rico. Int J Environ Health Res. 2015:1-10.
4. Chang YC, Hsieh KH. The study of house dust mites in Taiwan. Ann Allergy. 1989; 62:101-106.
5. Thomas WR, Smith WA, Hales BJ. The allergenic specificities of the house dust mite. Chang Gung Med J. 2004; 27:563-569.
6. Jeong KY, Park JW, Hong CS. House dust mite allergy in Korea: The most important inhalant allergen in current and future. Allergy Asthma Immunol Res. 2012; 4:313-325.
7. Calderon MA, Linneberg A, Kleine-Tebbe J, De Blay F, Hernandez Fernandez de Rojas D, Virchow JC, Demoly P. Respiratory allergy caused by house dust mites: What do we really know? J Allergy Clin Immunol. 2015; 136:38-48.
8. Lorenz AR, Luttkopf D, May S, Scheurer S, Vieths S. The principle of homologous groups in regulatory affairs of allergen products--a proposal. Int Arch Allergy Immunol. 2009; 148:1-17.
9. Krieger J, Jacobs DE, Ashley PJ, Baeder A, Chew GL, Dearborn D, Hynes HP, Miller JD, Morley R, Rabito F, Zeldin DC. Housing interventions and control of asthma-related indoor biologic agents: A review of the evidence. J Public Health Manag Pract. 2010; 16:S11-20.
10. Sporik R, Holgate ST, Platts-Mills TA, Cogswell JJ. Exposure to house-dust mite allergen (Der p I) and the development of asthma in childhood. A prospective study. N Engl J Med. 1990; 323:502-507.
11. Morgan WJ, Crain EF, Gruchalla RS, O'Connor GT, Kattan M, Evans R, 3rd, Stout J, Malindzak G, Smartt E, Plaut M, Walter M, Vaughn B, Mitchell H, Inner-City Asthma Study G. Results of a home-based environmental intervention among urban children with asthma. N Engl J Med. 2004; 351:1068-1080.
12. Yu SJ, Liao EC, Tsai JJ. House dust mite allergy: Environment evaluation and disease prevention. Asia Pac Allergy. 2014; 4:241-252.
13. Canonica GW, Bachert C, Hellings P, Ryan D, Valovirta E, Wickman M, De Beaumont O, Bousquet J. Allergen Immunotherapy (AIT): A prototype of Precision Medicine. World Allergy Organ J. 2015; 8:31.
14. Hales BJ, Martin AC, Pearce LJ, Laing IA, Hayden CM, Goldblatt J, Le Souef PN, Thomas WR. IgE and IgG anti-house dust mite specificities in allergic disease. J Allergy Clin Immunol. 2006; 118:361-367.
15. Valenta R, Linhart B, Swoboda I, Niederberger V. Recombinant allergens for allergen-specific immunotherapy: 10 years anniversary of immunotherapy with recombinant allergens. Allergy. 2011; 66:775-783.
16. Liao EC, Lin YH, Tsai JJ. Detection of group 2 Dermatophagoides pteronyssinus allergen for environmental monitoring of dust mite infestation. Biosci Trends. 2013; 7:82-88.
17. Calderon MA, Kleine-Tebbe J, Linneberg A, De Blay F, Hernandez Fernandez de Rojas D, Virchow JC, Demoly P. House Dust Mite Respiratory Allergy: An Overview of Current Therapeutic Strategies. J Allergy Clin Immunol Pract. 2015; 3:843-855.
18. Gao J, Wu M, Gao J, Wang X, Zhang Y, Zhu S, Yu

Y, Han W. Generation and Characterization of a New Monoclonal Antibody Against CXCL4. Monoclon Antib Immunodiagn Immunother. 2015; 34:110-115.
19. Soukhtanloo M, Talebian E, Golchin M, Mohammadi M, Amirheidari B. Production and characterization of monoclonal antibodies against aflatoxin B1. J Immunoassay Immunochem. 2014; 35:335-343.
20. Leenaars M, Hendriksen CF. Critical steps in the production of polyclonal and monoclonal antibodies: Evaluation and recommendations. ILAR J. 2005; 46:269-279.
21. Gillette RW. Alternatives to pristane priming for ascitic fluid and monoclonal antibody production. J Immunol Methods. 1987; 99:21-23.
22. Li J, Sun B, Huang Y, Lin X, Zhao D, Tan G, Wu J, Zhao H, Cao L, Zhong N. China Alliance of Research on Respiratory Allergic D. A multicentre study assessing the prevalence of sensitizations in patients with asthma and/or rhinitis in China. Allergy. 2009; 64:1083-1092.
23. Sun HL, Lue KH. Household distribution of house dust mite in central Taiwan. J Microbiol Immunol Infect. 2000; 33:233-236.
24. Arlian LG, Platts-Mills TA. The biology of dust mites and the remediation of mite allergens in allergic disease. J Allergy Clin Immunol. 2001; 107:S406-413.
25. Valenta R, Lidholm J, Niederberger V, Hayek B, Kraft D, Gronlund H. The recombinant allergen-based concept of component-resolved diagnostics and immunotherapy (CRD and CRIT). Clin Exp Allergy. 1999; 29:896-904.
26. Cox L, Esch RE, Corbett M, Hankin C, Nelson M, Plunkett G. Allergen immunotherapy practice in the United States: Guidelines, measures, and outcomes. Ann Allergy Asthma Immunol. 2011; 107:289-299; quiz 300.
27. Cox L, Nelson H, Lockey R, *et al*. Allergen immunotherapy: A practice parameter third update. J Allergy Clin Immunol. 2011; 127:S1-55.
28. Ewbank PA, Murray J, Sanders K, Curran-Everett D, Dreskin S, Nelson HS. A double-blind, placebo-controlled immunotherapy dose-response study with standardized cat extract. J Allergy Clin Immunol. 2003; 111:155-161.
29. Frew AJ, Powell RJ, Corrigan CJ, Durham SR, Group UKIS. Efficacy and safety of specific immunotherapy with SQ allergen extract in treatment-resistant seasonal allergic rhinoconjunctivitis. J Allergy Clin Immunol. 2006; 117:319-325.
30. Lent AM, Harbeck R, Strand M, Sills M, Schmidt K, Efaw B, Lebo T, Nelson HS. Immunologic response to administration of standardized dog allergen extract at differing doses. J Allergy Clin Immunol. 2006; 118:1249-1256.
31. Nanda A, O'Connor M, Anand M, Dreskin SC, Zhang L, Hines B, Lane D, Wheat W, Routes JM, Sawyer R, Rosenwasser LJ, Nelson HS. Dose dependence and time course of the immunologic response to administration of standardized cat allergen extract. J Allergy Clin Immunol. 2004; 114:1339-1344.

(Received April 2, 2016; Revised April 20, 2016; Accepted April 21, 2016)

Brief Report

DOI: 10.5582/ddt.2016.01010

Inhibition of PA endonuclease activity of influenza virus RNA polymerase by Kampo medicines

Riku Shirayama[1], Masaki Shoji[1], Nongluk Sriwilaijaroen[2,3], Hiroaki Hiramatsu[3], Yasuo Suzuki[3], Takashi Kuzuhara[1,*]

[1] *Laboratory of Biochemistry, Faculty of Pharmaceutical Sciences, Tokushima Bunri University, Yamashiro-cho, Tokushima, Japan;*
[2] *Faculty of Medicine, Thammasat University (Rangsit Campus), Pathumthani, Thailand;*
[3] *College of Life and Health Sciences, Chubu University, Aichi, Japan.*

Summary **To find a novel influenza inhibitor targeting the endonuclease activity of influenza A virus polymerase acidic protein (PA), which is essential for the acquisition of primers for viral mRNA transcription, seven Kampo extracts were tested *in vitro* for their ability to inhibit endonuclease activity of the recombinant PA protein that was expressed and purified from *Escherichia coli*. The Kampo medicines Kakkonto, Shosaikoto, Saikokeishito, Keishito, Maobushisaishinto, and Maoto, but not Chikujountanto, inhibited PA endonuclease activity in a dose-dependent manner. Our results indicate that Kampo medicines are good sources providing a structural lead for optimization of an influenza endonuclease inhibitor.**

Keywords: Influenza virus, RNA polymerase, endonuclease, Kampo medicine

1. Introduction

By far, the worst influenza pandemic to date was the 1918 Spanish influenza A (H1N1) virus, which caused 50 million deaths worldwide (*1,2*). Currently, the H3N2 Hong Kong/68 and H1N1 swine/09 pandemic variants cause severe illnesses in 3-5 million people and 250-500 thousand deaths per year (*3,4*). In addition to annual epidemics, non-human influenza A viruses sporadically infect humans. These infections can cause a severe disease and are associated with a high death rate. Highly mutable influenza A viruses not only cause occasional pandemics with unpredictable pathogenesis and annual epidemics, but also may cause the annual seasonal vaccine to fail and the development of resistance to antivirals (accordingly, vaccine formulation should be reviewed annually (*5*)). Both currently circulating H3N2 and H1N1 viruses are highly resistant to adamantanes targeting the viral M2 ion channel (*6,7*) and 1.8% of H1N1 viruses tested in 2013-2014 were resistant to oseltamivir, which targets viral neuraminidase (*8*). These observations indicate the urgent need for novel antivirals targeting essential viral proteins at sites that are highly conserved among strains to effectively control influenza outbreaks and prevent the development of drug resistance.

Influenza A viruses have a segmented single-stranded RNA (-) genome, and transcription and replication of the viral genome is catalyzed by a heterotrimeric RNA-dependent RNA polymerase consisting of polymerase basic protein 1 (PB1) and 2 (PB2) and polymerase acidic protein (PA) (*9,10*). The *N*-terminal domain (residues 1-220) of the PA subunit harbors endonuclease activity by which capped host pre-mRNAs are cleaved and then used as primers for viral mRNA synthesis, which is essential for virus multiplication (*11,12*). Unlike other polymerase parts with mutations that are associated with virulence and interspecies transmission, the PA *N*-terminal active site is highly conserved between humans and avian species (*11*). This suggests that the PA *N*-terminal endonuclease is a promising therapeutic target for influenza. Our previous results showed that catechins, phenethyl phenyl phthalimide analogs, marchantins, and fullerene C_{60} analogs inhibit PA endonuclease activity (in the influenza A virus H1N1 strain) and possess antiviral activity against influenza viruses A (H1N1 and/or H3N2) and/or B strains (*13-16*), supporting the hypothesis that the PA endonuclease is a candidate for the development

Released online in J-STAGE as advance publication February 22, 2016.

*Address correspondence to:
Dr. Takashi Kuzuhara, Laboratory of Biochemistry, Faculty of Pharmaceutical Sciences, Tokushima Bunri University, Yamashiro-cho, Tokushima 770-8514, Japan.
E-mail: kuzuhara@ph.bunri-u.ac.jp

Table 1. Composition of Kampo medicines

Composition	Weight ratio						
	Kakkonto	Keishito	Shosaikoto	Shosaikoto	Maoto	Maobushisaishinto	Chikujountanto
JP[a] Pueraria Root	4.0		-	-	-	-	-
JP Jujube	3.0	4.0	2.0	3.0	-	-	-
JP Ephedra Herb	3.0	-	-	-	5.0	4.0	-
JP Glycyrrhiza	2.0	2.0	2.0	2.0	1.5	-	1.0
JP Cinnamon Bark	2.0	4.0	2.0	-	4.0	-	-
JP Peony Root	2.0	4.0	2.0	-	-	-	-
JP Ginger	2.0	1.5	1.0	1.0	-	-	1.0
JP Bupleurum Root	-	-	5.0	7.0	-	-	-
JP Pinellia Tuber	-	-	4.0	5.0	-	-	-
JP Scutellaria Root	-	-	2.0	3.0	-	-	-
JP Ginseng	-	-	2.0	3.0	-	-	1.0
JP Asiasarum Root	-	-	-	-	-	3.0	-
JP Powdered Processed Aconite Root	-	-	-	-	-	1.0	-
JP Apricot Kernel	-	-	-	-	5.0	-	-
JP Pinellia Tuber	-	-	-	-	-	-	5.0
JP Bupleurum Root	-	-	-	-	-	-	3.0
JP Ophiopogon Tuber	-	-	-	-	-	-	3.0
JP Poria Sclerotium	-	-	-	-	-	-	3.0
JP Platycodon Root	-	-	-	-	-	-	2.0
JP Immature Orange	-	-	-	-	-	-	2.0
JP Cyperus Rhizome	-	-	-	-	-	-	2.0
JP Citrus Unshiu Peel	-	-	-	-	-	-	2.0
JP Coptis Rhizome	-	-	-	-	-	-	1.0
Bamboo Culm.	-	-	-	-	-	-	3.0
Total (g)	18.0	15.5	22.0	24.0	15.5	8.0	29.0

[a]JP: The Japanese Pharmacopoeia.

of the next generation of antivirals targeting a broad range of influenza A virus strains.

Kampo medicines are traditional Japanese herbal medicines that typically consist of several mixed herbs (*17,18*). Recently, a Kampo medicine, maoto, was reported to have anti-influenza activity (*18*). Here, we provide evidence for anti-PA endonuclease activity in 6 of the 7 tested Kampo medicines, suggesting that Kampo medicines are potential sources of compounds for the development of new, selective PA endonuclease inhibitors.

2. Materials and Methods

2.1. *Kampo medicines*

Kampo medicines, including Kakkonto, Shosaikoto, Saikokeishito, Keishito, Maobushisaishinto, Maoto, and Chikujountanto, were obtained from Tsumura & Co. (Tokyo, Japan). Based on the data sheets of Tsumura & Co., the composition of Kampo medicines are summarized in Table 1. Kampo medicines were dissolved in the purified water at 10 mg/mL for *in vitro* assay.

2.2. *Bacterial expression and purification of influenza virus PA endonuclease*

The recombinant PA endonuclease was produced as described previously (*13-16*). Briefly, the influenza A/PR/8/34 (H1N1) PA coding sequence corresponding to *N*-terminal endonuclease residues 1-220 was amplified from the plasmid pBMSA-PA (Riken BioResource Center, Tsukuba, Japan) and was cloned into the bacterial expression plasmid pET28a(+) with the T7/*lac* promoter plus 6 x histidine (His)-tag sequence (Novagen, Madison, WI, USA). After the introduction of the plasmid into BL21-CodonPlus *Escherichia coli* cells (Stratagene, La Jolla, CA, USA), expression of the PA endonuclease protein-6xHis was induced by the addition of IPTG. The recombinant PA endonuclease-6xHis was purified in a two-step process using Ni^{2+}-affinity chromatography, followed by HiTrap™ Q FF anion exchange chromatography with the AKTA™ Prime Plus System (GE Healthcare, Buckinghamshire, UK).

2.3. *PA endonuclease inhibition assay*

The recombinant PA endonuclease activity of the influenza A virus was determined following previously described methods (*13-16*), with modifications. The assay was performed in a 100 µL reaction mixture containing 20 mM Tris-HCl (pH 7.3), 100 mM NaCl, 2.5 mM $MnCl_2$, 10-50 µg/mL circular single-stranded DNA (M13mp18) as a substrate, and 5 µM recombinant PA endonuclease. After 30 min of digestion at 37°C, the digestion reaction was stopped by the addition of 20 mM EGTA. The undigested M13mp18 substrate remaining in the reaction as well as a reaction without

the recombinant PA endonuclease were analyzed by 0.7% agarose gel electrophoresis in Tris-borate-EDTA buffer and visualized by staining the gel with ethidium bromide. For the inhibition assay, each Kampo medicine at various concentrations was preincubated with the PA endonuclease in the reaction mixture at 37°C for 5 minutes, before adding the substrate to initiate the digestion reaction. The inhibitory effects of each Kampo medicine on PA endonuclease activity were determined on the basis of the ability the medicine to maintain the same intensity of the M13mp18 band as that of the reaction mixture without the PA endonuclease. The reaction that did not include the inhibitor was defined as the maximum diminution of the substrate band (*i.e.*, full PA endonuclease activity).

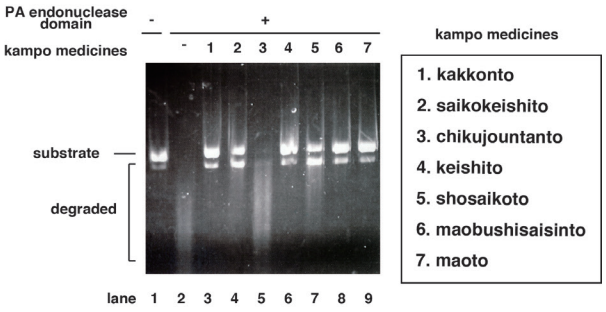

Figure 1. Inhibition of PA endonuclease activity by Kampo medicine extracts. The recombinant PA endonuclease (5 μM) was pre-incubated with the solvent (water) control (each Kampo medicine was dissolved in water) (Lane 2) or different Kampo medicines (1 mg/ml) as indicated (Lanes 3-9) prior to starting the reaction by the addition of M13mp18 substrate (50 μg/mL). As a negative control, the reaction was performed in the absence of the endonuclease; thus, the substrate should remain intact in the reaction (Lane 1). The remaining substrate for each reaction after endonuclease digestion (20 μL from a total reaction volume of 100 μL) was analyzed by 0.7% agarose gel electrophoresis.

3. Results and Discussion

After transformation of the pET28a(+) plasmid, which carries the influenza PA cDNA coding region spanning the first 220 *N*-terminal amino acid residues (responsible for endonuclease activity) from the pBMSA-PA plasmid by PCR-based cloning in BL21-CodonPlus *E. coli* cells, the recombinant PA endonuclease was induced and purified for the *in vitro* endonuclease assay. An assay of the cleavage of the phosphodiester bond within a polynucleotide chain by the recombinant PA endonuclease was performed at pH 7.3 to mimic the nucleus of an infected cell, where the cap-snatching endonuclease is located (*11*), using M13mp18 circular single-stranded DNA as a substrate. In the absence of the endonuclease, the M13mp18 substrate remained intact after the reaction, as shown in Lane 1, Figure 1. In the presence of the endonuclease, the substrate was cleaved and thus reduced upon the endonuclease cleavage activity. The complete reduction of band intensities was observed (Lane 2, Figure 1), indicating that 5 μM PA endonuclease can achieve complete cleavage of all of the 50 μg/mL substrate within 30 min under the assay conditions. The addition of 1 mg/mL Kakkonto, Shosaikoto, Saikokeishito, Keishito, Maobushisaishinto, or Maoto, but not Chikujountanto, significantly inhibited the digestion of the M13mp18 substrate.

To examine the dose-dependent effects of Kampo medicines on recombinant PA endonuclease activity, 5 μM endonuclease was pre-treated with serial 10-fold dilutions of Kampo medicines in the reaction mixture before the addition of 10 μg/mL M13mp18. All Kampo medicines, except Chikujountanto, at 100 μg/mL could abolish recombinant PA endonuclease activity as evidenced by the lack of a change in substrate levels (Figure 2). Similar decreases in substrate band

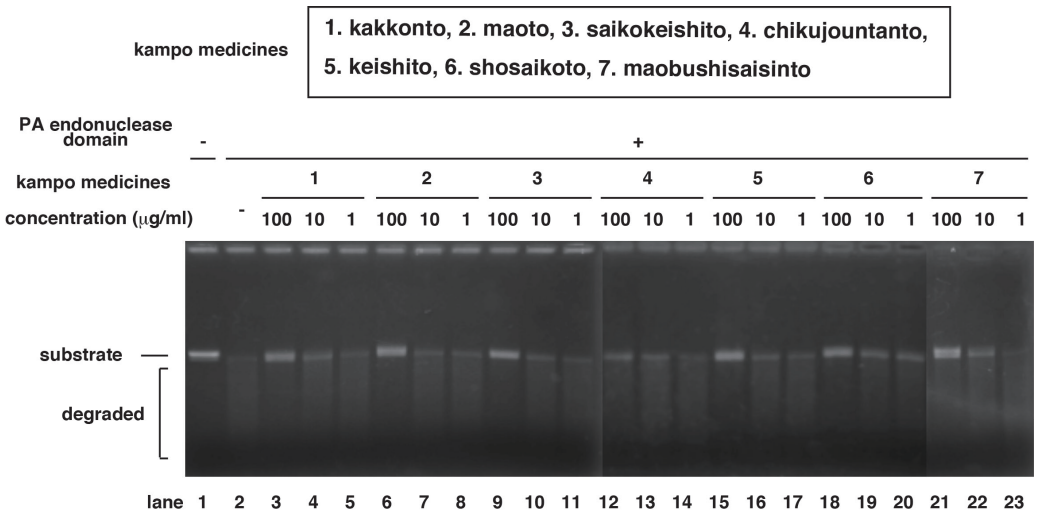

Figure 2. Dose-dependent inhibition of PA endonuclease by Kampo medicines. The activity of the recombinant PA endonuclease (5 μM) was determined in the absence (Lane 2) or the presence of various concentrations (from 1 to 100 μg/mL, as indicated) of different Kampo medicines as indicated (Lanes 3-23) using M13mp18 (10 μg/mL) as a substrate. A negative control without the endonuclease was evaluated in parallel (Lane 1). A 20-μL volume of each reaction from a total reaction volume of 100 μL was examined by 0.7% agarose gel electrophoresis.

intensities were observed using 1 and 10 μg/mL Kampo medicines, but the band intensities remained slightly higher than that of the reaction without a Kampo medicine (Lane 2), indicating that 1 and 10 μg/mL Kampo medicines can slightly decrease endonuclease activity. These results confirmed that Chikujountanto does not demonstrate significant inhibitory activity against the endonuclease under these assay conditions and that the Kampo medicines Kakkonto, Shosaikoto, Saikokeishito, Keishito, Maobushisaishinto, and Maoto, at concentrations greater than 10 μg/mL, significantly inhibit endonuclease activity.

The endonuclease activity of the *N*-terminus of PA, which has a highly conserved sequence and has an essential function for influenza virus transcription and multiplication, has been identified as a potential target for developing novel anti-influenza virus drug (*19*) with low susceptibility to viral resistance. We demonstrate here that several Kampo medicines including Kakkonto, Shosaikoto, Saikokeishito, Keishito, Maobushisaishinto, and Maoto are able to inhibit recombinant PA endonuclease activity, whereas Kampo medicine Chikujountanto at a highest tested concentration of 100 μg/mL is unable to inhibit the enzyme activity. Variation in composition between active Kampo medicines and the inactive Kampo medicine chikujountanto might account for the observed differences in endonuclease susceptibility (Table 1). Investigation of chemical compounds in Kampo medicine composition using three-dimensional HPLC analyses indicated that cinnamic acid is present in all tested Kampo medicines, except Chikujountanto. However, cinnamic acid at 2.5-20 μM does not appear to inhibit recombinant PA endonuclease activity (data not shown). Further studies are thus required to isolate and identify the active compounds of Kampo medicines that target the PA endonuclease.

In summary, we showed that the Kampo medicines Kakkonto, Shosaikoto, Saikokeishito, Keishito, Maobushisaishinto, and Maoto possess inhibitory activity against influenza viral PA endonuclease. They cleave the 5' cap of host pre-mRNAs for use as primers for the synthesis of viral mRNAs as templates for viral protein synthesis, which is critical for viral multiplication (*20*). These Kampo medicines are thus valuable materials for the future discovery and development of active anti-PA compounds for novel anti-influenza therapeutics.

Acknowledgements

The RNA polymerase PA plasmid pBMSA-PA of the influenza A/PR/8/34 (H1N1) virus was provided by the DNA bank, Riken BioResource Center (Tsukuba, Japan; originally deposited by Susumu Nakada (*21*)). We thank Tsumura & Co. (Tokyo, Japan) for providing Kampo medicines with the results of the 3D-HPLC analyses.

This work was supported by the National Bio-Resources Project of the Ministry of Education, Culture, Sports, Science, and Technology of Japan and the Japan Society for the Promotion of Science (JSPS), Grants-in-Aid for Scientific Research (C) 25460574 (to T.K.).

References

1. Horimoto T, Kawaoka Y. Influenza: lessons from past pandemics, warnings from current incidents. Nat Rev Microbiol. 2005; 3:591-600.
2. Neumann G, Noda T, Kawaoka Y. Emergence and pandemic potential of swine-origin H1N1 influenza virus. Nature. 2009; 459:931-939.
3. Sriwilaijaroen N, Suzuki Y. Molecular basis of a pandemic of avian-type influenza virus. Methods Mol Biol. 2014; 1200:447-480.
4. WHO. Influenza (Seasonal). *http://www.who.int/mediacentre/factsheets/fs211/en/* (accessed September 20, 2015).
5. CDC. Key facts about seasonal flu vaccine. *http://www.cdc.gov/flu/protect/keyfacts.htm* (accessed September 20, 2015).
6. CDC. Antiviral drug resistance among influenza viruses. *http://www.cdc.gov/flu/professionals/antivirals/antiviral-drug-resistance.htm* (accessed September 20, 2015).
7. Hayden FG, de Jong MD. Emerging influenza antiviral resistance threats. J Infect Dis. 2011; 203:6-10.
8. CDC. Influenza Antiviral Drug Resistance. *http://www.cdc.gov/flu/about/qa/antiviralresistance.htm* (accessed September 20, 2015).
9. Kuzuhara T, Kise D, Yoshida H, Horita T, Murazaki Y, Nishimura A, Echigo N, Utsunomiya H, Tsuge H. Structural basis of the influenza A virus RNA polymerase PB2 RNA-binding domain containing the pathogenicity-determinant lysine 627 residue. J Biol Chem. 2009; 284:6855-6860.
10. Sriwilaijaroen N, Suzuki Y. Molecular basis of the structure and function of H1 hemagglutinin of influenza virus. Proc Jpn Acad Ser B Phys Biol Sci. 2012; 88:226-249.
11. Dias A, Bouvier D, Crépin T, McCarthy AA, Hart DJ, Baudin F, Cusack S, Ruigrok RW. The cap-snatching endonuclease of influenza virus polymerase resides in the PA subunit. Nature. 2009; 458:914-918.
12. Yuan P, Bartlam M, Lou Z, Chen S, Zhou J, He X, Lv Z, Ge R, Li X, Deng T, Fodor E, Rao Z, Liu Y. Crystal structure of an avian influenza polymerase PA(N) reveals an endonuclease active site. Nature. 2009; 458:909-913.
13. Iwai Y, Takahashi H, Hatakeyama D, Motoshima K, Ishikawa M, Sugita K, Hashimoto Y, Harada Y, Itamura S, Odagiri T, Tashiro M, Sei Y, Yamaguchi K, Kuzuhara T. Anti-influenza activity of phenethylphenylphthalimide analogs derived from thalidomide. Bioorg Med Chem. 2010; 18:5379-5390.
14. Iwai Y, Murakami K, Gomi Y, Hashimoto T, Asakawa Y, Okuno Y, Ishikawa T, Hatakeyama D, Echigo N, Kuzuhara T. Anti-influenza activity of marchantins, macrocyclic bisbibenzyls contained in liverworts. PLoS One 2011; 6:e19825.
15. Kuzuhara T, Iwai Y, Takahashi H, Hatakeyama D, Echigo N. Green tea catechins inhibit the endonuclease activity of influenza A virus RNA polymerase. PLoS Curr. 2009; 1:RRN1052.

16. Shoji M, Takahashi E, Hatakeyama D, Iwai Y, Morita Y, Shirayama R, Echigo N, Kido H, Nakamura S, Mashino T, Okutani T, Kuzuhara T. Anti-influenza activity of C_{60} fullerene derivatives. PLoS One. 2013; 8:e66337.
17. Mantani N, Andoh T, Kawamata H, Terasawa K, Ochiai H. Inhibitory effect of *Ephedrae herba*, an oriental traditional medicine, on the growth of influenza A/PR/8 virus in MDCK cells. Antiviral Res. 1999; 44:193-200.
18. Nagai T, Kataoka E, Aoki Y, Hokari R, Kiyohara H, Yamada H. Alleviative effects of a Kampo (a Japanese herbal) medicine "maoto (ma-huang-tang)" on the early phase of influenza virus infection and its possible mode of action. Evid Based Complement Alternat Med. 2014, 2014:187036.
19. Baughman BM, Jake Slavish P, DuBois RM, Boyd VA, White SW, Webb TR. Identification of influenza endonuclease inhibitors using a novel fluorescence polarization assay. ACS Chem Biol. 2012; 7:526-534.
20. Plotch SJ, Bouloy M, Ulmanen I, Krug RM. A unique cap(m7GpppXm)-dependent influenza virion endonuclease cleaves capped RNAs to generate the primers that initiate viral RNA transcription. Cell. 1981; 23:847-858.
21. Nakamura Y, Oda K, Nakada S. Growth complementation of influenza virus temperature-sensitive mutants in mouse cells which express the RNA polymerase and nucleoprotein genes. J Biochem. 1991; 110:395-401.

(Received January 27, 2016; Revised February 16, 2016; Accepted February 17, 2016)

Case Report

DOI: 10.5582/ddt.2016.01005

Angiosarcoma of the thoracic wall responded well to nanoparticle albumin-bound paclitaxel: A case report

Naofumi Hara[1], Nobukazu Fujimoto[2,*], Yosuke Miyamoto[1], Tomoko Yamagishi[1], Michiko Asano[1], Yasuko Fuchimoto[1], Sae Wada[1], Shinji Ozaki[1], Hideyuki Nishi[3], Takumi Kishimoto[4]

[1] *Department of Respiratory Medicine, Okayama Rosai Hospital, Okayama, Japan;*
[2] *Department of Medical Oncology, Okayama Rosai Hospital, Okayama, Japan;*
[3] *Department of Surgery, Okayama Rosai Hospital, Okayama, Japan;*
[4] *Department of Internal Medicine, Okayama Rosai Hospital, Okayama, Japan.*

Summary **An 81-year-old woman visited a local clinic due to chest pain and a skin induration on the right precordia. She had a history of right breast cancer, and she had undergone a mastectomy and radiation therapy 10 years prior. Computed tomography (CT) imaging of the chest demonstrated a lobular mass that involved the right anterior thoracic wall and partially extruded from the thoracic cavity into the subcutaneous tissue. The tumor was surgically excised, and pathological analyses yielded a diagnosis of angiosarcoma. Five months after the operation, CT imaging showed multiple masses on the right pleura, indicating a local relapse and pleural dissemination of the angiosarcoma. Systemic chemotherapy composed of nanoparticle albumin-bound paclitaxel (nab-PTX) (80 mg/m^2) was delivered weekly. After 4 courses of chemotherapy, the tumors regressed remarkably. Nab-PTX may be an effective treatment option for recurrent or metastatic angiosarcoma.**

Keywords: Angiosarcoma, paclitaxel, chemotherapy

1. Introduction

Angiosarcoma is an extremely rare malignant vessel tumor that comprises 1% of all soft tissue sarcomas (*1*). It develops in subcutaneous tissue at many sites in the body, and a previous medical history of trauma, breast cancer, and/or radiotherapy are considered risk factors for the disease. Localized tumors are treated with surgical removal. However, for recurrent and unresectable conditions, there is limited evidence to support chemotherapy regimens. Here, we describe a patient with angiosarcoma that developed in the thoracic wall, which responded well to systemic chemotherapy composed of nanoparticle albumin-bound paclitaxel (nab-PTX).

Released online in J-STAGE as advance publication February 15, 2016.

**Address correspondence to:*
Dr. Nobukazu Fujimoto, Department of Medical Oncology, Okayama Rosai Hospital, 1-10-25 Chikkomidorimachi, Okayama 702-8055, Japan.
E-mail: nobufujimot@gmail.com

2. Case report

An 81-year-old woman was referred to our hospital for an examination due to right chest pain. She had a history of right breast cancer and had undergone a mastectomy and adjuvant radiotherapy 10 years prior. Upon examination, a skin induration with tenderness was found on the right precordia. Computed tomography (CT) imaging of the chest demonstrated right pleural effusion and a lobular mass that involved the right anterior thoracic wall; this mass had partially extruded from the thoracic cavity into the subcutaneous tissue (Figure 1A). On enhanced CT images, the mass showed a contrast effect in the early stages of the arterial phase. The tumor was surgically excised. Pathological analyses of the tumor showed disarrayed growth of hyperchromatic and vasoformative mesenchymal tumor cells with abnormal mitosis (Figure 2A). Immunohistochemical analyses revealed that the cells were positive for CD31 (Figure 2B) and CD34 (Figure 2C), but negative for epithelial markers, S-100 (Figure 2D) and D2-40 (Figure 2E). Based on these findings, the diagnosis was confirmed as angiosarcoma. Five months after the operation, CT images showed

multiple masses on the right pleura, indicating a local relapse and pleural dissemination of the angiosarcoma (Figure 1B). Systemic chemotherapy composed of nab-PTX (80 mg/m^2) was delivered weekly. After 4 courses of chemotherapy, the masses in the pleura regressed remarkably (Figure 1C). The only adverse event was alopecia, no myelosuppression or neurotoxicity was observed. After a total of 14 courses of chemotherapy, multiple tumors reappeared, and the patient died at 18 months after the initial diagnosis. Autopsy was not allowed.

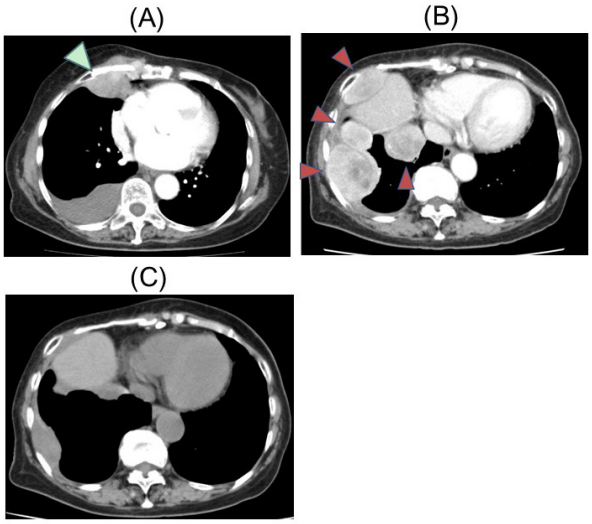

Figure 1. Computed tomography images of the chest. (A) Right pleural effusion and a lobular mass (white arrowhead) were observed at the initial examination. **(B)** Multiple masses on the right pleura (red arrowheads) appeared 5 months after the operation. **(C)** Regressed masses on the pleura after 4 courses of chemotherapy.

3. Discussion

Angiosarcoma is an uncommon malignant vessel tumor. Angiosarcoma can develop in the subcutaneous tissue in almost all parts of the body, but the most common sites are the head and neck, followed by the breast and liver (*2*). Angiosarcoma of the pleura is extremely rare (*3*). A history of breast cancer and radiation therapy are known risk factors for this disease (*4,5*), and both these factors were present in the current case study. There is limited evidence to support chemotherapy regimens for unresectable and recurrent angiosarcomas; however, a few reports have suggested that anthracyclines, ifosfamide, and taxanes are potential treatment options. A retrospective study showed that, when paclitaxel was used to treat unresectable angiosarcomas, progression-free survival was achieved for 6.8 months for scalp angiosarcoma and 2.8 months for sites below the clavicle (*6*). Nab-PTX is a novel, soluble, polyoxyethylated, castor oil-free, biologically interactive form of paclitaxel, which allows shorter infusion times and requires no premedication for hypersensitive reactions. Nab-PTX has been approved for breast cancer (*7*), non-small cell lung cancer (*8*), and gastric cancer (*9*) in Japan. Moreover, in the future, it will be used in more patients as an alternative to PTX. In the current case, nab-PTX was delivered to an aged patient with recurrent angiosarcoma that had disseminated in the pleura. This

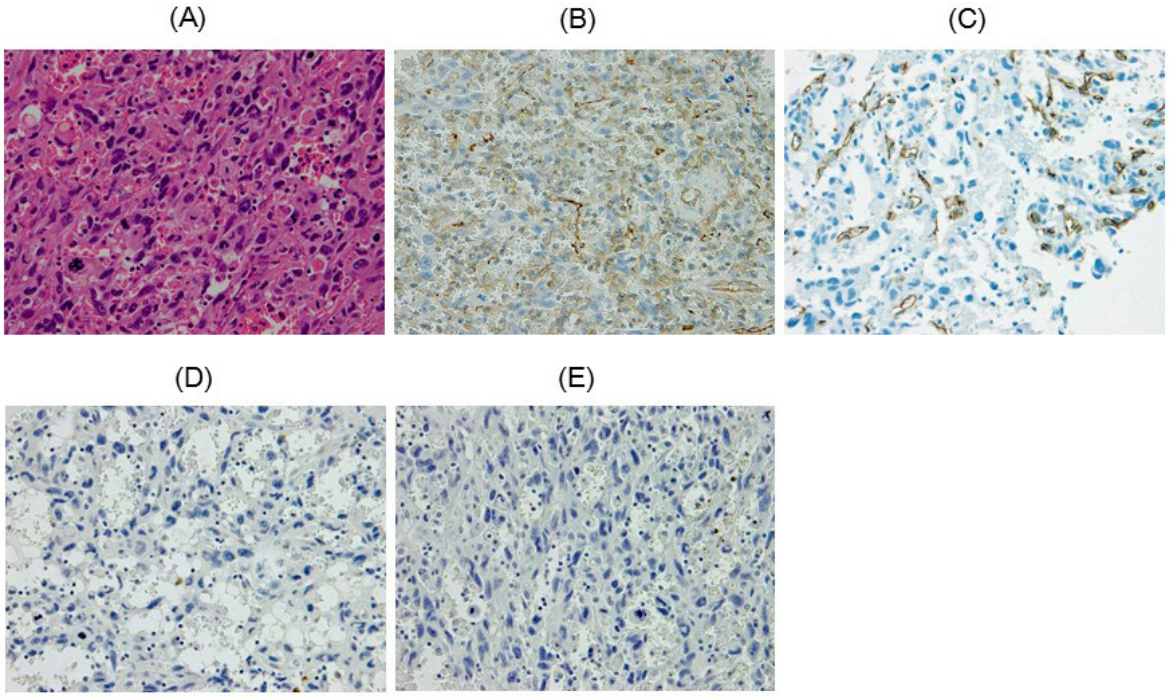

Figure 2. Pathological analyses. (A) Resected tumor specimen showed disarrayed growth of hyperchromatic and vasoformative mesenchymal tumor cells with abnormal mitosis (×40). Immunohistochemical analyses revealed that the cells were positive for CD31 **(B)** and CD34 **(C)**, but negative for epithelial markers, S-100 **(D)** and D2-40 **(E)** (×40).

treatment elicited a favorable response and few adverse events, though the tumor acquired resistance eventually. To our knowledge, the current case was the first to show that angiosarcoma significantly responded to nab-PTX. Our results suggested that weekly administration of nab-PTX may be an effective treatment option for recurrent angiosarcoma.

In conclusion, we described a case of angiosarcoma in the pleura, which showed a significant response to nab-PTX.

Acknowledgements

Supported by "The research, development, and dissemination of projects related to nine fields of occupational injuries and illnesses" of the Japan Labour Health and Welfare Organization and by grants-in-aid from the Ministry of Health, Labor and Welfare, Japan.

References

1. Wanebo HJ, Koness RJ, MacFarlane JK, Eilber FR, Byers RM, Elias EG, Spiro RH. Head and neck sarcoma: report of the Head and Neck Sarcoma Registry. Society of Head and Neck Surgeons Committee on Research. Head Neck. 1992; 14:1-7.
2. Albores-Saavedra J, Schwartz AM, Henson DE, Kostun L, Hart A, Angeles-Albores D, Chable-Montero F. Cutaneous angiosarcoma. Analysis of 434 cases from the Surveillance, Epidemiology, and End Results Program, 1973-2007. Ann Diagn Pathol. 2011; 15:93-97.
3. Zhang S, Zheng Y, Liu W, Yu X. Primary epithelioid angiosarcoma of the pleura: a case report and review of literature. Int J Clin Exp Pathol. 2015; 8:2153-2158.
4. Karlsson P, Holmberg E, Johansson KA, Kindblom LG, Carstensen J, Wallgren A. Soft tissue sarcoma after treatment for breast cancer. Radiother Oncol. 1996; 38:25-31.
5. Blanchard DK, Reynolds C, Grant CS, Farley DR, Donohue JH. Radiation-induced breast sarcoma. Am J Surg. 2002; 184:356-358.
6. Fury MG, Antonescu CR, Van Zee KJ, Brennan MF, Maki RG. A 14-year retrospective review of angiosarcoma: clinical characteristics, prognostic factors, and treatment outcomes with surgery and chemotherapy. Cancer J. 2005; 11:241-247.
7. Gradishar WJ, Tjulandin S, Davidson N, Shaw H, Desai N, Bhar P, Hawkins M, O'Shaughnessy J. Phase III trial of nanoparticle albumin-bound paclitaxel compared with polyethylated castor oil-based paclitaxel in women with breast cancer. J Clin Oncol. 2005; 23:7794-7803.
8. Rizvi NA, Riely GJ, Azzoli CG, Miller VA, Ng KK, Fiore J, Chia G, Brower M, Heelan R, Hawkins MJ, Kris MG. Phase I/II trial of weekly intravenous 130-nm albumin-bound paclitaxel as initial chemotherapy in patients with stage IV non-small-cell lung cancer. J Clin Oncol. 2008; 26:639-643.
9. Koizumi W, Morita S, Sakata Y. A randomized Phase III trial of weekly or 3-weekly doses of nab-paclitaxel versus weekly doses of Cremophor-based paclitaxel in patients with previously treated advanced gastric cancer (ABSOLUTE Trial). Jpn J Clin Oncol. 2015; 45:303-306.

(Received January 5, 2016; Revised February 8, 2016; Accepted February 9, 2016)

Case Report

DOI: 10.5582/ddt.2016.01033

Low-temperature infiltration identified using infrared thermography in patients with subcutaneous edema revealed ultrasonographically: A case report

Maiko Oya[1], Toshiaki Takahashi[1], Hidenori Tanabe[2,3], Makoto Oe[2], Ryoko Murayama[2], Koichi Yabunaka[1], Yuko Matsui[4], Hiromi Sanada[1,*]

[1] *Department of Gerontological Nursing/Wound Care Management, Graduate School of Medicine, The University of Tokyo, Tokyo, Japan;*
[2] *Department of Advanced Nursing Technology, Graduate School of Medicine, The University of Tokyo, Tokyo, Japan;*
[3] *Terumo Corporation, Tokyo, Japan;*
[4] *School of Nursing, Kanazawa Medical University, Ishikawa, Japan.*

Summary **Infiltration is a frequent complication of infusion therapy. We previously demonstrated the usefulness of infrared thermography as an objective method of detecting infiltration in healthy people. However, whether thermography can detect infiltration in clinical settings remains unknown. Therefore, we report two cases where thermography was useful in detecting infiltration at puncture sites. In both cases, tissue changes were verified ultrasonographically. The patients were a 56-year-old male with cholangitis and a 76-year-old female with hepatoma. In both cases, infiltration symptoms such as swelling and erythema occurred one day after the insertion of a peripheral intravenous catheter. Thermographic images from both patients revealed low-temperature areas spreading from the puncture sites; however, these changes were not observed in other patients. The temperature difference between the low-temperature areas and their surrounding skin surface exceeded 1.0°C. Concurrently, ultrasound images revealed that tissues surrounding the vein had a cobblestone appearance, indicating edema. In both patients, subcutaneous tissue changes suggested infiltration and both had low-temperature areas spreading from the puncture sites. Thus, subcutaneous edema may indicate infusion leakage, resulting in a decrease in the temperature of the associated skin surface. These cases suggest that infrared thermography is an effective method of objectively and noninvasively detecting infiltration.**

Keywords: Peripheral intravenous catheter, complications, early detection, ultrasonography

1. Introduction

Infiltration, one of the most frequent complications of infusion therapy with peripheral intravenous catheters (*1*), is defined as "inadvertent administration into the surrounding tissue" by the Infusion Nurses Society (INS) (*2*). When infusion agents leak from vessels and soak into the subcutaneous tissue, the contents, *i.e.*, anticancer drugs and contrast media as well as other types of agents, can cause erythema, induration, and even necrosis (*3-5*). Patients with infiltration often experience pain and in severe cases are left with persistent disabilities in their arms (*6*). Thus, infiltration can be a serious adverse event that warrants careful observation to detect abnormalities early during administration.

The INS have created an Infiltration Scale that is used to assess signs and symptoms such as "skin blanched", "edema", "cool to touch", "pain", and "numbness" (*1*). Even if patients are closely monitored for these signs and symptoms, confusion can often occur; as an example, agents can continue flowing despite obvious infiltration symptoms or can stop flowing without obvious infiltration symptoms. Hence, the assessment of infiltration can often be difficult in

**Address correspondence to:*
Hiromi Sanada, Department of Gerontological Nursing/ Wound Care Management, Graduate School of Medicine, The University of Tokyo, 7-3-1 Hongo, Bunkyo-ku, Tokyo 113-0033, Japan.
E-mail: hsanada-tky@umin.ac.jp

clinical settings.

Our group has sought to develop an objective method for early detection of infiltration by focusing on the symptom "cool to touch". Although infiltrating drugs are thought to lower the temperature of the surrounding tissues and the skin surface, few studies have examined this phenomenon. An experiment in dogs showed that microwave radiometry could be used to observe the decline in skin temperature during extravasation of doxorubicin into subcutaneous tissues (*7*). In addition, we used infrared thermography in an experiment to examine a model of infiltration in healthy adults (*8*). A circle-like low-temperature area around the puncture site was produced by intentionally allowing normal saline to leak into subcutaneous tissue; the resulting temperature differed from that obtained by the infusion of normal saline into the vessel. This thermal change occurred prior to pain manifesting, suggesting that thermography would be useful at early and noninvasive detection of infiltration. However, infiltration was intentionally produced in the model, so whether thermography could detect infiltration in patients with actual changes in their subcutaneous tissue was unknown.

Recently, ultrasonography has advanced greatly, particularly with respect to the depiction of peripheral veins. We previously reported that edema of the subcutaneous fat layer could be observed with ultrasound in patients with infiltration (*9*). To confirm whether thermographic images can practically indicate infiltration in patients with subcutaneous changes, we report two cases where thermal changes were evident in patients along with ultrasonographic signs and symptoms. Our contention is that the efficacy of thermography in detecting infiltration can be enhanced with ultrasonography.

2. Case Report

Adults undergoing peripheral intravenous catheterization in an internal medicine ward of a university hospital in Tokyo, Japan were monitored for infiltration. Infrared thermography and ultrasonography were performed on puncture sites immediately after catheter insertion and before removal. Ultrasonography was performed using portable ultrasound equipment (Noblus, Hitachi Aloka Medical Ltd., Tokyo, Japan) with a linear-array transducer (5-18.0 MHz). To identify the catheterized vein, the focus range and the image depth were set at 1.5-2.5 cm. Infrared thermography images (Thermo Shot, Nippon Avionics Co. Ltd., Tokyo, Japan) were obtained with a range of 5.0°C and an emissivity value of 0.98 and those images were analyzed using the InfReC Analyzer NS9500 Lite (Nippon Avionics Co. Ltd., Tokyo, Japan). This study was approved by the Research Ethics Committee of the Graduate School of Medicine, the University of Tokyo (approval No. #10348).

Figures 1 and 2 show the results for a patient who completed four days of infusion therapy without any complications. There were no macroscopic signs and symptoms, and none of the ultrasound images showed marked changes in the subcutaneous tissue, the vessel, or the catheter position upon insertion and removal. Both thermographic images showed similar temperature patterns around the puncture site. Two cases of patients with symptoms and signs of infiltration will now be reported.

2.1. *Case 1*

A 56-year-old man was admitted for cholangitis and a 22-gauge ethylene tetrafluoroethylene catheter (Surshield Surflo2, Terumo Corporation, Tokyo, Japan) was inserted in his right forearm to administer two doses of antibiotics and a continuous maintenance solution. A problem was noted at the puncture site, and the catheter removed approximately 23 h after insertion. Upon examination, swelling with a minor axis of 5 cm and a major axis of 6 cm, cool skin, and paresthesia were noted at the puncture site, indicating Grade 2 infiltration according to the Infiltration Scale.

Ultrasound images taken before the removal of the catheter revealed subcutaneous edema as indicated by tissue with a cobblestone appearance that was not present at the time of insertion; however, the catheter was still in the vessel (Figure 3). Thermographic images showed a low-temperature area mainly at the dressing site at the time of insertion (Figure 4A), but a low-temperature area spreading from the puncture site was observed when the catheter was removed (Figure 4B). This low-temperature area corresponded to the site of the swelling. The temperature at the center of the low-temperature area was 32.2°C and that in the surrounding area was 33.4°C, indicating a temperature difference of 1.2°C.

2.2. *Case 2*

A 76-year-old woman was admitted for radiofrequency ablation of a hepatoma. A 22-gauge catheter of the same type used in Case 1 was inserted in her left forearm and retained with a heparin lock. During the procedure, glucose and Ringer's lactate solutions were administered together with antibiotics and an analgesic. However, a problem at the puncture site was noted approximately 25 h after catheter insertion while the patient was receiving postoperative glucose and Ringer's lactate infusions. Examination revealed swelling and erythema with a minor axis of 2 cm and a major axis of 3 cm, pain on movement, and cool skin, indicating Grade 2 infiltration according to the Infiltration Scale.

Ultrasound images before catheter removal showed tissue with a cobblestone appearance and thicker subcutaneous tissue than was noted at the time of insertion (Figure 5). Although the vein was barely visible

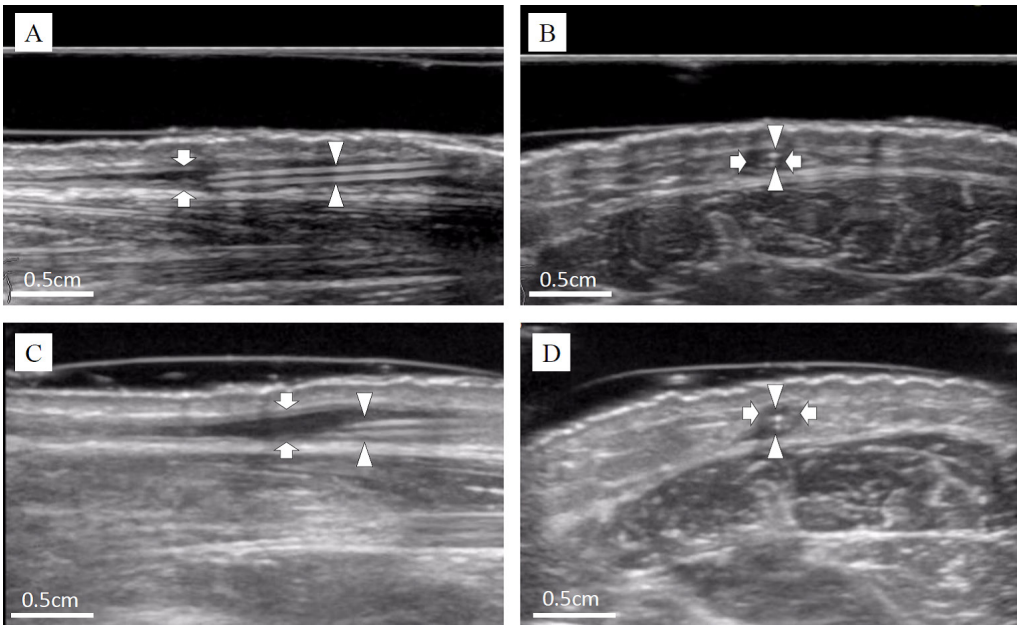

Figure 1. Representative ultrasound images from a normal patient. (A) Longitudinal and **(B)** transverse scan after catheter insertion; **(C)** longitudinal and **(D)** transverse scan before removal (4 days after insertion). Arrowheads indicate the catheter, with the vein shown between arrows. There were no marked differences between the time of insertion and removal.

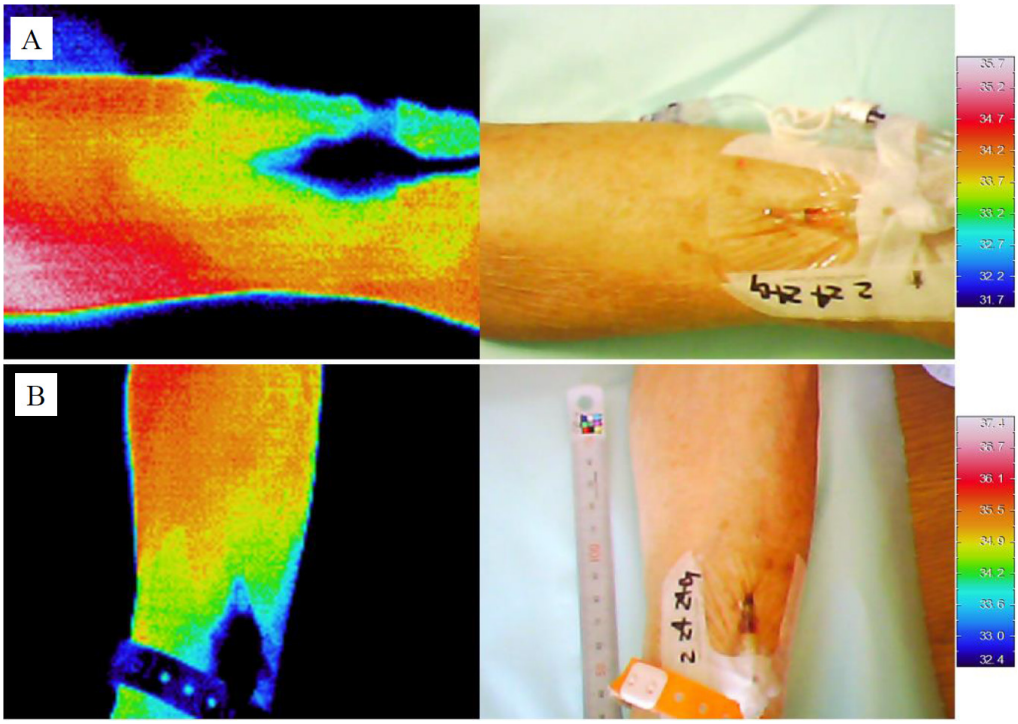

Figure 2. Representative thermographic and macroscopic images from a normal patient. (A) After insertion and **(B)** before removal. There were no complications at the time of removal, and similar temperature patterns were observed.

because of its small diameter, the catheter appeared to be within the vessel. Figure 6B shows a thermographic image with a widely spread low-temperature area at the time of removal, whereas figure 6A shows no low-temperature area at the time of insertion. The temperature was 31.9°C at the center of the low-temperature area and 33.3°C outside that area, indicating a temperature difference of 1.4°C.

3. Discussion

Both of the current patients displayed infiltration symptoms during peripheral intravenous catheterization. Infrared thermography revealed a low-temperature area in both patients, and the temperature of this area differed by more than 1.0°C in comparison to the temperature of the surrounding tissue. Ultrasonographic changes in

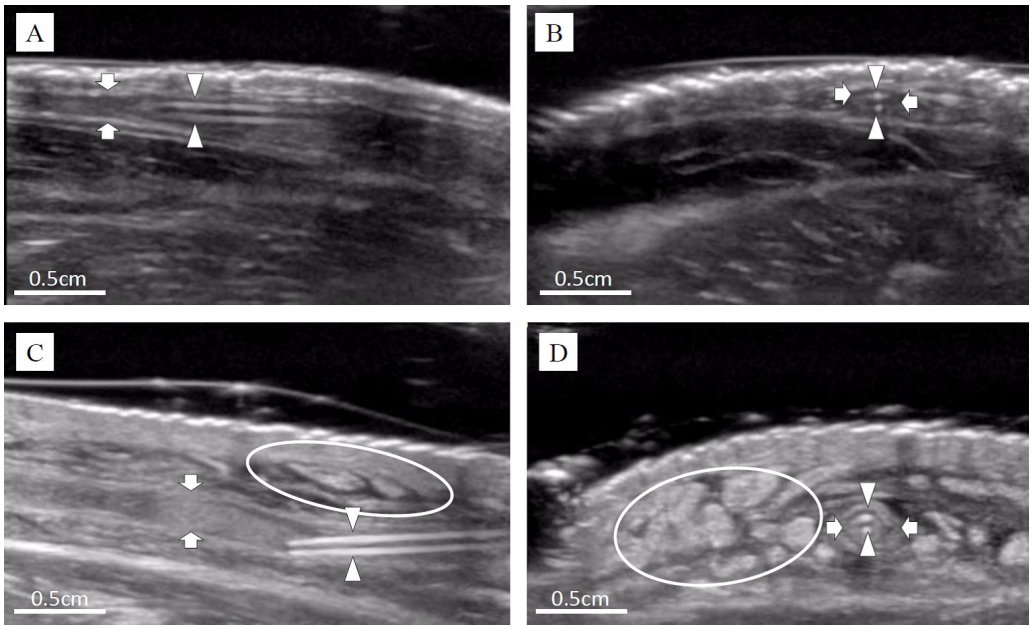

Figure 3. Ultrasound images from the patient in Case 1. Images **(A)** and **(B)** are after insertion and images **(C)** and **(D)** are before removal, when infiltration symptoms were observed. Arrowheads indicate the catheter, and the vein is between the arrows. Images **(C)** and **(D)** show tissue with a cobblestone appearance around the vein (circled area).

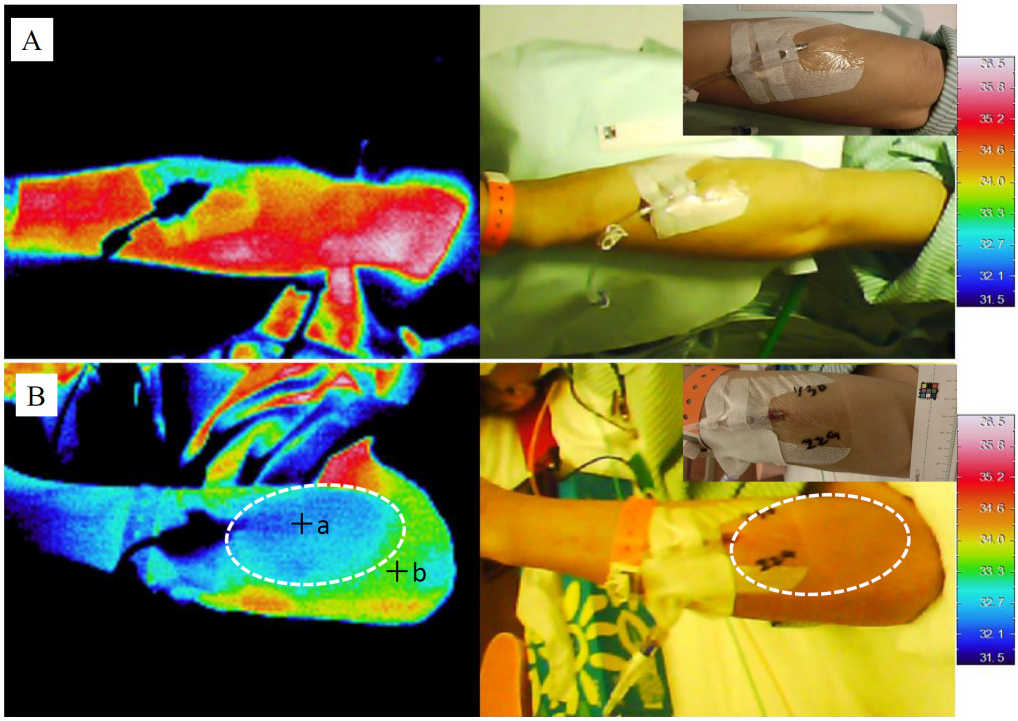

Figure 4. Thermographic and macroscopic images from the patient in Case 1. (A) After insertion; **(B)** before removal (with clear visible images). Image **(B)** shows a low-temperature area spreading from the puncture site. The center of the low-temperature area (a) was 32.2°C and the surrounding area (b) was 33.4°C.

subcutaneous tissue were evident in both patients, and these changes (*e.g.* tissue with a cobblestone appearance) were indicative of edema. The drop in the temperature of the tissue and skin surface may have been the result of an infusion leaking into surrounding tissues. Thermographic observation of the puncture site was therefore a useful method of detecting subcutaneous abnormalities during infusion in these patients.

An experiment involving extravasation of doxorubicin in dogs showed that a temperature decrease of more than 1.0°C was likely to indicate infiltration (*7*). This finding is supported by evidence that skin temperature decreases less than 1.0°C during proper intravenous therapy. In both of the current patients, the

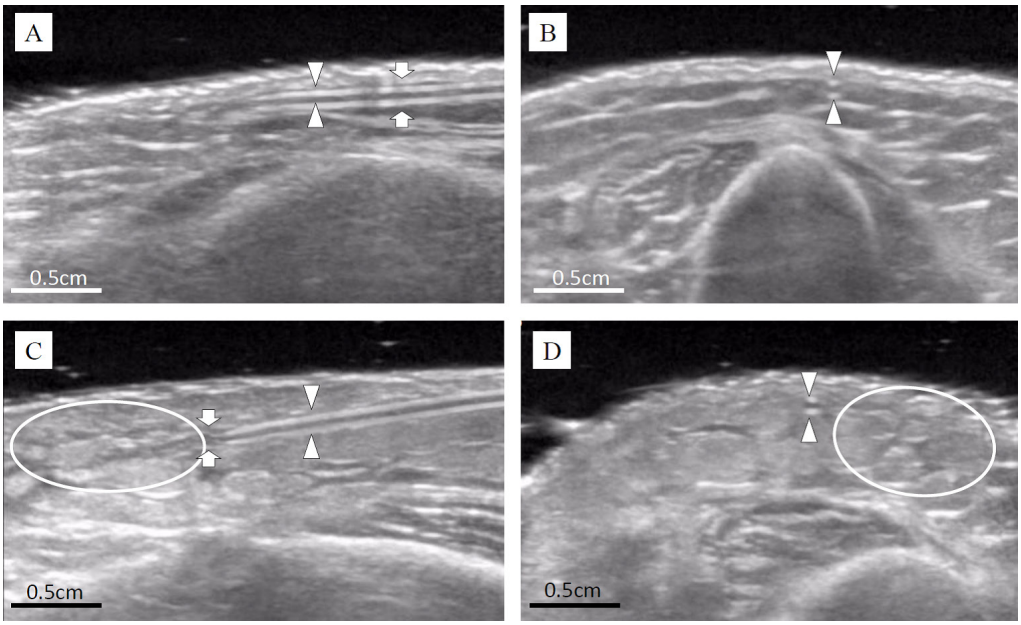

Figure 5. Ultrasound images from the patient in Case 2. Images **(A)** and **(B)** are after insertion and images **(C)** and **(D)** are before removal, when infiltration symptoms were observed. Arrowheads indicate the catheter, and the vein is between the arrows. Images **(C)** and **(D)** show surrounding tissue with a cobblestone appearance.

Figure 6. Thermographic and macroscopic images from the patient in Case 2. (A) After insertion and **(B)** before removal (with clear visible images). The rectangle represents the position of the catheter hub. Image **(B)** shows a low-temperature area spreading widely from the puncture site (circled area). The center of the low-temperature area (a) was 31.9°C, and the area beyond the low-temperature area (b) was 33.3°C.

temperature decrease in comparison to surrounding areas was greater than 1.0°C, suggesting a potential threshold for the detection of abnormalities during peripheral intravenous catheterization. However, the experiment in dogs showed that greater amounts of extravasation and more rapid flow rates caused a sharper drop in temperature. The thermography images in this case report were taken after infusions were stopped, but observations at different times and different rates of infusion could result in substantial disparities in the temperature difference.

In a previous study, we examined a model of infiltration by inserting a catheter directly into subcutaneous tissue, producing a low-temperature area

that appeared as a localized circle at the tip of the catheter on thermography (*8*). In both of the current cases, the low-temperature area spread from the puncture site but ultrasound images showed no deviation of the catheter from the vessel. The actual phenomena of infiltration may produce different thermal patterns on the skin surface depending on where a catheter is inserted. Further research with a larger sample is needed to identify patterns of temperature changes, but the current cases do offer clues to diagnostic information to help with the objective and noninvasive diagnosis of infiltration.

Several techniques have been reported to decrease complications in infusion therapy (*10,11*). However, evaluating macroscopic symptoms objectively is difficult. For example, patients who are unconscious or who have peripheral neuropathy cannot feel or complain of pain. In such instances, thermographic evaluation could provide an objective and reliable method of detecting infiltration.

In both of the current patients with infiltration, there was evidence of a relationship between a spreading low-temperature area and subcutaneous edema depicted ultrasonographically. However, further research is needed to determine when and how to judge abnormalities based on thermal changes during peripheral intravenous catheterization. Those findings could allow infrared thermography to be used to detect infiltration.

Acknowledgements

This work was conducted as a part of a project funded by the JSPS KAKENHI Grant Number 26670915.

References

1. Rickard CM, Webster J, Wallis MC, Marsh N, McGrail MR, French V, Foster L, Gallagher P, Gowardman JR, Zhang L, McClymont A, Whitby M. Routine versus clinically indicated replacement of peripheral intravenous catheters: A randomised controlled equivalence trial. Lancet. 2012; 380:1066-1074.
2. Infusion Nurses Society. Infusion Nursing Standards of Practice. J Infus Nurs. 2006; 29:S1-S92.
3. European Oncology Nursing Society. Extravasation guidelines 2007. *http://www.cancernurse.eu/documents/EONSClinicalGuidelinesSection6-en.pdf* (accessed September 30, 2015).
4. Wang CL, Cohan RH, Ellis JH, Adusumilli S, Dunnick NR. Frequency, management, and outcome of extravasation of nonionic iodinated contrast medium in 69,657 intravenous injections. Radiology. 2007; 243:80-87.
5. Dychter SS, Gold DA, Carson D, Haller M. Intravenous therapy: A review of complications and economic considerations of peripheral access. J Infus Nurs. 2012; 35:84-91.
6. Hadaway L. Infiltration and extravasation. Am J Nurs. 2007; 107:64-72.
7. Shaeffer J, el-Mahdi AM, Hamwey AE Jr, Carr KL. Detection of extravasation of antineoplastic drugs by microwave radiometry. Cancer Lett. 1986; 31:285-291.
8. Matsui Y, Murayama R, Tanabe H, Oe M, Fukuda M, Motoo Y, Wagatsuma T, Kinoshita S, Sakai K, Konya C, Sugama J, Sanada H. Analysis of thermographic images in an extravasation model of intravenous infusion in healthy adults. Journal of Nursing Science and Engineering. 2014; 1:4-11. (in Japanese)
9. Yabunaka K, Murayama R, Takahashi T, Tanabe H, Kawamoto A, Oe M, Arai R, Sanada H. Ultrasonographic appearance of infusion via the peripheral intravenous catheters. Journal of Nursing Science and Engineering. 2015; 2:40-46. (in Japanese)
10. Doellman D, Hadaway L, Bowe-Geddes LA, Franklin M, LeDonne J, Papke-O'Donnell L, Schulmeister L, Stranz M. Infiltration and extravasation: Update on prevention and management. J Infus Nurs. 2009; 32:203-211.
11. Schulmeister L. Extravasation management: Clinical update. Semin Oncol Nurs. 2011; 27:82-90.

(Received April 12, 2016; Accepted April 16, 2016)

DD&T
Drug Discoveries & Therapeutics

Guide for Authors

1. Scope of Articles

Drug Discoveries & Therapeutics welcomes contributions in all fields of pharmaceutical and therapeutic research such as medicinal chemistry, pharmacology, pharmaceutical analysis, pharmaceutics, pharmaceutical administration, and experimental and clinical studies of effects, mechanisms, or uses of various treatments. Studies in drug-related fields such as biology, biochemistry, physiology, microbiology, and immunology are also within the scope of this journal.

2. Submission Types

Original Articles should be well-documented, novel, and significant to the field as a whole. An Original Article should be arranged into the following sections: Title page, Abstract, Introduction, Materials and Methods, Results, Discussion, Acknowledgments, and References. Original articles should not exceed 5,000 words in length (excluding references) and should be limited to a maximum of 50 references. Articles may contain a maximum of 10 figures and/or tables.

Brief Reports definitively documenting either experimental results or informative clinical observations will be considered for publication in this category. Brief Reports are not intended for publication of incomplete or preliminary findings. Brief Reports should not exceed 3,000 words in length (excluding references) and should be limited to a maximum of 4 figures and/or tables and 30 references. A Brief Report contains the same sections as an Original Article, but the Results and Discussion sections should be combined.

Reviews should present a full and up-to-date account of recent developments within an area of research. Normally, reviews should not exceed 8,000 words in length (excluding references) and should be limited to a maximum of 100 references. Mini reviews are also accepted.

Policy Forum articles discuss research and policy issues in areas related to life science such as public health, the medical care system, and social science and may address governmental issues at district, national, and international levels of discourse. Policy Forum articles should not exceed 2,000 words in length (excluding references).

Case Reports should be detailed reports of the symptoms, signs, diagnosis, treatment, and follow-up of an individual patient. Case reports may contain a demographic profile of the patient but usually describe an unusual or novel occurrence. Unreported or unusual side effects or adverse interactions involving medications will also be considered. Case Reports should not exceed 3,000 words in length (excluding references).

News articles should report the latest events in health sciences and medical research from around the world. News should not exceed 500 words in length.

Letters should present considered opinions in response to articles published in Drug Discoveries & Therapeutics in the last 6 months or issues of general interest. Letters should not exceed 800 words in length and may contain a maximum of 10 references.

3. Editorial Policies

Ethics: Drug Discoveries & Therapeutics requires that authors of reports of investigations in humans or animals indicate that those studies were formally approved by a relevant ethics committee or review board.

Conflict of Interest: All authors are required to disclose any actual or potential conflict of interest including financial interests or relationships with other people or organizations that might raise questions of bias in the work reported. If no conflict of interest exists for each author, please state "There is no conflict of interest to disclose".

Submission Declaration: When a manuscript is considered for submission to Drug Discoveries & Therapeutics, the authors should confirm that 1) no part of this manuscript is currently under consideration for publication elsewhere; 2) this manuscript does not contain the same information in whole or in part as manuscripts that have been published, accepted, or are under review elsewhere, except in the form of an abstract, a letter to the editor, or part of a published lecture or academic thesis; 3) authorization for publication has been obtained from the authors' employer or institution; and 4) all contributing authors have agreed to submit this manuscript.

Cover Letter: The manuscript must be accompanied by a cover letter signed by the corresponding author on behalf of all authors. The letter should indicate the basic findings of the work and their significance. The letter should also include a statement affirming that all authors concur with the submission and that the material submitted for publication has not been published previously or is not under consideration for publication elsewhere. The cover letter should be submitted in PDF format. For example of Cover Letter, please visit http://www.ddtjournal.com/downcentre.php (Download Centre).

Copyright: A signed JOURNAL PUBLISHING AGREEMENT (JPA) must be provided by post, fax, or as a scanned file before acceptance of the article. Only forms with a hand-written signature are accepted. This copyright will ensure the widest possible dissemination of information. A form facilitating transfer of copyright can be downloaded by clicking the appropriate link and can be returned to the e-mail address or fax number noted on the form (Please visit Download Centre). Please note that your manuscript will not proceed to the next step in publication until the JPA form is received. In addition, if excerpts from other copyrighted works are included, the author(s) must obtain written permission from the copyright owners and credit the source(s) in the article.

Suggested Reviewers: A list of up to 3 reviewers who are qualified to assess the scientific merit of the study is welcomed. Reviewer information including names, affiliations, addresses, and e-mail should be provided at the same time the manuscript is submitted online. Please do not suggest reviewers with known conflicts of interest, including participants or anyone with a stake in the proposed research; anyone from the same institution; former students, advisors, or research collaborators (within the last three years); or close personal contacts. Please note that the Editor-in-Chief may accept one or more of the proposed reviewers or may request a review by other qualified persons.

Language Editing: Manuscripts prepared by authors whose native language is not English should have their work proofread by a native English speaker before submission. If not, this might delay the publication of your manuscript in Drug Discoveries & Therapeutics.

The Editing Support Organization can provide English proofreading, Japanese-English translation, and Chinese-English translation services to authors who want to publish in Drug Discoveries & Therapeutics and need assistance before submitting a manuscript. Authors can visit this organization directly at http://www.iacmhr.com/iac-eso/support.php?lang=en. IAC-ESO was established to facilitate manuscript preparation by researchers whose native language is not English and to help edit works intended for international academic journals.

4. Manuscript Preparation

Manuscripts should be written in clear, grammatically correct English and submitted as a Microsoft Word file in a single-column format. Manuscripts must be paginated and typed in 12-point Times New Roman font with 24-point line spacing. Please do not embed figures in the text. Abbreviations should be used as little as possible and should be explained at first mention unless the term is a well-known abbreviation (*e.g.* DNA). Single words should not be abbreviated.

Title page: The title page must include 1) the title of the paper (Please note the title should be short, informative, and contain the major key words); 2) full name(s) and affiliation(s) of the author(s), 3) abbreviated names of the author(s), 4) full name, mailing address, telephone/fax numbers, and e-mail address of the corresponding author; and 5) conflicts of interest (if you have an actual or potential conflict of interest to disclose, it must be included as a footnote on the title page of the manuscript; if no conflict of interest exists for each author, please state "There is no conflict of interest to disclose"). Please visit Download Centre and refer to the title page of the manuscript sample.

Abstract: The abstract should briefly state the purpose of the study, methods, main findings, and conclusions. For article types including Original Article, Brief Report, Review, Policy Forum, and Case Report, a one-paragraph abstract consisting of no more than 250 words must be included in the manuscript. For News and Letters, a brief summary of main content in 150 words or fewer should be included in the manuscript. Abbreviations must be kept to a minimum and non-standard abbreviations explained in brackets at first mention. References should be avoided in the abstract. Key words or phrases that do not occur in the title should be included in the Abstract page.

Introduction: The introduction should be a concise statement of the basis for the study and its scientific context.

Materials and Methods: The description should be brief but with sufficient detail to enable others to reproduce the experiments. Procedures that have been published previously should not be described in detail but appropriate references should simply be cited. Only new and significant modifications of previously published procedures require complete description. Names of products and manufacturers with their locations (city and state/country) should be given and sources of animals and cell lines should always be indicated. All clinical investigations must have been conducted in accordance with Declaration of Helsinki principles. All human and animal studies must have been approved by the appropriate institutional review board(s) and a specific declaration of approval must be made within this section.

Results: The description of the experimental results should be succinct but in sufficient detail to allow the experiments to be analyzed and interpreted by an independent reader. If necessary, subheadings may be used for an orderly presentation. All figures and tables must be referred to in the text.

Discussion: The data should be interpreted concisely without repeating material already presented in the Results section. Speculation is permissible, but it must be well-founded, and discussion of the wider implications of the findings is encouraged. Conclusions derived from the study should be included in this section.

Acknowledgments: All funding sources should be credited in the Acknowledgments section. In addition, people who contributed to the work but who do not meet the criteria for authors should be listed along with their contributions.

References: References should be numbered in the order in which they appear in the text. Citing of unpublished results, personal communications, conference abstracts, and theses in the reference list is not recommended but these sources may be mentioned in the text. In the reference list, cite the names of all authors when there are fifteen or fewer authors; if there are sixteen or more authors, list the first three followed by *et al*. Names of journals should be abbreviated in the style used in PubMed. Authors are responsible for the accuracy of the references. Examples are given below:

Example 1 (Sample journal reference):
Nakata M, Tang W. Japan-China Joint Medical Workshop on Drug Discoveries and Therapeutics 2008: The need of Asian pharmaceutical researchers' cooperation. Drug Discov Ther. 2008; 2:262-263.

Example 2 (Sample journal reference with more than 15 authors):
Darby S, Hill D, Auvinen A, *et al*. Radon in homes and risk of lung cancer: Collaborative analysis of individual data from 13 European case-control studies. BMJ. 2005; 330:223.

Example 3 (Sample book reference):
Shalev AY. Post-traumatic stress disorder: Diagnosis, history and life course. In: Post-traumatic Stress Disorder, Diagnosis, Management and Treatment (Nutt DJ, Davidson JR, Zohar J, eds.). Martin Dunitz, London, UK, 2000; pp. 1-15.

Example 4 (Sample web page reference):
World Health Organization. The World Health Report 2008 – primary health care: Now more than ever. *http://www.who.int/whr/2008/whr08_en.pdf* (accessed September 23, 2010).

Tables: All tables should be prepared in Microsoft Word or Excel and should be arranged at the end of the manuscript after the References section. Please note that tables should not in image format. All tables should have a concise title and should be numbered consecutively with Arabic numerals. If necessary, additional information should be given below the table.

Figure Legend: The figure legend should be typed on a separate page of the main manuscript and should include a short title and explanation. The legend should be concise but comprehensive and should be understood without referring to the text. Symbols used in figures must be explained.

Figure Preparation: All figures should be clear and cited in numerical order in the text. Figures must fit a one- or two-column format on the journal page: 8.3 cm (3.3 in.) wide for a single column, 17.3 cm (6.8 in.) wide for a double column; maximum height: 24.0 cm (9.5 in.). Please make sure that artwork files are in an acceptable format (TIFF or JPEG) at minimum resolution (600 dpi for illustrations, graphs, and annotated artwork, and 300 dpi for micrographs and photographs). Please provide all figures as separate files. Please note that low-resolution images are one of the leading causes of article resubmission and schedule delays. All color figures will be reproduced in full color in the online edition of the journal at no cost to authors.

Units and Symbols: Units and symbols conforming to the International System of Units (SI) should be used for physicochemical quantities. Solidus notation (*e.g.* mg/kg, mg/mL, mol/mm^2/min) should be used. Please refer to the SI Guide www.bipm.org/en/si/ for standard units.

Supplemental data: Supplemental data might be useful for supporting and enhancing your scientific research and Drug Discoveries & Therapeutics accepts the submission of these materials which will be only published online alongside the electronic version of your article. Supplemental files (figures, tables, and other text materials) should be prepared according to the above guidelines, numbered in Arabic numerals (*e.g.*, Figure S1, Figure S2, and Table S1, Table S2) and referred to in the text. All figures and tables should have titles and legends. All figure legends, tables and supplemental text materials should be placed at the end of the paper. Please note all of these supplemental data should be provided at the time of initial submission and note that the editors reserve the right to limit the size and length of Supplemental Data.

5. Submission Checklist

The Submission Checklist will be useful during the final checking of a manuscript prior to sending it to Drug Discoveries & Therapeutics for review. Please visit Download Centre and download the Submission Checklist file.

6. Online submission

Manuscripts should be submitted to Drug Discoveries & Therapeutics online at http://www.ddtjournal.com. The manuscript file should be smaller than 5 MB in size. If for any reason you are unable to submit a file online, please contact the Editorial Office by e-mail at office@ddtjournal.com

7. Accepted manuscripts

Proofs: Galley proofs in PDF format will be sent to the corresponding author *via* e-mail. Corrections must be returned to the editor (proof-editing@ddtjournal.com) within 3 working days.

Offprints: Authors will be provided with electronic offprints of their article. Paper offprints can be ordered at prices quoted on the order form that accompanies the proofs.

Page Charge: A page charge of $140 will be assessed for each printed page of an accepted manuscript. The charge for printing color figures is $340 for each page. Under exceptional circumstances, the author(s) may apply to the editorial office for a waiver of the publication charges at the time of submission.

(Revised February 2013)

Editorial and Head Office:

Pearl City Koishikawa 603
2-4-5 Kasuga, Bunkyo-ku
Tokyo 112-0003
Japan
Tel: +81-3-5840-9697
Fax: +81-3-5840-9698
E-mail: office@ddtjournal.com

DD&T
Drug Discoveries & Therapeutics

JOURNAL PUBLISHING AGREEMENT (JPA)

Manuscript No.:

Title:

Corresponding author:

The International Advancement Center for Medicine & Health Research Co., Ltd. (IACMHR Co., Ltd.) is pleased to accept the above article for publication in Drug Discoveries & Therapeutics. The International Research and Cooperation Association for Bio & Socio-Sciences Advancement (IRCA-BSSA) reserves all rights to the published article. Your written acceptance of this JOURNAL PUBLISHING AGREEMENT is required before the article can be published. Please read this form carefully and sign it if you agree to its terms. The signed JOURNAL PUBLISHING AGREEMENT should be sent to the Drug Discoveries & Therapeutics office (Pearl City Koishikawa 603, 2-4-5 Kasuga, Bunkyo-ku, Tokyo 112-0003, Japan; E-mail: office@ddtjournal.com; Tel: +81-3-5840-9697; Fax: +81-3-5840-9698).

1. Authorship Criteria

As the corresponding author, I certify on behalf of all of the authors that:

1) The article is an original work and does not involve fraud, fabrication, or plagiarism.
2) The article has not been published previously and is not currently under consideration for publication elsewhere. If accepted by Drug Discoveries & Therapeutics, the article will not be submitted for publication to any other journal.
3) The article contains no libelous or other unlawful statements and does not contain any materials that infringes upon individual privacy or proprietary rights or any statutory copyright.
4) I have obtained written permission from copyright owners for any excerpts from copyrighted works that are included and have credited the sources in my article.
5) All authors have made significant contributions to the study including the conception and design of this work, the analysis of the data, and the writing of the manuscript.
6) All authors have reviewed this manuscript and take responsibility for its content and approve its publication.
7) I have informed all of the authors of the terms of this publishing agreement and I am signing on their behalf as their agent.

2. Copyright Transfer Agreement

I hereby assign and transfer to IACMHR Co., Ltd. all exclusive rights of copyright ownership to the above work in the journal Drug Discoveries & Therapeutics, including but not limited to the right 1) to publish, republish, derivate, distribute, transmit, sell, and otherwise use the work and other related material worldwide, in whole or in part, in all languages, in electronic, printed, or any other forms of media now known or hereafter developed and the right 2) to authorize or license third parties to do any of the above.

I understand that these exclusive rights will become the property of IACMHR Co., Ltd., from the date the article is accepted for publication in the journal Drug Discoveries & Therapeutics. I also understand that IACMHR Co., Ltd. as a copyright owner has sole authority to license and permit reproductions of the article.

I understand that except for copyright, other proprietary rights related to the Work (*e.g.* patent or other rights to any process or procedure) shall be retained by the authors. To reproduce any text, figures, tables, or illustrations from this Work in future works of their own, the authors must obtain written permission from IACMHR Co., Ltd.; such permission cannot be unreasonably withheld by IACMHR Co., Ltd.

3. Conflict of Interest Disclosure

I confirm that all funding sources supporting the work and all institutions or people who contributed to the work but who do not meet the criteria for authors are acknowledged. I also confirm that all commercial affiliations, stock ownership, equity interests, or patent-licensing arrangements that could be considered to pose a financial conflict of interest in connection with the article have been disclosed.

Corresponding Author's Name (Signature):

Date: